Summer 8-15-2018

Kdm6b is Required for Self-Renewal of Normal and Leukemic Mouse Stem Cells Under Proliferative Stress

Cates Mallaney
Washington University in St. Louis

WASHINGTON UNIVERSITY IN ST. LOUIS

Division of Biology and Biomedical Sciences
Human and Statistical Genetics

Dissertation Examination Committee:
Grant A. Challen, Chair
Todd E. Druley
Daniel C. Link
Jeffrey A. Magee
Laura G. Schuettpelz
Matthew J. Walter

Kdm6b is Required for Self-Renewal of Normal and Leukemic Mouse Stem Cells Under Proliferative Stress

by

Cates N. Mallaney

A dissertation presented to
The Graduate School
of Washington University
in partial fulfillment of the
requirements for the degree
of Doctor of Philosophy

August 2018
St. Louis, Missouri

Table of Contents

List of Figures

List of Tables

Acknowledgements

Starting off as a graduate student, I knew that I wanted to focus on leukemia research, but was not sure if I would be able to combine that with my interest in genetic regulation and genetic disease that results not from mutations, but rather from dysregulation of expression. When I first saw Grant Challen present his research, I knew that I had found my lab. From day one, Grant's enthusiasm for science, drive for therapeutic discover, and mentorship has helped shape me as a scientist and molded my thesis into a piece of science of which I am incredibly proud. I consider myself very fortunate to be able to say that I personally learned and was trained by someone that I feel is well on his way to being a leader in the field. I thank him for not only personally training me, but for always pushing scientific excellence, and for fostering an environment that leads to the success of his trainees.

As only the third member of the Challen lab and first graduate student to join, one of the greatest things I have gotten to be a part of is the shaping of the lab environment. The friendship, collaboration and eagerness that exists within the Challen lab is incomparable. To that end, I would like to thank the past and present lab members Beth Ostrander, Andy Martens, Hamza Celik, Beth Eultgen, Won Kyun Koh, Casey Wilson, Emily Haussler, and Greg Fishberger, Alok Kothari, and Ashley Kramer. They have all been instrumental in my growth as a scientist, and have helped shape the work presented in this thesis with their help and their ideas. I would also like to thank Challen Lab collaborators: Siteman Flow Cytometry Core, WUSTL Pathology Flow Core, WUSTL Genome Editing Core, and WUSTL Genome Technology Access Center

(GTAC). One of the reasons that makes WUSTL so excellent is the collaboration between labs. I would like to thank the labs of Drs. Daniel Link, Todd Druley, Laura Schuettpelz, Jeff Magee, Matthew Walter, Timothy Ley, and Lukas Wartman for their generosity with equipment, reagents, and resources.

I would like to thank the members of my thesis committee for pushing me to become a better researcher. Their knowledge in the field is incomparable and their feedback and concepts have led to some of my favorite experiments and ideas. I appreciate their belief in me and the time they have taken to meet, discuss, and generate ideas. Each individual on my committee is a wonderful mentor and excellent resource.

To the Division of Biology and Biomedical Sciences (DBBS), and specifically, Jeanne Silvestrini, Shirley McTigue, and Dana Kharibian, I have immeasurable gratitude. Jeanne has helped guide me throughout graduate school and has always been a great person to get advice from as well as to chat and laugh with, and I am incredibly grateful to her. Shirley and Dana were instrumental in my F31 fellowship and I thank them for all their hard work and guidance.

The Human and Statistical Genetics (HSG) division of DBBS and the Division of Biostatistics have had such a huge influence on my life. I would like to thank the faculty and staff of both divisions for their knowledge and enthusiasm. I would like to thank Dr. D.C. Rao and my master's mentor, Dr. Yun Ju Sung who are undoubtedly the reason I was able to pursue my Ph.D.

I would also like to thank my friends and fellow HSG classmates, as well as fellow graduate students from other programs. It is incredible to see the work that has

been done by everyone in advancing science. To be able to spend so many hours a week working next to and with one of my favorite people, Beth Ostrander, has been a privilege and a constant source of entertainment.

I would like to thank my family. To my mom and dad who allowed all of my siblings to pursue all our interests, thank you. Thank you for supporting me, for always being excited for me, and for believing in me. Also, thank you for the weird familial genetics, as they set me on the path to where I am! To all my siblings, the ones I grew up with, and the ones I gained through marriage, thank you for always having high expectations of me, and for your love and friendship. And to Gary, my better half, who has encouraged me, pushed me to pursue my degree, and shown immeasurable patience as he supported me in every single way possible, thank you for you, your love, and every other possible thing.

To my motivation and inspiration to research leukemia, my late nephew, Theo: the impact you made in so many peoples' lives in such a short amount of time is incalculable. Not a day has gone by where I have not remembered your beautiful smile and your sweet spirit. I will always continue to fight in your memory.

Cates Mallaney

Washington University in St. Louis

August 2018

Dedicated to my nephew, Theo.

ABSTRACT OF THE DISSERTATION

Kdm6b is Required for Self-Renewal of Normal and Leukemic Mouse Stem Cells Under Proliferative Stress

by

Cates N. Mallaney

Doctor of Philosophy in Biology and Biomedical Sciences

Human and Statistical Genetics

Washington University in St. Louis, 2018

Assistant Professor Grant A. Challen, Chair

KDM6B (JMJD3) is one of two known epigenetic modifiers responsible for the removal of the repressive histone mark, histone-3 lysine-27 trimethylation (H3K27me3), and has been shown to play a role in development, differentiation, and inflammatory stress response. Unlike the other H3K27me3 demethylase, UTX (KDM6A), which is frequently mutated in hematopoietic malignancies, KDM6B is upregulated in a myriad of blood disorders. This suggests that it may have important functions in the pathogenesis of hematopoietic cancers. Here, we examined the role of Kdm6b in hematopoietic stem cell (HSC) fate decisions under normal and malignant conditions to evaluate its potential as a therapeutic target. Loss of *Kdm6b* leads to a significant reduction in phenotypic and functional HSCs in adult mice, which increases with increased age. Loss of *Kdm6b* results in the inability to maintain the HSC population post-transplantation in a dose-dependent manner. In addition, *Kdm6b* is necessary for HSC self-renewal in response to inflammatory, genotoxic and oncogenic stress. *Kdm6b* HSCs have a stress response

gene expression signature which overlaps significantly with immediate early response genes, genes associated with aged HSCs and genes involved in quiescence of HSCs. When stimulated with an inflammatory or proliferative agent, *Kdm6b*–deficient HSCs are not able to efficiently resolve gene expression programs, leading to delayed cell cycle entry and a self-renewal block, forcing them to differentiate once they commit to divide. Thus, *Kdm6b* is necessary for self-renewal of normal and leukemic stem cells, and *KDM6B* inhibition combined with proliferative agents may force differentiation and eventual depletion of leukemic stem cells in patients.

Chapter 1: Introduction

1.1 Epigenetic Modifications are Dynamic and Reversible

Within the nucleus, DNA is highly organized into chromatin consisting of nucleosome complexes comprised of histone proteins that can be modified at their N-terminal tails. These covalent post-translational modifications, termed epigenetic, including methylation and acetylation of the lysine (K) and arginine (R) residues, play a vital role in transcriptional regulation and chromatin architecture. The epigenetic landscape also serves a role in cell type identity with modifications being inherited by daughter cells and serving as memory for those cells[1–4]. There have been many enzymes that have been identified that are responsible for the placement of post-translational modifications of the histone tails. These epigenetic 'writers' include histone acetyltransferases and histone methyltransferases. EZH2, a histone 3 lysine 27 (H3K27) methyltransferase, is the well-characterized writer component of the polycomb repressive complex 2 (PRC2) which also includes the subunits SUZ12, EED, and RbAp48[5]. PRC2 is responsible for the trimethylation of H3K27, which is associated with transcriptional repression[6], and paused RNA polymerase II (RNA Pol II) at the promoters of PRC2 targeted genes[7]. The placement of H3K27me3 by PRC2 has been shown to play an important role in X-linked inactivation[8,9], as well as embryonic stem cell pluripotency (ESC) and development[10–14].

Because H3K27me3 repression plays a vital role in maintaining pluripotency of ESCs[14], it stood to reason there must be a way to resolve expression of the genes necessary for differentiation. Evidence of histone demethylases, so called 'erasers',

came when LSD1 (KDM1A), was discovered to act as a transcriptional repressor by removing the activating H3K4me2/1 chromatin modification by oxidative demethylation requiring the cofactor flavin[15]. Since then an even larger family of proteins, the Jumonji C (JmjC) domain containing proteins have been discovered. These enzymes also act as oxidative demethylases, but require iron Fe(II) and α-ketoglutarate as cofactors[16,17]. Bioinformatic analyses to identify JmjC domain proteins indicate that in humans this class of proteins contains 30 different genes that cluster into seven groups[16–20]. Since the discovery of the enzymatic activity of JmjC proteins, many studies have uncovered their substrate specificities, including those responsible for the removal of the H3K27me3 repressive mark: KDM6B and UTX.

1.2 KDM6B as a Demethylase

One of the seven phylogenetic branches of the JmjC protein groups is the UTX/UTY/KDM6B group of proteins. UTX (also called KDM6A) protein is X-linked and escapes inactivation[21] whereas the UTY protein in Y-linked. These two proteins contain six tetratricopeptide repeats (TPR) domains along with a JmjC domain and are 88% homologous, with 82% homology within their JmjC domains[22]. KDM6B, located on chromosome 17p13.1 in humans, is another member of this family. While KDM6B still retains high sequence homology to UTX within its JmjC domain at 84%, it lacks TPR domains and the full length proteins are only 70% homologous[22]. Computational modeling of the KDM6B:H3 complex shows three conserved domains: the JmjC domain, the linker domain, and the zinc binding domain, similar to that of UTX; however, within the zinc binding domain, there is a different angle of an α-helix which shifts the zinc atom

as well as the bound H3 peptide giving a slight difference in conformation between the two proteins[23]. Additionally, while it has been shown that UTX undergoes a conformational change upon binding to H3 peptide[24], KDM6B does not[23].

In 2007, six independent groups identified UTX and/or KDM6B as H3K27me2/3 demethylases, but interestingly, despite the highly conserved sequence, UTY lacks demethylase activity[18,19,22,25–27]. Agger et al showed that ectopic expression of UTX and KDM6B, led to a reduction of H3K27me2/3 levels in HeLa cells in a dose-dependent manner and indicated a higher specificity to trimethylation[19]. The experimental approach by Hong et al in HEK293T cells indicated that as well as having H3K27me2/3 specificity, UTX can also demethylase H3K27me1, and the TPR domains may be necessary for this specific interaction[22]. Conversely, while overexpression of KDM6B showed a global reduction in H3K27me3 and H3K27me2 in HEK293T cells, it also led to an increase in H3K27me1 levels due to the conversion of H3K27me3 and H3K27me2 indicating that while UTX can demethylase H3K27me1, KDM6B can not[26]. While overexpression of both proteins led to a global reduction in H3K27me2/3 levels, knockdown of either protein led to varying results depending on the cell type.

Enzymatic kinetics utilizing MALDI-TOF mass spectrometry indicate that KDM6B has a higher affinity for its substrates over UTX[28,29], however, demethylation still required a high enzyme-to-substrate ratio[19,25–27]. Jones et al. found that despite the slight conformational changes discussed previously, the same residues of the histone peptides needed for substrate recognition were identical between the KDM6B and UTX and they hypothesize that these shifts in conformation may explain higher KDM6B affinity[23,28]. Within the JmjC domain of KDM6B, there are three amino acids residues necessary for

chelating iron: His1390, Glu1392 and His1470[18]. Any one mutation, or combination of mutations, renders KDM6B catalytically dead, leaving it unable to demethylate H3K27me2/3 showing its dependency on iron[18,19,27,28]. Additionally, KDM6B and UTX were both shown to have diminished enzymatic activity on synthetic peptides, with UTX unable to recognize or demethylate H3K27me1 without the presence of intact H3 histone, indicating the necessity of the core histones and the possibility of other cofactors of KDM6B and UTX to exist[22,26].

In addition to being methylated at H3K27 the histone tail has also been shown to be phosphorylated by mitogen- and stress-activated kinases (MSK) at S28 creating a double H3K27me3S28p post-translational modification. This modification leads to a disassociation of the PRC2 complex and an increase in gene expression[30]. The presence of phosphorylation at S28 was also shown to result in the inability of KDM6B to demethylate H3K27me3[28].

While the majority of the experimental evidence suggests that KDM6B is specific to H3K27me2/3, a more recent group studied its role as a methylarginine demethylase (RDM). Using truncated recombinant proteins containing the catalytic domain of several JmjC proteins, they found that KDM6B was capable of demethylating synthetic H3K27Rme2a, and the method of methyl group oxidation to release formaldehyde is conserved between lysine and arginine demethylation. Interestingly, formaldehyde dehydrogenase-coupled demethylation assays indicated that KDM6B demethylation of arginine is more efficient than lysine. Given all this, however, KDM6B failed to show enzymatic demethylase activity on natural histone peptides[31]. Despite its inability to act on natural occurring peptides in the context of the experimental design of Walport et al, it

is the first time that it has been shown that JmjC proteins, and KDM6B specifically, may play a dual role in demethylation.

In addition to having possible histone demethylase role outside of H3K27me2/3, KDM6B has also been shown to regulate p53 post-translational modifications which influence its regulatory roles, protein interactions, and subcellular localizations[32–37]. Overexpression of KD6MB in neuronal stem cells (NSC) was shown to increase p53 independent of transcription indicating that it helps stabilize p53 during NSC differentiation[38]. In addition to stabilizing p53 the two proteins were shown to interact in NSCs, and wild-type KDM6B but not catalytically inactive KDM6B led to a reduction in p53 demethylation. This demethylation correlated to an increase of p53 in the nucleus, whereas the mutant KDM6B led to an accumulation of p53 in the cytoplasm indicating that during neuronal differentiation KDM6B plays a very important role in regulating p53 subcellular location in a demethylase-dependent manner[38].

1.3 KDM6B Plays an Important Role in Development

Given the role that H3K27me3 was seen to play in maintaining the pluripotency of ESCs, it stood to reason that one of the major roles H3K27me3 demethylases play an important role in the regulation of development. Indeed, the pattern of KDM6B expression in embryonic stem cells has been shown to increase throughout differentiation[12]. It has been shown that KDM6B begins regulating development at the first step of mammalian cell lineage commitment, prior to embryo implantation. In order for implantation to occur the eight-cell blastomeres must first differentiate the outside cells into the trophectoderm (TE) and inside cells into the inner cell mass (ICM). The TE is essential for implantation

as it interacts with the maternal uterus and forms placental tissue[39]. KDM6B has been shown to play an important role in this lineage commitment by balancing PRC2 and controlling TE gene expression. In mouse trophoblastic stem cells, PRC2 was found to be localized to the ICM, but KDM6B was expressed in both lineages. Interestingly, this expression was found to be higher in the cytoplasm than the nucleus. Within the TE, KDM6B was found to bind to and decrease H3K27me3 at the promoters of *Cdx2* and *Gata3* leading to an increase in expression[40]. These genes are previously defined master-transcription factors necessary for TE development[41–43], and are repressed by PRC2 in the ICM[40]. This pattern of KDM6B expression was also seen in bovine preimplanted embryos, and knockdown of maternal *KDM6B* mRNA led to impaired embryonic development[44]. Taken together, these two studies point out the importance of KDM6B regulation in the earliest stages of cell lineage commitment, showing it is a necessary component for TE development and proper embryonic implantation.

Within embryonic stem cells (ESC), the WNT and Nodal/BMP/SMAD signaling pathways have been implicated in playing crucial roles in maintaining the balance between self-renewal and differentiation[45,46]. Experimental evidence suggests that KDM6B plays a role in both of these signaling pathways in determining ESC fate decisions. It was shown that in murine (m)ESCs Nodal signaling activates Smads2/3. These proteins can directly interact and recruit KDM6B to developmental genes and reverse PRC2 silencing. Interestingly, these genes are only dependent on this pathway in the presence of PRC2 indicating that KDM6B plays a specific role in balancing PRC2 in mESCs[47]. While this group showed that KDM6B interacts with Smads2/3 to initiate transcription, Teng Fei et al, showed that in mESCs the promoter of *Kdm6b* is a direct

target of BMP4 mediated SMAD1/5 and SMAD4 transcriptional repression. As differentiation begins, SMAD binding at the promoter decreases indicating that the repression of KDM6B is necessary for the self-renewal of mESCs[48]. In contrast, during osteogenic differentiation of human mesenchymal stem cells (hMSC), BMP4 signaling increased the expression of KDM6B by SMAD1/4 which in turn activated *Hox* and osteogenic genes[49,50]. To add to the complexity, differentiation of hMSCs in odontogenic cell lineages required KDM6B to bind to and activate BMP2, a master transcription factor of odontogenic genes[51]. Taken together, this all suggests that the regulation of KDM6B within the Nodal/BMP/SMAD pathway is cell context specific and it can either be repressed or serve as a transcriptional activator depending on the cell fate, and in some cases may act in a negative-feedback loop. This is best illustrated in developing spinal cord, where hyperactivation of BMP causes SMAD1/4 to recruit KDM6B to the *Noggin* promoter which then allows NOGGIN, the BMP inhibitor, to regulate the increased activity of BMP4[52]. While the regulation of KDM6B by SMAD proteins seems to be unique to KDM6B, both UTX and KDM6B were found to be regulators of the WNT signaling pathway during endoderm differentiation from human ESCs[53] suggesting that there may be functional redundancy between the H3K27me3 demethylases in other pathways.

While KDM6B functions in gonad development[19], MSC differentiation[49–51], mesodermal and cardiovascular differentiation[54], epidermis[55], and retinal bipolar cells[56] have all been described, the role of KDM6B in neural stem cells (NSC) and differentiation has been best characterized. In 2007, the same year KDM6B was identified as a histone demethylase, it was shown to play a vital role in retinoic-acid induced mouse forebrain development. Kristin Jepsen et all showed that KDM6B is repressed by SMRT in NSCs

and is a direct target of RA-receptor. When KDM6B expression is increased it in turn demethylates and activates the gene expression profile necessary for differentiation[57]. In agreement with KDM6B being needed for neuronal cell fate, it has been shown that KDM6B is more highly expressed in differentiating neural precursors and not self-renewing ESCs, and KDM6B expression is necessary for neural commitment. Interestingly, KDM6B role in neuronal cell fate seemed to be acting in both a demethylase-dependent and independent manner. Neural regulators such as *Nestin, Pax6,* and *Sox6* gene expression depends on KDM6B expression. All showed increased expression as neuronal differentiation occurred but *Nestin* showed decreased H3K27me3 levels at the promoter and *Pax6* and *Sox1* had increased H3K27me3 levels at their promoters[58]. Though this seems counterintuitive, it was shown that while the role of KDM6B in neuronal differentiation from ESCs is dependent on its demethylase activity, it is not dependent upon the presence or maintenance of H3K27me3[52]. As previously discussed, it is possible that KDM6B histone demethylase-independent role in NSC differentiation is a result of its influence on p53 subcellular localization in NSCs, and the demethylation of p53 and localization to the nucleus may contribute to gene expression changes that do not affect the H3K27me3 levels[38].

In addition to being essential in the neuronal development from ESCs, KDM6B has also been shown to play a critical role in adult NSCs. KDM6B was found to be required for neuron survival in the hippocampus after pilocarpine-induced seizures in adult mice[59]. It was found that in post-mitotic cerebellar granule neurons, KDM6B is required to induce a gene signature that is required for synapse maturation[60]. In addition to this, ablation of KDM6B in the adult subventricular zone results in impaired differentiation of adult NSCs[61].

While the all of these studies were conducted *in vitro,* constitutive knockout of KDM6B using a gene trap method in mice resulted in perinatal death due to respiratory failure, however lung development and cardiac rhythm was unaffected. Further analysis of the knockout mice indicated that loss of KDM6B disrupts the Bötzinger complex of the respiratory rhythm generator in the brain[62]. Surprisingly, the anticipated effects that KDM6B would have on preimplantation, embryogenesis, and neuronal development were not seen in this study, or another study using a neomycin-cassette to replace exons 14-21 of *Kdm6b* to create a germline knockout mouse[63], indicating that *in vitro* analysis of KDM6B function may not correlate with *in vivo* outcomes.

1.4 KDM6B Regulates Transcription in a Demethylase-Independent Manner

While KDM6B has been shown demethylate both histones and other proteins, and its role in development seems mainly reliant upon its demethylation activity, accumulating evidence also suggests that KDM6B also regulates transcription by demethylase-independent mechanisms. Using a double UTX-KDM6B knockout mouse model, it was seen that this genetic combination was embryonic lethal in females but the catalytically inactive UTY was capable of rescuing male mice. This suggests that these proteins may play a role in development beyond that of demethylation, or there are additional proteins acting in this pathway[64]. Evidence also suggests that KDM6B plays a role in DNA damage response. In ESCs inhibition of KDM6B by the small molecule inhibitor GSK-J4 led to an increase in γH2AX[65]. However, GSK-J4 has been shown to inhibit both UTX and KDM6B[28], indicating that the results seen in this study may not be directly due to inhibition of KDM6B. However, Kristine Williams et al, showed that upon irradiation, p53 recruits

KDM6B to its targeted promoters of genes involved in cell cycle response to stress and apoptosis. Furthermore, no detectable decrease in H3K27me3 was observed[66]. While p53 bound promoters have been shown to have decreases in H3K27me3[67], it was not observed in this study indicating a possible demethylase-independent role.

During cellular reprogramming of mouse embryonic fibroblasts to induced pluripotent stem cells, KDM6B has also been shown to interact with TRIM26, recruiting it to target protein PHF20 for ubiquitination and subsequent degradation and thus inhibiting cellular reprogramming. Both wild-type and catalytically inactive KDM6B are capable of bridging this interaction between TRIM26 and PHF20 indicating that it is not dependent upon its demethylation activity[68]. Another protein that KDM6B has been shown to interact with is the T-box factor, T-bet, to alter chromatin architecture. In differentiating T-helper 1 (Th1) cells, KDM6B was shown to be necessary for *Ifng*, *Ccl3,* and *Cxcr3* to be expressed, and catalytically-inactive KDM6B was capable of eliciting these transcriptional responses with the exception of *Ccl3*[69]. Further analysis showed that KDM6B physically interacts with SWI/SNF remodeling complex and allows it to interact with T-bet acting as a bridge[69]. The interaction between KDM6B and the SWI/SNF complex was not dependent on T-bet and occurred in unstimulated cells indicating KDM6B may play a role in remodeling chromatin architecture in other contexts[69]. In addition to remodeling chromatin structure to make promoters more accessible, KDM6B has also been shown to influence transcriptional elongation. In 12-O-tetradecanoylphorbol 13-acetate (TPA)-induced macrophage-like differentiation of HL-60 cells, chromatin-immunoprecipitation (ChIP) and gene expression data suggested that KDM6B acts in both demethylase-dependent and –independent ways[70]. Data suggests that KDM6B aids in the assembly of full-length

mRNAs and it does so by recruiting elongation factors SPT6 and SPT16 to its target genes and releases RNA Pol II[70]. Taken together, the data from these studies suggests that along with being a histone and protein demethylase, KDM6B is capable of interacting with proteins, aiding in protein localization, recruiting protein-protein interactions, bridging the interaction between chromatin remodeling complexes and transcription factors, and increasing transcriptional elongation.

1.5 KDM6B as a Regulator of Inflammatory Response

Many studies have identified KDM6B as an inflammatory and stress response gene to a variety of stimuli. One of the first groups to identify KDM6B as a H3K27-demethylase did so in the context of macrophages in response to bacterial exposure. Francesca De Santa et al showed that upon stimulation of macrophages with lipopolysaccharide (LPS), *Kdm6b* gene expression increases immediately after exposure, and the expression is induced by NF-κB binding to two consensus sites in the first intron[27]. This paper provided evidence of two promoters for KDM6B: one that is active in ESCs and one that is active in macrophages[27]. They saw that *HoxA* genes as well as *Bmp2* were targets of KDM6B and their expressions were demethylase-dependent. Additionally, this study provided evidence that upon inflammatory stimuli, newly transcribe KDM6B proteins associate with MLL- complexes[27]. Previously, it had been shown that UTX also associates with MLL- complexes[71], however, it should be noted that in this context only *Kdm6b,* and not *Utx,* increased in expression upon LPS stimulation[27]. Follow-up studies by the same group, however, had surprising results, whereas in the first study they found examples of KDM6B demethylating *Bmp2*, ChIP-SEQ showed no difference in H3K27me3 peaks before or after LPS-stimulation in macrophages. In fact,

KDM6B was found to be bound to genes that had the activating H3K4me3 marker and transcriptionally active RNA Pol II. 73% of bound KDM6B genes had increased RNA Pol II activity post-LPS stimulation. Additionally, they were able to show that when H3K27me3 was lost, it was due to the loss of nucleosomes and not demethylation[72]. Of note, fetal-liver derived macrophages from *Kdm6b*-KO mice showed no differentiation defects and very few gene expression changes, however, they did show in a subset of genes, loss of KDM6B results in reduced RNA Pol II recruitment[72]. While these studies provided direct evidence of NF-κB controlling *Kdm6b* expression, another study has shown that ablating KDM6B in THP-1 cells not only led to a 2-fold decrease in NF-κB signaling pathway proteins, but also in the ablation of NF-κB itself[73], indicating that the expression of these two proteins is tightly linked, and a possible regulatory feedback loop may exist.

A key component to innate immunity is the polarization of macrophages into M1 or M2 cells depending on the stimuli[74–76]. The polarization into M1 macrophages supports a pro-inflammatory response and typically involves IFNγ activation[77,78], whereas the polarization into M2 macrophages promotes anti-inflammatory responses and is activated by IL-4 and IL-13[76,79]. In a study to identify key components in macrophage response to IFNγ or IL-4, it was shown that *Kdm6b* expression increases after treatment of either of these stimuli indicating it has an important role in the polarization of macrophages[80]. While differentiation into macrophages did not seem to be affected by loss of KDM6B[72], polarization of M2 macrophages, but not M1, required *Kdm6b* in a demethylase-dependent manner. Takashi Satoh et al, found that in response to chitin or helminth infection, *Kdm6b*-KO M2 macrophages are made in equal numbers but fail to recruit eosinophils. While H3K27me3 levels did not correlate to differences in gene expression

between wild-type and *Kdm6b*-KO macrophages, polarization of M2 macrophages was reliant upon the expression of transcription factor *Irf4*, which could only be rescued by ectopic expression of wild-type KDM6B and not catalytically inactive KDM6B[63]. The reliance of KDM6B for M2 polarization was further explored in microglia. In microglia it was shown that suppression of KDM6B inhibited M2 polarization[81], similar to what was previously shown in macrophages[63]. In contrast to the previous study, however, they found that the inhibition of M2 polarization led to an increase in the M1 inflammatory responses and subsequent neuron death[81]. Possibly linking KDM6B to Parkinson's disease, KDM6B regulation of neuronal development, inflammation, and aging, they also found that in aged mice KDM6B expression in the midbrain is lower than that of young mice, and as a result there is an increased ratio of M1 to M2 polarized macrophages[81]. Taken together, this suggests that KDM6B plays a vital role in both the pro- and anti-inflammatory pathways, and loss of KDM6B prevents M2 macrophages from acting in an anti-inflammatory manor, while potentially promoting the pro-inflammatory effects of M1 macrophages. Given that polarization of M1 macrophages was unaffected by loss of KDM6B, but that it has been shown to be a direct target of M1 polarizing stimuli, it may suggest that in M1 macrophages, KDM6B may work to suppress the pro-inflammatory pathways post-stimulus.

Further characterizing the role of KDM6B in LPS activated microglia, another group showed that the increase in KDM6B expression is reliant on the expression of both STAT1 and STAT3, and in the absence of both of these proteins, KDM6B cannot activate the inflammatory gene expression signature[82]. This is interesting, because in glioblastoma stem cells, STAT3 inhibits KDM6B expression to promote self-renewal[83], but in the

presence of inflammatory stimuli in microglia, it is necessary for KDM6B activation, indicating once again the importance of cellular context on KDM6B regulation. In addition to being a target of primary stimuli such as LPS, INFγ, and IL-4, KDM6B was also shown to be upregulated by serum amyloid A (SAA)[84], which is a biproduct of inflammatory tissue in response to inflammatory stimuli[85,86]. This suggests that regardless of the pathway KDM6B is a key component to macrophage response signatures. Foam cell macrophages play an important role in atherosclerotic lesion formation and have been shown to exhibit an M2 polarization anti-inflammatory signature[87]. Interestingly, loss of KDM6B in foam cells led to a reduction in the pro-fibrotic gene signature[88] indicating that KDM6B may control other pathways in M2 macrophages beyond the anti-inflammatory gene signature.

KDM6B plays vital roles in immune response of cells beyond macrophages. As previously discussed, KDM6B plays a crucial role in the differentiation of naïve CD4+ T-cells into Th1 cells. This transition requires the expression of *Ifng,* and conversely this expression needs to be sequestered in order to Th2 cell differentiation[89]. The demethylase-independent interaction between KDM6B, T-BET, and the SWI/SNF complex was required in order to ensure chromatin accessibility of the *Ifng* locus and subsequent transcription[69]. This also points to the fact that KDM6B not only increases in expression in response to INFγ in macrophages, but is responsible for its expression in TH1 cells which are responsible for providing the IFNγ signal to activate macrophages. Interestingly, inhibition of KDM6B in a mouse experimental autoimmune encephalomyelitis (EAE) model, led to reduced severity of disease and increased the production of Treg cells and not the pro-inflammatory TH1 or TH17 cells, but this was

found to be regulated by its effect on dendritic cells (DC), and not on the T-cells[90]. Beyond affecting how T-cells differentiate or respond to environmental cues, KDM6B has also shown to be crucial for the thymic egression of CD4+ cells, and loss of KDM6B leads to an accumulation of CD4+ in the thymus and a reduction in splenic CD4+ cells, however, this function of KDM6B was shown to be redundant with UTX[91]. Given its role in immunity it comes as no surprise that KDM6B has been shown several times that to be induced after viral infections[92,93]. While the role of KDM6B in macrophages and the immune system has been studied extensively, it has also been shown to be upregulated during amino acid deprivation[94] and under hypoxic conditions[95] indicating that it is a key component to cellular stress responses beyond inflammation.

1.6 KDM6B as a Tumor Suppressor

Epigenetic modifiers are frequently mutated or dysregulated in malignancies, and therefore often studied as potential therapeutic targets. KDM6B is no exception, however, unlike many epigenetic modifiers, the effects of KDM6B in different malignancies have been widely variable. In many cancers, KDM6B has been identified as a tumor suppressor. In non-small cell lung cancer (NSCLC) cell growth correlated with KDM6B expression levels, with the lowest expression conferring to the fastest growth. It was shown that overexpressing KDM6B in NSCLC cells led to apoptosis. Further mechanistic studies showed that KDM6B interacts with FOXO1, an inducer of apoptosis. Overexpression of KDM6B leads to decreased phosphorylation of FOXO1 and relocation into the nucleus[96]. Overexpression of KDM6B in glioblastoma stem cells leads to decreased neurosphere formation which are associated with poor patient prognosis[97],

and as previously discussed it was shown that in glioblastoma cells *KDM6B* is inhibited by STAT3, which maintains the self-renewal of the glioblastoma stem cells[83]. Another group additionally showed that in glioblastoma stem cells KDM6B acts as a tumor suppressor via its ability to control p53 cellular localization, and increased KDM6B expression led to increased accumulation of p53 in the nucleus[98]. In pancreatic ductal adenocarcinoma (PDAC), there is frequently a loss of heterozygousity of *KDM6B*[99]. Analysis of expression of KDM6B in normal pancreatic ducts compared to both PDAC and the precursor lesions pancreatic intraepithelial neoplasms (PanIN) indicated that as disease progresses KDM6B expression decreases[100]. Further, knockdown of KDM6B in PDAC cells led to increased cell growth and when transplanted into xenographic mice showed reduced survival due to the decreased expression of the tumor suppressor CEBPα[100]. Analysis Vitamin D has been identified as a potential therapy[101,102] for several cancers, including colon. Fábio Pereira et al, showed that when colon cancer cells are treated with the active vitamin D metabolite 1α,25-dihydroxyvitamin D_3, KDM6B expression was increased, and furthermore, was necessary for the induction of vitamin D target genes which act to prevent epithelial-mesenchymal transition (EMT). Additionally, they saw that in patient colon cancer cells *Kdm6b* and vitamin D receptor (*Vdr*) gene expression had a strong correlation[103].

Possibly the most extensively studied mechanism of tumor suppression by KDM6B is its role in oncogenic induced senescence (OIS) via the regulation of *INK4A/ARF* locus. It has been shown that KDM6B is a direct regulator of OIS. KDM6B increases in expression following RAS or RAF oncogenic exposure in human fibroblasts which leads to reduction in EZH2 levels[104], as well as the increased expression of the OIS regulator

p16^{INK4A} [104,105]. This increase in p16^{INK4A} protein is dependent upon KDM6B demethylase activity, and further the increase of *KDM6B* expression is activated via the macrophage promoter of *KDM6B*[104,105]. In colorectal cancer, KDM6B expression leads to an increase in p15^{INK4B}, and in patient samples these two proteins expression levesl are highly correlated with low expression of either of these proteins being a poor prognostic factor in patients[106]. In addition to controlling the *INK4A/ARF* locus, KDM6B has also been shown to be critical in the formation of senescence-associated heterochromatin foci (SAHF) due to its interaction with and demethylation of retinoblastoma (pRB) protein at K810[68,107]. Taken together, these studies suggest that KDM6B can play a role as a tumor suppressor through multiple different mechanisms of action.

1.7 KDM6B as an Oncogene

Indicating the importance of cellular context in conjunction with KDM6B, there have also been numerous studies that indicate KDM6B plays a role as an oncogene. Perhaps most surprisingly, in human papillomavirus E7 (HPV-E7) oncoprotein induced cervical carcinomas, KDM6B is highly expressed and in turn increases p16^{INK4A} protein[108]. However, because HPV-E7 also simultaneously degrades pRB[109], this activation does not lead to OIS. HPV-E7 cervical cells are dependent upon KDM6B and have been termed “KDM6B addicted”. Further, they also show addiction to the downstream p16^{INK4A} [110], indicating that the very same pathway in which KDM6B acts as a tumor suppressor in many different cancers, can also make it a oncogene in the right cellular context. Epstein-Barr virus (EBV) is another oncogenic virus that is associated with Burkitt’s and Hodgkin’s lymphoma, was shown to upregulate the expression of KDM6B, and it is

hypothesized that KDM6B contributes to the pathogenesis of this malignancy as well[92]. Supporting this hypothesis, KDM6B also shows high expression in diffuse large B-cell lymphoma (DLBCL), and inhibition of KDM6B induced apoptosis and increased sensitivity of DLBCL cells to chemotherapy agents[111].

In breast cancer, KDM6B has been shown to act as an oncogene in several ways. It was shown that in anti-oestrogen (AE) sensitive breast cancer cells, KDM6B demethylates the enhancer of the anti-apoptotic *BCL2* gene, and loss of KDM6B subsequently leads to an increase in apoptosis[112]. While in colon cancer, KDM6B was shown to act as a tumor suppressor by preventing EMT after vitamin D treatment[103], in breast cancer cells, KDM6B has been shown to be necessary for breast carcinoma invasion[113]. KDM6B expression increased in more invasive breast cancers, and it was shown that KDM6B is required for TGF-β EMT[113]. It should be noted that overexpression of KDM6B is not always indicative of a good therapeutic target, as it was shown in pleural mesothelioma that inhibition of KDM6B induced a cytokine storm which would be detrimental to the normal tissue[114].

1.8 KDM6B in Hematopoietic Malignancies

While *UTX* and other epigenetic modifiers are frequently mutated in hematopoietic malignancies[115–118], mutations in KDM6B are rare in blood cancers. In fact, only one study in a rare CD4+ mature T-cell leukemia, Sézary syndrome, did find that 47.5% of patients harbored 17p13.1 deletions that included KDM6B, but only one was predicted to be deleterious, and an additional 16.7% of patients had mutations including one frameshift[119]. The role KDM6B plays on CD4+ T-cell development may explain the finding

that KDM6B is mutated or deleted in this cancer, but found to be overexpressed in T-cell acute lymphoblastic leukemia (T-ALL)[120], multiple myeloma (MM)[121], and myelodysplastic syndrome (MDS)[122] but not frequently mutated. In NOTCH1-driven T-ALL, it was shown that KDM6B may play an oncogenic role[120]. Interestingly, in both MM and MDS, reducing *KDM6B* expression resulted in changes in immune signaling[121,122], indicating that KDM6B may be playing a role in stress response in hematopoietic malignancies. MSCs lack immunogenicity[51], however, hematopoietic stem cells (HSCs) and their progenitors express immune receptors[123], so it stands to reason that KDM6B may be required for immune and stress response in these cells. While bone marrow transplants (BMT) of fetal liver cells of *Kdm6b*-KO did not show any deficits in the peripheral blood[63,120], other epigenetic modifiers have been shown to have differing roles in fetal versus adult hematopoiesis[124].

Our study aimed to elucidate the role KDM6B plays in normal adult hematopoiesis and its effect on proliferative and oncogenic stress in hematopoiesis. We found that contrary to what was seen in fetal livers, KDM6B is required for adult HSC self-renewal and the maintenance of the stem cell compartment, and it plays a vital role in quiescence and stress response to a variety of stimuli. Moreover, we show that KDM6B serves an oncogenic function in adult acute myeloid leukemia as genetic inhibition results in increased latency to AML and a reduced self-renewal of leukemia-initiating cells in an MLL-AF9 model. Taken together, our results suggest that *KDM6B* mutations are not common in hematopoietic cancers because this protein is essential for normal HSC functions.

Chapter 2: Kdm6b is Required for Self-Renewal of Normal and Leukemic Stem Cells Under Proliferative Stress

2.1 Introduction

KDM6B, also known as JMJD3, is one of two known epigenetic modifiers responsible for enzymatic removal of the repressive histone H3 lysine 27 trimethylation (H3K27me3) mark[18,19,22,25,26]. This modification is associated with transcriptional repression and gene silencing[6,126]. Removal of H3K27me3 by either KDM6B or KDM6A (UTX1) is required for lineage-specific gene expression and differentiation in embryonic stem cells[19,26,55,58]. In addition, KDM6B has been shown to play a role in stress response in macrophages[27,28,72], hippocampal neurons[59], and fibroblasts[104,105]. The role of KDM6B in the inflammatory response is not redundant with UTX1, and evidence suggests that KDM6B may have demethylase-independent functions in response to stress[72,121].

Genome sequencing of hematopoietic malignancies has identified recurrent somatic mutations in many epigenetic modifiers[115–117]. While mutations in KDM6A are found in blood cancers such as acute myeloid leukemia (AML), KDM6B mutations have not been identified[117,118]. In contrast, gene expression analysis has found that KDM6B is over-expressed in a range of blood disorders including myelodysplastic syndromes (MDS)[122], Hodgkin's lymphoma (HL)[92], multiple myeloma (MM)[121], and T-cell acute lymphoblastic leukemia (T-ALL)[120]. In NOTCH1-driven T-ALL, it was shown that while UTX1 acts as a tumor suppressor[120,127], KDM6B plays an oncogenic role[120]. These data

may suggest that KDM6B is necessary for hematopoiesis and aberrant expression is a contributing factor in blood cancers. Germline deletion in mice of *Kdm6b* led to perinatal lethality due to incomplete respiratory development, however transplantation of fetal liver cells did not show a defect in hematopoietic development[63,120]. To date, the role of KDM6B in hematopoietic stem cell (HSC) biology has not been studied in adult hematopoiesis. Given that *Kdm6b* is upregulated in numerous adult hematopoietic malignancies, and that other epigenetic modifiers have been shown to have differing roles in embryonic and adult hematopoiesis[124], we developed a conditional loss-of-function mouse model to study the role of *Kdm6b* in hematopoietic development and HSC fate decisions in adult mice. We show that loss of *Kdm6b* leads to a significant reduction in phenotypic and functional HSCs, which increases with age, and is required for self-renewal of leukemia-initiating cells in AML. Additionally, we show that loss of *Kdm6b* leads to the inability for HSCs to respond to proliferative stress signals, resulting in defective self-renewal and a differentiation cascade leading to the inability to maintain the HSC compartment.

2.2 Results

2.2.1 Loss of Kdm6b results in depletion of phenotypic hematopoietic stem cells

To study the role of Kdm6b in hematopoiesis, a conditional knockout mouse was generated by crossing the Vav-CRE driver[128] to delete floxed exons 14-20 of *Kdm6b*[129] in hematopoietic cells[128]. Complete floxed allele recombination was observed in phenotypically-defined hematopoietic stem cells (HSCs; Lineage- Sca-1$^+$ c-Kit$^+$ CD48$^-$ CD150$^+$ EPCR$^+$, **Supplementary Fig. 2.1.1A**). In thymocytes, where *Kdm6b* is highly

expressed, we observed complete ablation of Kdm6b protein, but no significant increase in global H3K27me3 levels **(Supplementary Fig. 2.1.1B,C)**. Mice were sacrificed at eight- and 80-weeks of age for analysis of mature and progenitor populations in blood, whole bone marrow (WBM), spleen and thymus. There was a slight reduction in WBM cellularity and spleen weight at eight-weeks of age **(Supplementary Fig. 2.1.1D,E)**. Both Vav-CRE:*Kdm6b*$^{fl/+}$ (*Kdm6b*-Het^{VAV}) and Vav-CRE:*Kdm6b*$^{fl/fl}$ (*Kdm6b*-KO^{VAV}) had a significant increase in B-cells and a reduction in myeloid cells compared to control mice (Vav-CRE:*Kdm6b*$^{+/+}$) in peripheral blood. However, no overt hematological disease was observed in mutant mice by 80-weeks of age **(Supplementary Fig. 2.1.1F,K)**.

HSCs and multipotent progenitors (MPPs; Lineage-, EPCR^{+}, c-Kit^{+}, Sca-1^{+}, CD48^{-} CD150^{-}) were analyzed in WBM **(Fig. 2.1A)**. *Kdm6b*-KO^{VAV} had a 26.77% and 46.61% reduction in HSC and MPP frequencies respectively, which when coupled with the reduction in WBM cellularity led to a significant reduction in absolute HSC and MPP numbers **(Fig. 2.1B,C)**. This depletion of HSCs and MPPs was even greater in aged mice **(Fig. 2.1D,E)**. At eight-weeks of age *Kdm6b*-Het^{VAV} mice had no difference in HSC or MPP frequency or count as compared to control^{VAV} mice **(Fig. 2.1B,C)**, however, at 80-weeks of age there was a significant reduction in both HSCs and MPPs, similar to that of complete knockout **(Fig. 2.1D,E)**. This suggests that *Kdm6b* is an important regulator in the aging hematopoietic compartment and older HSCs are more sensitive to dose-dependent losses of *Kdm6b.* We also analyzed WBM for oligopotent progenitors, spleen for erythroid progenitors, and thymus for thymic progenitors **(Supplementary Fig. 2.1.2A-O)**. There was a reduction in myeloid progenitors in old mice, most prominently granulocyte/macrophage progenitors (GMPs, **Supplementary Fig. 2.1.2C**). In

agreement with previous studies[91], there was an increase in CD4+ and CD8a+ cells in the thymus of *Kdm6b*-KO^{VAV} mice **(Supplementary Fig 2.1.2N)**.

2.2.2 Loss of Kdm6b results in depletion of functional long-term repopulating HSCs

To determine if the loss of phenotypic HSCs in *Kdm6b*-KO^{VAV} mice correlated to a functional loss of repopulating activity, 2.5 x 10^5 wild-type WBM cells were transplanted into lethally irradiated recipients along with limiting dilution doses of WBM from control^{VAV}, *Kdm6b*-Het^{VAV} and *Kdm6b*-KO^{VAV} mice. 16-weeks post-transplant, blood chimerism was assessed **(Fig. 2.2A, Supplementary Fig. 2.2.1A)** and mice were classified to have long-term multi-lineage reconstitution (LTMR) if all three blood lineages (B-cell, T-cell and myeloid) had >1% engraftment from donor-derived cells **(Fig 2.2B, Supplementary Fig. 2.2.1B,C)**. The proportion of LTMR mice at each dose was used to calculate long-term repopulating cell frequency[130]. While control^{VAV} and *Kdm6b*-Het^{VAV} mice had a comparable frequency of long-term repopulating cells (1:49,984 and 1:55,422 respectively), *Kdm6b*-KO^{VAV} WBM was estimated to have a two-fold reduction (1:108,101; p-value 0.054, **Fig. 2.2C**). In agreement with this observation, there was a significant reduction in donor-derived HSCs in *Kdm6b*-KO^{VAV} recipient mice 18-weeks post-transplant **(Fig. 2.2D)**.

To assess the effect of *Kdm6b* on self-renewal, 3.0 x 10^6 WBM from LTMR mice was transplanted into secondary recipients. *Kdm6b*-KO^{VAV} secondary recipients had no donor-cell engraftment beyond four-weeks post-transplant **(Fig. 2.2E)**. While overall engraftment was equivalent between control^{VAV} and *Kdm6b*-Het^{VAV} recipients, only 37.5% of *Kdm6b*-Het^{VAV} recipient mice were considered LTMR at the end of secondary

transplant as opposed to 83.3% of control^{VAV} recipients **(Fig. 2.2F-G)**. Post-secondary transplant, *Kdm6b*-Het^{VAV} HSCs were reduced in recipient bone marrow **(Fig. 2.2H)**, similar to *Kdm6b*-KO^{VAV} primary recipient mice, indicating that *Kdm6b* is necessary for HSC self-renewal in a dose-dependent manner. in vitro assay of 1.0 x 10^4 WBM cells recapitulated what was seen in vivo with *Kdm6b*-Het^{VAV} and *Kdm6b*-KO^{VAV} WBM having reduced colony-forming potential **(Fig. 2.2I)**.

In aged mice there was an even greater reduction in phenotypic HSCs and MPPs in both the *Kdm6b*-Het^{VAV} and *Kdm6b*-KO^{VAV} mice. Because the phenotypic reduction observed in eight-week old mice correlated with a functional reduction, 5.0x10^5 aged WBM from control^{VAV}, *Kdm6b*-Het^{VAV} and *Kdm6b*-KO^{VAV} mice was transplanted in a 1:1 ratio with wild-type WBM into lethally irradiated recipient mice. There was a significant reduction in engraftment of both the *Kdm6b*-Het^{VAV} and *Kdm6b*-KO^{VAV} compared to controls in a dose-dependent manner **(Supplementary Fig. 2.2.2A)**. Interestingly, *Kdm6b*-Het^{VAV} recipient mice had equivalent engraftment of myeloid cells 16-weeks post-transplant, but a significant reduction in lymphoid lineages, whereas *Kdm6b*-KO^{VAV} recipients had significant reductions in all three lineages **(Supplementary Fig. 2.2.2B)**. HSC analysis 18-week post-transplant showed a significant reduction in both *Kdm6b*-Het^{VAV} and *Kdm6b*-KO^{VAV} recipients **(Supplementary Fig. 2.2.2C)**.

2.2.3 Kdm6b is required for HSC self-renewal

To more specifically determine the function of *Kdm6b* in HSC self-renewal, 200 HSCs from control^{VAV}, *Kdm6b*-Het^{VAV} and *Kdm6b*-KO^{VAV} mice were transplanted with 2.5 x 10^5 wild-type WBM competitor cells into lethally irradiated recipients. While donor-

derived engraftment was comparable at four-weeks post-transplant, subsequent timepoints showed a significant decrease in blood chimerism from *Kdm6b*-KO^{VAV} HSCs **(Fig. 2.3A)**, although both *Kdm6b*-Het^{VAV} and *Kdm6b*-KO^{VAV} HSCs contributed to all three blood lineages **(Fig. 2.3B)**. 18-weeks post-transplant, HSCs from primary recipients were resorted and 200 HSCs were transplanted into secondary recipients. The significant reduction in donor-derived HSCs **(Fig. 2.3C)** in *Kdm6b*-KO^{VAV} primary recipient mice limited the number of secondary recipients for this genotype. Secondary transplant saw a reduction in donor-derived chimerism in both *Kdm6b*-Het^{VAV} and *Kdm6b*-KO^{VAV} recipient mice, with myeloid cells comprising the majority their output **(Fig. 2.3D)**. The majority of recipient mice of *Kdm6b*-Het^{VAV} and *Kdm6b*-KO^{VAV} HSCs did not have tri-lineage long-term engraftment **(Fig. 2.3E)**. This may indicate that the HSCs remaining post-primary transplant were no longer multipotent, and that *Kdm6b* is necessary for maintenance of lymphoid potential in HSCs. 18-weeks post-secondary transplant, there was a significant reduction in donor-derived HSCs in mutant HSC recipient mice **(Fig. 2.3F)**, indicating loss of *Kdm6b* results in compromised self-renewal.

2.2.4 Kdm6b is required for self-renewal of leukemia-initiating cells

To determine if *Kdm6b* also regulates self-renewal in malignant stem cells, c-Kit enriched WBM from control^{VAV}, *Kdm6b*-Het^{VAV} and *Kdm6b*-KO^{VAV} mice was transduced with the MLL-AF9 oncogene[131], and 1.0 x 10^5 cells were transplanted into recipient mice. Transduction efficiency and frequency of MLL-AF9+ GMPs (the leukemia-initiating cells in this model) were comparable between genotypes **(Supplementary Fig. 2.4.1A,B)**. Four-weeks post-transplant there was a significant reduction in GFP+ cells

in the blood in both *Kdm6b*-Het^{VAV} and *Kdm6b*-KO^{VAV} recipient mice **(Supplementary Fig. 2.4.1C)**. Notably, no engraftment defect was observed from *Kdm6b*-Het^{VAV} and *Kdm6b*-KO^{VAV} cells transduced with the control (MIG) retrovirus, suggesting that viral transduction is not contributing to the reduced GFP+ blood **(Supplementary Fig. 2.4.1C)**. The reduction in MLL-AF9-GFP+ blood correlated with a significant increase in survival of *Kdm6b*-Het^{VAV} and *Kdm6b*-KO^{VAV} transplanted mice compared to control^{VAV} recipients **(Fig. 2.4A)**. There was no difference in spleen weights of moribund mice **(Supplementary Fig. 2.4.1D)**, but there was a significant decrease in the number of leukemic GMPs in the bone marrow of *Kdm6b*-Het^{VAV} and *Kdm6b*-KO^{VAV} recipient mice **(Fig. 2.4B,C)**. Secondary transplant was performed with limiting doses of WBM from primary MLL-AF9 tumors to determine the frequency of leukemia-initiating cells. Recipient mice were scored as positive if they developed AML **(Fig. 2.4E)**, and that metric was used to estimate leukemia-initiating cell frequency. *Kdm6b*-Het^{VAV} and *Kdm6b*-KO^{VAV} tumors had a three-fold reduction in leukemia-initiating cell frequency compared to controls **(Fig. 2.4F)**, suggesting *Kdm6b* also regulates self-renewal of leukemia-initiating cells.

2.2.5 Interferon response and NF-κB signaling are increased in Kdm6b-deficient HSCs

To elucidate potential mechanisms underlying the phenotype of *Kdm6b*-KO^{VAV} HSCs, global transcriptomic analysis was performed. Comparison of gene expression profiles of control^{VAV} and *Kdm6b*-KO^{VAV} HSCs to identify genes that >2-fold increased or decreased expression (adjusted p-value <0.05) found 649 genes that met this criteria **(Tables 2.1 and 2.2)**. Surprisingly, 88.3% of these genes showed increased expression in *Kdm6b*-KO^{VAV} HSCs, with only 76 genes having decreased expression **(Fig. 2.5A)**,

which was not anticipated following depletion of a protein that removes a repressive epigenetic mark. Gene Set Enrichment Analysis (GSEA) was performed to identify dysregulated pathways[132,133]. GSEA identified NF-κB target genes as the gene set most significantly upregulated (p-value 0.0, FDR=0.155) in *Kdm6b*-KO^{VAV} HSCs, in addition to interferon response genes **(Fig. 2.5B)**. In macrophages, *Kdm6b* has been shown to become upregulated immediately upon inflammatory stress induced by lipopolysaccharide (LPS) and/or interferon gamma (IFNγ) treatment, and has been shown to be a direct target of NF-κB[28,72]. In HSCs, it appears that loss of *Kdm6b* results in expression of a stress-response signature in the native state.

As *Kdm6b* has been described as a H3K27me3 histone demethylase, ChIPmentation[134] for H3K27me3 was performed on control^{VAV} and *Kdm6b*-KO^{VAV} HSCs. H3K4me3 ChIPmentation was also performed because KDM6B has been shown to associate with transcriptionally-activated NF-κB target genes in MDS patients[122]. Principal component analysis (PCA) showed no difference in H3K4me3 between control^{VAV} and *Kdm6b*-KO^{VAV} HSCs, but a distinct separation in H3K27me3 profiles **(Supplementary Fig. 2.5.1A)**. H3K4me3 peaks were highly overlapping between genotypes with 99.98% of peaks within 5kB of a transcriptional start site conserved **(Supplementary Fig. 2.5.1B)**. H3K27me3 domains showed 67.90% conservation between control^{VAV} and *Kdm6b*-KO^{VAV} HSCs, with the majority of the differential peaks being unique to *Kdm6b*-KO^{VAV} HSCs **(Fig. 2.5C)**. While there was an increase in the number of called H3K27me3 peaks in *Kdm6b*-KO^{VAV} HSCs (as would be expected following depletion of an enzyme that removes H3K27me3), the overall H3K27me3 pattern was comparable between control^{VAV} and *Kdm6b*-KO^{VAV} HSCs **(Fig. 2.5D)**, and

H3K27me3 changes did not correlate with altered gene expression **(Fig. 2.5E,F, Table 2.3)**. Similarly, there was no difference in H3K4me3 patterns **(Supplementary Fig. 2.5.1C-E)**. Two of the top dysregulated genes in the NF-κB (*Fos*) and INFγ response (*Jun*) genesets showed no difference in chromatin profile, but a difference in gene expression **(Fig. 2.5G)**. Thus, while loss of *Kdm6b* generates unique H3K27me3 peaks, the gene expression differences in *Kdm6b*-KO^{VAV} HSCs are H3K27me3-independent, similar to what is seen in *Kdm6b*-KO macrophages[72].

2.2.6 Inflammatory stress forces differentiation of *Kdm6b*-deficient HSCs

To study the role of *Kdm6b* more specifically in adult HSC maintenance, *Kdm6b*$^{fl/fl}$ mice were crossed to the inducible Mx1-CRE driver[135]. Mx1-CRE becomes active in hematopoietic cells following administration of polyinosinic:polycytidylic (pIpC) acid, an immunostiumulant that mimics viral infection and elicits an IFNα response[136]. Mx1-CRE:*Kdm6b*$^{+/+}$ (Control^{MX1}), Mx1-CRE:*Kdm6b*$^{fl/+}$ (*Kdm6b*-Het^{MX1}), and Mx1-CRE:*Kdm6b*$^{fl/fl}$ (*Kdm6b*-KO^{MX1}) mice were treated with six-doses of pIpC and allowed to recover for six-weeks. 200 HSCs from control^{MX1}, *Kdm6b*-Het^{MX1} and *Kdm6b*-KO^{MX1} mice were transplanted with 2.5 x 10^5 wild-type WBM competitor cells into lethally irradiated recipients. *Kdm6b*-KO^{MX1} HSCs showed a significant reduction in engraftment at all timepoints **(Fig. 2.6A, Supplementary Fig. 2.6.1A)**, and a significant reduction in *Kdm6b*-KO^{MX1} HSCs in the bone marrow of recipient mice **(Fig. 2.6)**. At the time of transplant, individual HSCs were concurrently sorted to determine floxing efficiency from Mx1-CRE. Surprisingly, 56.9% of HSCs from *Kdm6b*-KO^{MX1} mice retained both floxed alleles (making them functionally wild-type), and only 22.3% of HSCs had deletion of both *Kdm6b* alleles **(Fig. 2.6C)**. While efficiency of floxed allele recombination in

Kdm6b-Het^{MX1} HSCs was higher, 30.5% of HSCs were still not recombined **(Fig. 2.6C)**. To determine if this CRE-deficiency was specific to the *Kdm6b* allele, we assessed floxing efficiency of *Utx1* using an Mx1-CRE:*Utx1*$^{fl/+}$ (*Utx1*-Het^{MX1}) mouse model[137]. Using the same pIpC regimen, only 9.1% of the HSCs from these mice were not recombined six-weeks post-treatment, indicating that the decreased floxing efficiency is likely linked to the biological role of *Kdm6b* in HSCs **(Supplementary Fig. 2.6.1C)**. Because Mx1-CRE is still activated upon bone marrow transplantation[138], donor-derived HSCs were purified from *Kdm6b*-Het^{MX1} recipients at 18-weeks post-transplant to determine if floxing efficiency was resolved. There was an increase in deletion efficiency post-primary transplant in these HSCs with only 10.8% retaining unrecombined alleles **(Fig. 2.6C)**. We were unable to recover any HSCs from *Kdm6b*-KO^{MX1} post-transplant to assess floxing efficiency.

Because *Kdm6b*-Het^{MX1} HSCs showed efficient floxing post-primary transplant, we assessed self-renewal in this model by transplanting 200 donor-derived HSCs from control^{MX1} and *Kdm6b*-Het^{MX1} into secondary recipients. While primary *Kdm6b*-Het^{MX1} recipients only showed a slight reduction in overall engraftment compared to control^{MX1} recipients **(Fig. 2.6A)**, secondary transplantation showed a significant decrease in *Kdm6b*-Het^{MX1} engraftment **(Fig. 2.6D)**. 16-weeks post-transplant, no *Kdm6b*-Het^{MX1} recipient mice had tri-lineage engraftment **(Supplementary Fig. 2.6.1B)**. 18-weeks post-secondary transplant, donor-derived HSCs were almost undetectable in *Kdm6*b-Het^{MX1} recipients **(Fig. 2.6E)**.

The presence of unrecombined HSCs in *Kdm6b*-KO^{MX1} WBM could be a result of two possibilities: (A) Mx1-CRE is not efficient in deleting the alleles, or (B) Mx-1-CRE is

efficient, but the recombined HSCs are rapidly outcompeted by the residual unrecombined HSCs in the inflammatory environment. To investigate these possibilities, 200 HSCs from untreated Mx1-CRE:*Kdm6b*$^{+/+}$ and Mx1-CRE:*Kdm6b*$^{fl/fl}$ mice were transplanted, allowed to engraft, and then treated with pIpC four-weeks post-transplant. Interestingly, even without prior pIpC treatment initial engraftment of *Kdm6b*-KO^{MX1} HSCs was still significantly reduced, which may be due to activation of Mx1-CRE upon transplantation into an inflammatory environment post-irradiation **(Supplementary Fig. 2.6.1D)**. Upon treatment with pIpC, there was a significant reduction in relative engraftment in the *Kdm6b*-KO^{MX1} recipients **(Fig. 2.6F)**. To determine efficiency of floxed allele recombination, granulocytes (Gr-1^{+}, Mac-1^{+}) were purified from WBM of the donor mice pre-transplant, and compared to donor-derived macrophages from the blood of *Kdm6b*-KO^{MX1} recipient mice at eight-weeks post-transplant. RT-PCR of genomic DNA indicated that the macrophages in the blood two-weeks post-pIpC were derived from efficiently recombined *Kdm6b*-KO^{MX1} HSCs as indicated by the significant increase in the ratio of deleted allele to the floxed allele **(Fig. 2.6G)**. Two-weeks post-pIpC, there was a significant reduction in donor-derived HSCs in the *Kdm6b*-KO^{MX1} recipients **(Fig. 2.6H)**, and functional assay of purified HSCs identified reduced colony-forming potential *Kdm6b*-KO^{MX1} HSCs **(Fig. 2.6I)**. Surprisingly, of the few colonies that were generated from *Kdm6b*-KO^{MX1} HSCs, ~90% did show complete recombination of both *Kdm6b* alleles **(Supplementary Fig. 2.6.1E)**. This indicates that pIpC-driven recombination of *Kdm6b* flox alleles using Mx1-CRE is efficient, but that either those HSCs differentiate quickly and do not remain in the HSC pool, or are rapidly outcompeted by the residual unrecombined HSCs in terms of self-renewal.

2.2.7 Kdm6b is necessary for HSC maintenance in response to proliferative stress

To investigate the role of Kdm6b in HSCs under stress conditions without the problem of variable floxed allele recombination by Mx1-CRE, control^{VAV} and *Kdm6b*-KO^{VAV} mice were treated with a short course (two doses) of pIpC and analyzed 24-hours after the second injection. While there was a significant increase in frequency of control^{VAV} HSCs (Lineage- c-Kit^{+} EPCR^{+} CD48^{-} CD150^{+}; Sca-1 is excluded because it is an IFN-responsive gene) post-pIpC treatment, *Kdm6b*-KO^{VAV} HSCs showed no change in abundance **(Figure 2.7A)**. This increase in control^{VAV} HSCs was coupled with a decrease in quiescence **(Figure 2.7B, Supplementary Figure 2.7.1A)**. While frequency of *Kdm6b*-KO^{VAV} HSCs was unchanged in response to pIpC, there was a significant increase in the total progenitor population (Lineage- c-Kit^{+} EPCR^{+}; **Figure 2.7C**), indicating that upon inflammatory stress, *Kdm6b*-KO^{VAV} HSCs differentiate to downstream progenitors, but fail to self-renew to sustain the HSC pool. *Kdm6b*-KO^{VAV} progenitors were also less proliferative than controls **(Figure 2.7D)**. There was no difference in apoptosis (cleaved PARP+) or DNA damage (γH2AX+) in HSCs or progenitors from control^{VAV} or *Kdm6b*-KO^{VAV} mice post-pIpC exposure **(Supplementary Figure 2.7.1B-E)** providing further evidence that the cause of depletion of *Kdm6b*-KO^{VAV} HSCs under inflammatory stress is commitment to terminal differentiation and not mechanisms (e.g. increased apoptosis) that would render the mutant HSCs less competitive.

The failure of *Kdm6b*-KO^{VAV} HSCs to exit quiescence after pIpC treatment led us to compare gene expression in *Kdm6b*-KO^{VAV} HSCs with a HSC quiescence geneset signature[139]. There was significant overlap between these genesets **(Figure 2.7E)**, with

all of the shared genes having increased expression in *Kdm6b*-KO^{VAV} HSCs. Furthermore, four of these overlapping genes were the top dysregulated NF-κB target genes **(Figure 2.7F)**. This may indicate that *Kdm6b*-KO^{VAV} HSCs have altered cell cycle kinetics in response to proliferative stress due the inability to silence genes associated with HSC quiescence.

To test the ability of *Kdm6b*-mutant HSCs to regenerate the hematopoietic system after proliferative stress, control^{VAV}, *Kdm6b*-Het^{VAV} and *Kdm6b*-KO^{VAV} mice were injected with 5-flurouracil (5-FU) which kills rapidly cycling hematopoietic cells and forces quiescent HSCs to proliferate. After a 10-day recovery, there was a slight decrease in white blood cell and neutrophil counts **(Supplementary Figure 2.7.1F,G)**, but no difference in red blood cell (RBC) or platelet (PLT) counts (**Supplementary Figure 2.7.1H,I)**, in *Kdm6b*-Het^{VAV} and *Kdm6b*-KO^{VAV} mice, indicating they are capable of initial hematopoietic recovery. However, upon serial 5-FU injection, both *Kdm6b*-Het^{VAV} and *Kdm6b*-KO^{VAV} mice had a significant decrease in survival compared to controlVAV mice **(Figure 2.7G)**. Interestingly, the loss of *Kdm6b* does not seem to be dose dependent under these conditions, unlike bone marrow transplantation but analogous to challenge with MLL-AF9 oncogenic stress **(Figure 2.4A)**. To examine HSC kinetics acutely after myeloablative stress, control^{VAV}, *Kdm6b*-Het^{VAV} and *Kdm6b*-KO^{VAV} mice were treated with one dose of 5-FU and assessed for HSC (Lineage- Sca-1^{+} EPCR^{+} CD150^{+} CD48^{-}; c-Kit is excluded from these analyses as it is downregulated upon 5-FU treatment) frequency and cell cycle. There was no discernable difference in HSC frequency between any of the groups **(Figure 2.7H)**, but an increase in the proportion of quiescent (G0) HSCs at both day two and day six post-5FU treatment in

Kdm6b-KO^{VAV} HSCs **(Figure 2.7I)**, as well as the total progenitor population (Lineage-Sca-1^{+} EPCR^{+}; **Supplementary Figure 2.7.1J,K**). HSC quiescence genes (*Fos, Dusp1, Zfp36,* and *Ier2*) that were over-expressed in *Kdm6b*-KO^{VAV} HSCs became further upregulated after treatment with pIpC (Figure 2.7j). Post-5-FU treatment, there was also a significant increase in these genes two-days post-treatment compared to control^{VAV} HSCs, however six-days post-5-FU treatment, the expression of these genes normalized **(Figure 2.7K)**. As a control, we showed *Gata2* (a gene identified in the HSC quiescence signature and an NF-κB target gene that is not dysregulated in *Kdm6b*-KOVAV HSCs) did not increase post-treatment with either pIpC (**Supplemental Figure 2.7.2A**) or 5-FU (**Supplemental Figure 2.7.2B**) in *Kdm6b*-KOVAV HSCs, indicating that *Kdm6b* regulates a specific subset of genes involved in this response. One HSC gene upregulated in *Kdm6b*-KO^{VAV} HSCs, *Fos,* associates with *Jun* to form the AP1 transcription factor complex, and loss of AP1 has been associated with differentiation block[140–142]. Additionally, chronic overexpression of *Fos* in HSCs was shown to decrease colony forming potential and increase dormancy of HSCs[143]. Like *Fos*, *Jun* is upregulated in *Kdm6b*-KO^{VAV} HSCs at baseline and increases further after pIpC **(Supplementary Figure 2.7.2C)** and 5-FU **(Supplemental Figure 2.7.2D)**. As loss of the AP1 complex inhibits differentiation, over-expression of this complex may promote differentiation of *Kdm6b*-KO^{VAV} HSCs over self-renewal after they have exited quiescence.

2.3 Summary

Unlike many epigenetic modifiers, including *KDM6A*, *KDM6B* is not frequently mutated in hematopoietic malignancies. Here, we show that loss of *Kdm6b*

compromises self-renewal of both normal and leukemic stem cells. In transplantation, *Kdm6b* is necessary for HSC self-renewal in a dose dependent manner. These results suggest that *KDM6B* mutations are not observed in hematopoietic malignancies as even corruption of one allele in a HSC would result in the eventual loss of that clone due to a competitive disadvantage against wild-type HSCs.

Our data suggests that the major roles of *Kdm6b* in HSCs are not directly related to histone demethylase activity, but rather demethylase-independent regulation of stress response gene expression programs. Upon proliferative stress, *Kdm6b*-deficient HSCs do not self-renew, but rather differentiate rapidly to more committed downstream progenitors **(Fig. 2.8)**. This could be in part due to the increased expression of the AP1 transcription factor complex subunits, *Jun* and *Fos*. Previous studies have shown that AP1 inhibition has been shown to increase cellular proliferation and inhibit differentiation[142], thus perhaps increased AP1 activity in *Kdm6b*-deficient HSCs leads to increased quiescence and a differentiation push when the mutant HSCs finally engage cell cycle similar to the phenotype that is seen when *Fos* is overexpressed in HSCs[143].

One of the hallmarks of aging HSCs is a skewing toward myeloid lineages[144] and a weakening of immune response[145]. We observed that in aged mice, loss of *Kdm6b* seems affect both heterozygous and homozygous knock-out mice in phenotypic HSC and MPPs equally. Further, in eight-week old transplanted WBM and HSCs, a difference between control^{VAV} and *Kdm6b*-Het^{VAV} engraftment and HSCs were not observed until secondary transplant, but in aged WBM transplantation the phenotype was observed in the primary transplant. The HSCs that were remaining in *Kdm6b*-Het^{VAV} recipients had a decreased lymphoid, but comparable myeloid contribution as

compared to control^{VAV} recipients. The ability to contribute to the myeloid lineage and less so to the lymphoid was also seen in secondary HSC transplants form eight-week old donors of both *Kdm6b*-Het^{VAV} and *Kdm6b*-KO^{VAV} recipients. Given the inflammatory signature of *Kdm6b*-KO^{VAV} HSCs as well as the myeloid skewing we observed, the phenotype associated with loss of *Kdm6b* is very similar to that of aged HSCs, suggesting *Kdm6b* plays an important role in the stem cell fate decisions of young HSCs.

Loss of *Kdm6b* in MLL-AF9-driven AML significantly increases survival and decreases self-renewal of leukemia-initiating cells, presenting KDM6B as a novel therapeutic target for hematopoietic malignancies. GSK-J4, a small molecule inhibitor of KDM6B and KDM6A, has been widely cited as a potential therapeutic agent for a variety of blood cancers[28,120]. GSK-J4 binds to the catalytic domain and inhibits demethylase activity of both KDM6B and KDM6A. Our data suggests that therapeutic agents targeting the demethylase activity of KDM6B would likely be ineffective, and that more specific effects could be achieved by development of small molecules targeting the domains which regulate its unique functions in HSCs. Additionally, therapeutic inhibition of KDM6B may be improved by combination with chemotherapies that induce HSC differentiation, as blocking KDM6B activity would lead to an inability of the leukemia-initiating cells to self-renew, leading to their eventual exhaustion by terminal differentiation.

2.4 Methods

2.4.1 Mice

All animal procedures were approved by the Institutional Animal Care and Use Committee and performed in strict adherence to Washington University School of Medicine institutional guidelines. All mice used in this study were the C57Bl/6 background. *Kdm6b*$^{fl/fl}$ mice[129] were kindly provided by Dr. Martin Matzuk (Baylor College of Medicine) and backcrossed to the C57Bl/6 background (The Jackson Laboratory strain # 000664) for over five generations. *Kdm6b*$^{fl/fl}$ mice were crossed to Mx1-CRE[135] or Vav-CRE[128] strains to generate hematopoietic conditional knockout mice. *Utx1*$^{fl/fl}$ mice[137] were kindly provided by Dr. Lukas Wartman (Washington University). Six doses (300 µg/mouse) of polyinosinic:polycytidylic acid (pIpC, Sigma #p1530) spaced in 48-hour intervals were administered via intraperitoneal (IP) injections into Mx1-CRE mice to induce recombination of floxed alleles. Genotyping primers are found listed in **Table 2.4**.

2.4.2 Bone Marrow Transplantation

C57Bl/6 CD45.1 (The Jackson Laboratory strain # 002014) mice were used as recipients for bone marrow transplantation. For competitive transplantation, recipient mice were given a split dose (~4-hours apart) of lethal irradiation totaling 10.5 Gy prior to transplantation via retro-orbital injection. For MLL-AF9 secondary transplants, recipient mice were given a single dose of 6.0 Gy sublethal irradiation. For limiting dilution transplants, either $2.0x10^4$, $5.0x10^4$, or $1.0x10^5$ whole bone marrow (WBM) from

CD45.2 donor mice was transplanted along with 2.5 x10^5 CD45.1 wild-type WBM cells into lethally irradiated recipients. Secondary WBM transplants of the limiting dilution recipients were performed by transplanting 3.0x10^6 WBM cells from individual primary recipients into secondary lethally irradiated mice.

For hematopoietic stem cell (HSC) transplantation, 200 donor HSCs (CD45.2^+, Lineage$^-$, c-Kit+, Sca1^+, CD48^-, and CD150^+) were purified by flow cytometry and transplanted along with 2.5 x10^5 CD45.1 wild-type WBM cells into lethally irradiated recipients. Secondary HSC transplants were established by re-purifying 200 donor-derived HSCs from primary recipients and transferring to secondary lethally irradiated recipient mice along with fresh wild-type WBM competitor.

For MLL-AF9 transplants, 1.0x10^5 c-Kit enriched WBM cells were transduced with MLL-AF9 retrovirus and transplanted into lethally irradiated recipient mice. For secondary transplantation, either 1x10^3 leukemic GMPs (CD45.2^+, GFP$^+$, Lineage$^-$, c-Kit$^+$, Sca1^-, CD16/32^+, CD34^+ cells), or 5x10^3, 1.5x10^4 or 5.0x10^4 WBM cells from individual tumors were transplanted into sublethally irradiated recipients.

Bone marrow chimeras were established by transplanting 2.5x10^5 donor WBM with 2.5x10^5 CD45.1 wild-type WBM cells into lethally irradiated recipients. The blood of transplanted recipient's was analyzed to assess donor-cell contribution every four-weeks by retro-orbital bleeding and flow cytometry.

2.4.3 Flow Cytometry

Flow cytometry panels used for phenotypic identification of hematopoietic cell populations used in this study are found in **Table 2.5**. Cell sorting and analysis was

performed at the Siteman Cancer Center flow cytometry core and the Washington University Department of Pathology and Immunology flow cytometry core.

All antibody staining was done at a cell density of $7.0x10^7$ in 100uL of complete Hanks Balanced Salt Solution (HBSS, Corning #21021CV) containing Pen/Strep (100Units/mL, Fisher Scientific #MT30002CI), HEPES (10μM, Life Technologies #15630080) and Serum Plus II (2%, Sigma #14009C). Samples were incubated on ice for 20 minutes with the appropriate antibodies **(Table 2.6)**.

WBM (tibias, femurs, and iliac crests), spleen and thymus were harvested and analyzed for analysis of stated cell populations in **Table 2.5**. Magnetic enrichment of WBM was used prior to HSC purification by flow cytometry and retroviral transduction. WBM was incubated on ice with mouse CD117-conjugated microbeads (Miltenyi Biotec #130-091-224) and the samples were enriched using the AutoMACS Pro Separator (Miltenyi Biotec #130-092-545). Following enrichment, the c-Kit+ fraction was stained with appropriate antibodies for flow cytometry. For transplant recipients, donor-cell versus wild-type competitor contribution to blood was distinguished using the different CD45 isoforms (CD45.2 vs. CD45.1 respectively). Lineage contribution was determined by assessing myeloid ($Gr\text{-}1^+$ and $Mac\text{-}1^+$), B-cell ($B220^+$) and T-cell ($CD3e^+$) populations.

For intracellular flow cytometry, samples were stained for surface markers overnight at 4°C. Samples were fixed and permeabilized using the Cytofix/Cytoperm Fixation/Permeabilization Kit (BD Biosciences #554714), then stained in the dark in a

total of 50μL with intracellular antibodies (PARP, γH2AX, KI67) for 20 minutes at room temperature.

2.4.4 Western Blotting

For Kdm6b western blots, total nuclear protein extract was isolated from $2.0x10^7$ thymocytes using Nuclear Extract Kit (Active Motif #40010). 50μg of sample was loaded into pre-casted 4-15% gradient SDS gels (Biorad #456-1084) and transferred to nitrocellulose membranes (Millipore #IPVH00010). Membranes were probed with Kdm6b antibody (Cell Signaling #3457), or Hdac2 (Cell Signaling #2540) and were detected using horseradish-peroxidase-conjugated secondary rabbit antibody (GE Healthcare #NA9340) and chemiluminescence HRP substrate (Millipore #WBKLS0100).

2.4.5 H3K27me3 quantification

Total histones from $1.0x10^7$ thymocytes were extracted using the EpiQuik Total Histone Extraction Kit (EpiGentek # OP-0006-100). H3K27me3 quantification from these extracts was determined using EpiQuik Global Tri-Methyl Histone H3K27 Quantification Kit (Colorimetric) (EpiGentek #P-3042-96). Input per sample was 50ng, and absorbance was read using the Epoch Microplate Spectrophotometer (BioTek).

2.4.6 LPS, pIpC, and 5-FU injections

Lipopolysaccharide (LPS) (Sigma Aldrich #L2880) was administered at a dose of 1ug/mouse via IP injections daily for 30 days. 5-fluorouracil (5-FU, Sigma Aldrich #F6627) was administered at a dose of 150mg/kg via IP injection. To assess initial recovery, mice were given a single 5-FU dose and allowed ten days for hematopoietic

regeneration. Following this dose, mice were given serial injections at seven-day intervals until morbidity or the end of experiment. For short-term stress response to pIpC, mice were given two 300ug doses of pIpC 48-hours apart via IP injection and analyzed 24-hours after the last injection.

2.4.7 Methocult Plating

Colony forming potential was assessed by plating $1.0x10^4$ WBM cells into a 6-well plate with 2mL of methocellulose-based medium (MethCultTM GF M3434, Stemcell Technologies #03434). Cells were given nine-days and then colonies were counted. Floxing efficiency was checked by sorting single HSCs into 96-well plates containing MethoCultTM GF M3434 and allowed two-weeks to grow. Individual colonies were collected and washed with Dulbecco's Phosphate Buffered Saline (Sigma #D8537), and genomic DNA was isolated using the KAPA Express Extract Kit (Sigma # KK7103).

2.4.8 Plasmids and Viral Transduction

pMSCV-IRES-GFP-MLL-AF9 (pMIG-MLL-AF9) retroviral plasmid was kindly provided by Dr. Jeff Magee (Washington University). For retroviral production, 293T (ATCC #CRL-3216) cells were co-transfected with retroviral packaging vector (pCL-Eco) and either empty vector control (pMIG-GFP) or pMIG-MLL-AF9 using lipofectamine 3000 (ThermoFisher Scientific #L3000008). Supernatents were collected 48-hours post-transfection and stored at -80°C until transduction.

For retroviral transduction, $1.0x10^6$ cells/500uL were plated in Stempro-34 medium (Gibco #10639011) supplemented with Pen-Strep (100 Units/mL), L-glutamine

(2 mM), murine stem cell factor (100 ng/mL), murine thrombopoietin (100ng/mL), murine Flt3L (50ng/mL), murine interleukin-3 (5 ng/mL), and polybrene (4 mg/mL; Sigma), and spin-fected in 48-well tissue culture plates (CytoOne #CC7682-7548) with retrovirus supernatant at 250g for two-hours on consecutive days.

2.4.9 Quantitative Real-Time PCR

Total RNA was isolated using the NucleoSpin RNA XS kit (Macherey-Nagel #740902.250) and converted to cDNA with the SuperScript VILO kit (Invitrogen #11754-050). Real-time PCR was performed on the StepOnePlus RealTime PCR System (Life Technologies), using a mix of standardized cDNA, Taqman Master Mix (Applied Biosystems #4304437), 18s rRNA probe (VIC-MGB; Applied Biosystems #74319413E), and a gene-specific probe (FAM-MGB; Applied Biosystems, see table below). Samples were normalized to 18s and fold-change was determined by the ΔΔCT method. Gene-specific probes are found in **Table 2.7**.

To assess efficiency of floxed allele recombination in Mx1-CRE:*Kdm6b*$^{fl/fl}$ transplant recipient mice post-pIpC treatment, macrophages (Mac-1^{+}, Gr-1^{+}) were sorted and gDNA was made using the PureLink Genomic DNA mini kit (Invitrogen #K1820-02). Real-time PCR was performed on the StepOnePlus RealTime PCR System (Life Technologies), using a standardized mix of gDNA, PowerSYBR Green PCR master mix (AppliedBiosystems #4367659), and the universal forward primer with either the WT/Floxed or deleted reverse primer. Samples were normalized to GAPDH and fold-change was determined by the ΔΔCT method.

2.4.10 RNA-SEQ data, quality control and analysis

HSCs were purified from three biological replicates (composed of pooled WBM from three male and three female mice) of either Control^{VAV} or *Kdm6b*-KO^{VAV} mice. Total RNA was isolated using the NucleoSpin RNA XS kit (Macherey-Nagel #740902.250). Library preparation, sequencing, and alignment was performed by the Genome Technology Access Center (Washington University). The SMARTer Ultra Low RNA kit (Clontech) was used to prepare the libraries from 3-5ng of total RNA. Sequencing was performed with an Illumina HiSeq-3000. RNA-seq reads were aligned to the Ensembl release 76 top-level assembly with STAR version 2.0.4b[146]. Gene counts were derived from the number of uniquely aligned unambiguous reads by Subread:featureCount version 1.4.5[147,148]. Transcript counts were produced by Sailfish version 0.6.3[149]. Sequencing performance was assessed for total number of aligned reads, total number of uniquely aligned reads, genes and transcripts detected, ribosomal fraction known junction saturation and read distribution over known gene models with RSeQC version 2.3[150,151].

Aligned reads were imported into Partek® Genomics Suite® software, verision 6.6 Copyright ©; 2016 (Parek Inc., St. Louis, USA) for statistical analysis. Quantification and normalization of gene RPKM was performed with an expectation maximization algorithm (EM) using the mouse mm10 genome. Principal component analysis (PCA) was used to check for sample outliers. Differential expression analysis using ANOVA was performed assigning each gene a p-value, and a differentially expressed gene list was generated using the conditions $p<0.05$ and a fold-change of >2.0 in *Kdm6b*-KO^{VAV} HSCs as compared to control^{VAV} **(Table 2.1 and 2.2)**. Gene set enrichment analysis

(GSEA)[132,133] was performed using expression data to identify genesets that were dysregulated in *Kdm6b*-KO^{VAV} HSCs. Primary RNA-SEQ data is available under GEO accession number GSE110378.

2.4.11 ChIPmentation

ChIPmentation was performed as previously described[134]. Briefly, 1.0x10^4 HSCs were sorted into PBS+10% FBS, and then crosslinked at room temperature for 8-minutes using 1% paraformaldehyde (VWR #J531). Chromatin was sheared using a Covaris E220 Focused-ultrasonicator until the DNA fragments were between 200 – 700 base pairs. Chromatin samples were incubated overnight at 4°C with either the H3K27me3 antibody (Diagenode #pAb-069-050) or the H3K4me3 antibody (Diagenode #pAb-003-050). Following overnight incubation, protein G dynabeads (Life Technologies #130-099-508) were added for 2-hours at 4°C. The beads were washed, and tagmented for 10-minutes at 37°C using the Nextera DNA Library Preperation Kit (Illumina #FC-121-1030). After additional washes, an overnight decrosslinking was performed and immunoprecipiated DNA was isolated using Ampure XP beads (Beckman Coulter #NC9959336). 2xKapa HiFi HotStart Ready Mix (Kapa #KB KK2601), along with Nextera custom primers, was used for library amplification of the ChIP DNA (12 cycles of PCR as determined by qPCR). Libraries were again purified with Ampure XP beads and run on an Illumina Hiseq 3000 (PE2X150).

Sequences were aligned to mm10 using Bowtie2[152]. Peak calling of H3K27me3 and H3K4me3 was performed with hiddenDomains[153], the R package ChIPQC[154] was used for quality control including PCA plots. HOMER plots for H3K27me3 and

H3K4me3 were made using deepTools[155]. BEDOPS[156] was used to determine overlapping and unique H3K27me3 and H3K4me3 regions between *Kdm6b*-KO^{VAV} HSCs and control^{VAV} HSCs. Primary ChIPmentation data is available under GEO accession number GSE110378.

2.4.12 Statistics

GraphPad Prism Version 6 (GraphPad Software Inc.) was used for statistics and graphing of data. Student t-test, one-way, and two-way ANOVA's were used for statistical comparisons where appropriate. Survival curves were analyzed using a Mantel-Cox logrank test. All graphs represent mean ± S.E.M.

2.5 Figures

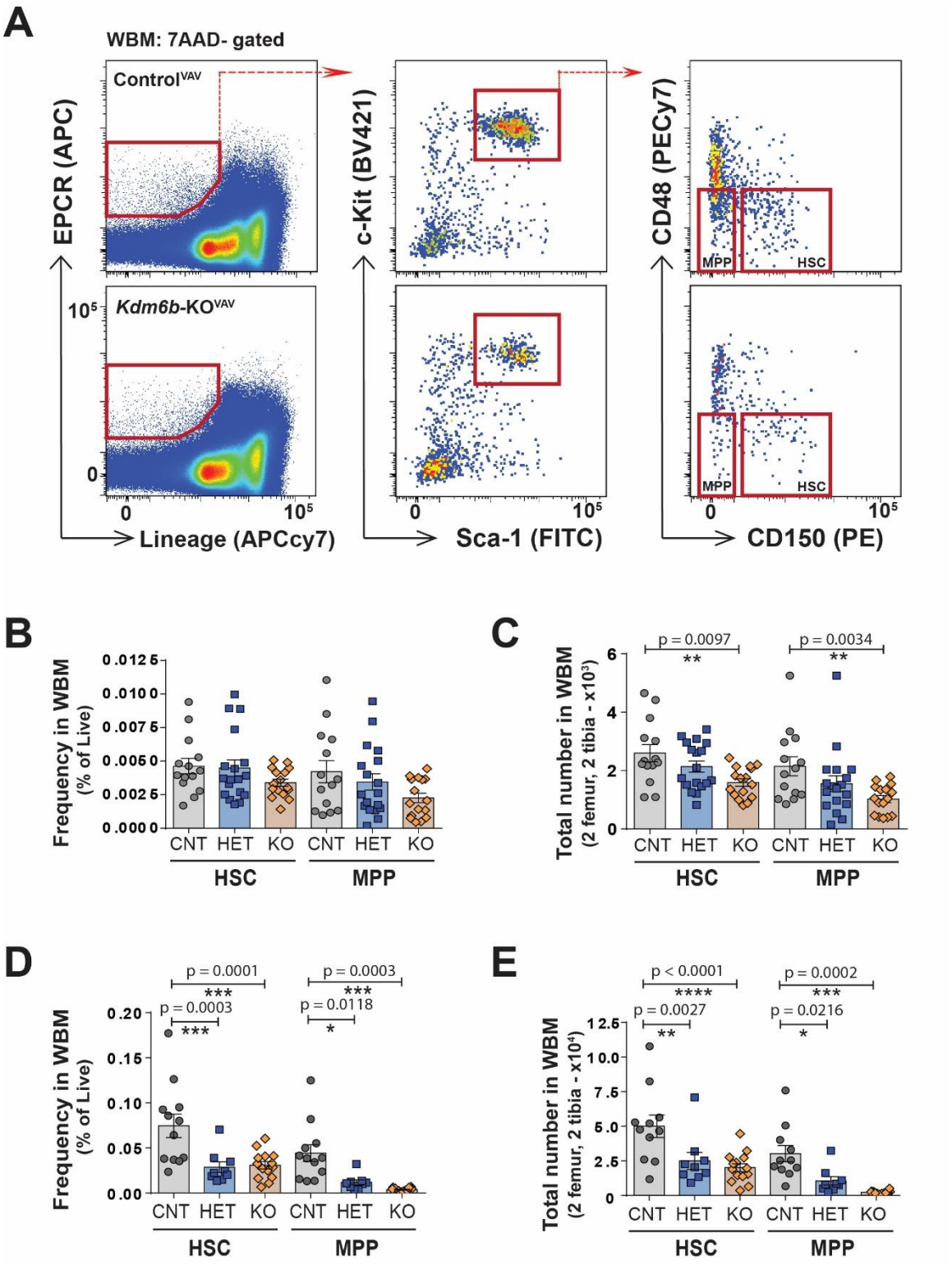
A
WBM: 7AAD- gated
Control^VAV
Kdm6b-KO^VAV
EPCR (APC)
c-Kit (BV421)
CD48 (PECy7)
Lineage (APCcy7)
Sca-1 (FITC)
CD150 (PE)
MPP
HSC
B
Frequency in WBM (% of Live)
C
Total number in WBM (2 femur, 2 tibia - x10³)
p = 0.0097
p = 0.0034
D
Frequency in WBM (% of Live)
p = 0.0001
p = 0.0003
p = 0.0003
p = 0.0118
E
Total number in WBM (2 femur, 2 tibia - x10⁴)
p < 0.0001
p = 0.0027
p = 0.0002
p = 0.0216
CNT HET KO CNT HET KO
HSC
MPP

Figure 2.1: Loss of Kdm6b results in depletion of phenotypic hematopoietic stem cells.

(A) Flow cytometry gating scheme to identify hematopoietic stem cells (HSCs) and multipotent progenitors (MPPs) in whole bone marrow (WBM) of eight-week old Control^{VAV} (top) or *Kdm6b*-KO^{VAV} mice (bottom). **(B)** Frequency of HSCs and MPPs in WBM of eight-week old Control^{VAV} (CNT, *n*=14), *Kdm6b*-Het^{VAV} (HET, *n*=18), and *Kdm6b*-KO^{VAV} (KO, *n*=16) mice (C) Absolute number of HSCs and MPPs in WBM of eight-week old Control^{VAV} (CNT, *n*=14), *Kdm6b*-Het^{VAV} (HET, *n*=18), and *Kdm6b*-KO^{VAV} (KO, *n*=16) mice. (D) Frequency of HSCs and MPPs in WBM of 80-week old Control^{VAV} (CNT, *n*=12), *Kdm6b*-Het^{VAV} (HET, *n*=9), and *Kdm6b*-KO^{VAV} (KO, *n*=14) mice. (E) Absolute number of HSCs and MPPs in WBM of 80-week old Control^{VAV} (CNT, *n*=12), *Kdm6b*-Het^{VAV} (HET, *n*=9), and *Kdm6b*-KO^{VAV} (KO, *n*=14) mice. Mean ± S.E.M. values are shown. *p<0.05, **p<0.01, ***p<0.001, ****p<0.0001.

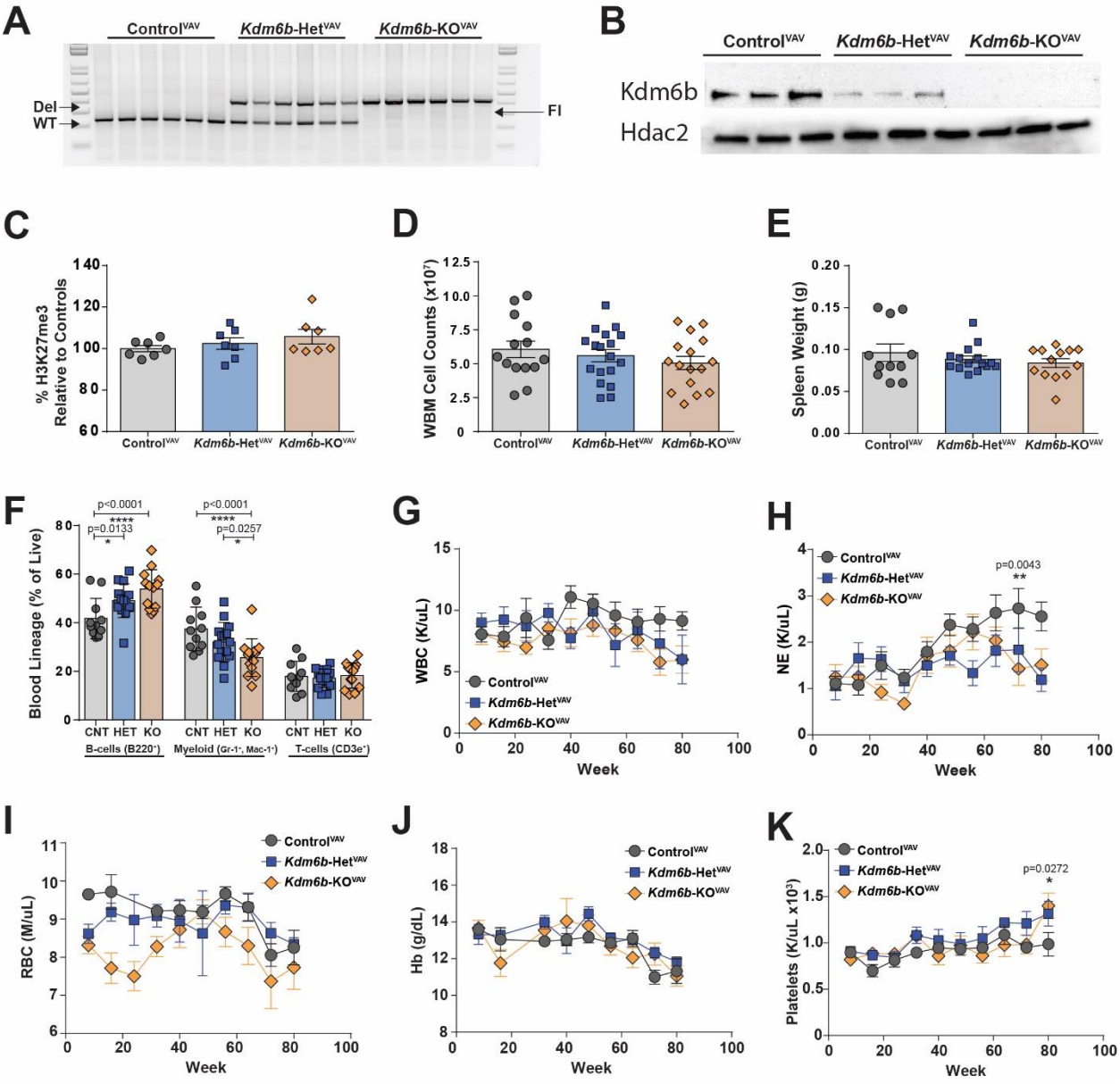
A
Control^VAV
Kdm6b-Het^VAV
Kdm6b-KO^VAV
Del
WT
Fl
B
Kdm6b
Hdac2
C
% H3K27me3 Relative to Controls
D
WBM Cell Counts (x10^7)
E
Spleen Weight (g)
F
Blood Lineage (% of Live)
p<0.0001
p=0.0133
p=0.0257
CNT HET KO
B-cells (B220+)
Myeloid (Gr-1+, Mac-1+)
T-cells (CD3e+)
G
WBC (K/uL)
Week
H
NE (K/uL)
p=0.0043
I
RBC (M/uL)
J
Hb (g/dL)
K
Platelets (K/uL x10^3)
p=0.0272

Supplementary Figure 2.1.1: Loss of Kdm6b does not generate hematopoietic malignancies.

(A) PCR showing complete recombination of *Kdm6b* floxed alleles in single HSCs from Control^{VAV}, Kdm6b-Het^{VAV}, and Kdm6b-KO^{VAV} mice. **(B)** Kdm6b protein expression by western blot in thymocytes from Control^{VAV}, *Kdm6b*-Het^{VAV}, and *Kdm6b*-KO^{VAV} mice. **(C)** Colorimetric assay quantifying H3K27me3 levels in thymocytes from Control^{VAV}, *Kdm6b*-Het^{VAV}, and *Kdm6b*-KO^{VAV} mice (*n*=7). **(D)** WBM cellularity of Control^{VAV} (*n*=14), *Kdm6b*-Het (*n*=18), and *Kdm6b*-KO^{VAV} mice (*n*=16) at eight-weeks of age. (E) Spleen weights of Control^{VAV} (*n*=11), *Kdm6b*-Het (*n*=15), and *Kdm6b*-KO^{VAV} mice (*n*=13) at eight-weeks of age. (F) Tri-lineage analysis of blood from Control^{VAV} (*n*=11), *Kdm6b*-Het (*n*=15), and *Kdm6b*-KO^{VAV} mice (*n*=13) at eight-weeks of age. Blood counts of (G) white blood cells (WBC), (H) neutrophils (NE), (I) red blood cells (RBC), (J) hemoglobin (Hb), and (K) platelets (PLT) from Control^{VAV} (*n*=13), *Kdm6b*-Het (*n*=9), and *Kdm6b*-KO^{VAV} (*n*=14) mice aged to 80-weeks. Mean ± S.E.M. values are shown. *p<0.05, **p<0.01, ****p<0.0001.

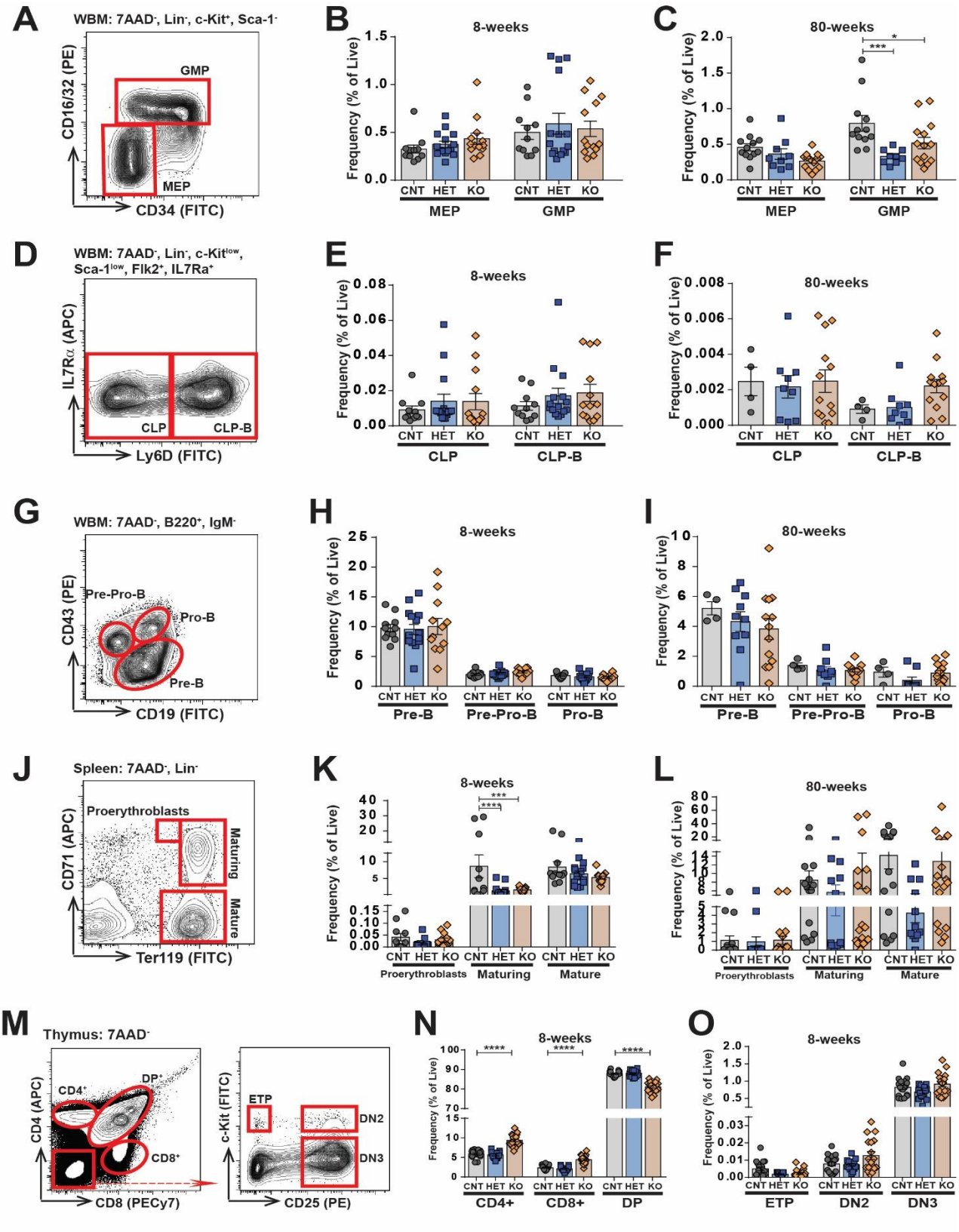
A
WBM: 7AAD-, Lin-, c-Kit+, Sca-1-
CD16/32 (PE)
GMP
MEP
CD34 (FITC)
B
8-weeks
Frequency (% of Live)
CNT HET KO
MEP
GMP
C
80-weeks
*
***
D
WBM: 7AAD-, Lin-, c-Kitlow, Sca-1low, Flk2+, IL7Ra+
IL7Rα (APC)
CLP
CLP-B
Ly6D (FITC)
E
F
G
WBM: 7AAD-, B220+, IgM-
CD43 (PE)
Pre-Pro-B
Pro-B
Pre-B
CD19 (FITC)
H
I
J
Spleen: 7AAD-, Lin-
Proerythroblasts
Maturing
Mature
CD71 (APC)
Ter119 (FITC)
K
L
M
Thymus: 7AAD-
CD4+
DP+
CD8+
CD4 (APC)
CD8 (PECy7)
ETP
DN2
DN3
c-Kit (FITC)
CD25 (PE)
N
****
CD4+
CD8+
DP
O
ETP
DN2
DN3

Supplementary Figure 2.1.2: Progenitor analysis in young and aged Kdm6b-deficient mice.

(A) Flow cytometry gating scheme for myeloid progenitors from WBM. Frequency of myeloid progenitors in eight-week **(B)** and 80-week **(C)** Control^{VAV}, *Kdm6b*-Het^{VAV}, and *Kdm6b*-KO^{VAV} mice (B, *n*=11, 15, 13; C, *n*=12, 9, 14 respectively). **(D)** Flow cytometry gating scheme for lymphoid progenitors from WBM. Frequency of lymphoid progenitors in eight-week **(E)** and 80-week **(F)** Control^{VAV}, *Kdm6b*-Het^{VAV}, and *Kdm6b*-KO^{VAV} mice (E, *n*=11, 15, 13; F, *n*=4, 9, 14 respectively). **(G)** Flow cytometry gating scheme for B-cell progenitors from WBM. Frequency of B-cell progenitors eight-week **(H)** and 80-week **(I)** Control^{VAV}, *Kdm6b*-Het^{VAV}, and *Kdm6b*-KO^{VAV} mice (H, *n*=11, 15, 13; I, Control^{VAV}, *Kdm6b*-Het^{VAV}, and *Kdm6b*-KO^{VAV} mice.=4, 9, 14 respectively). **(J)** Flow cytometry gating scheme for erythrocyte progenitors from spleen. Frequency of spleen erythrocyte progenitors eight-week **(K)** and 80-week **(L)** Control^{VAV}, *Kdm6b*-Het^{VAV}, and *Kdm6b*-KO^{VAV} mice (H, *n*=11, 15, 13; I, *n*=12, 9, 14 respectively). **(M)** Flow cytometry gating scheme for mature thymocytes and thymic progenitor cells. **(N)** Frequency of mature thymocytes in eight-week old Control^{VAV}, *Kdm6b*-Het^{VAV}, and *Kdm6b*-KO^{VAV} mice (*n*=18, 15, 18 respectively). **(O)** Frequency of thymic progenitors in eight-week old Control^{VAV}, *Kdm6b*-Het^{VAV}, and *Kdm6b*-KO^{VAV} mice (*n*=18, 15, 18 respectively). Mean ± S.E.M. values are shown. *p<0.05, ***p<0.001, ****p<0.0001.

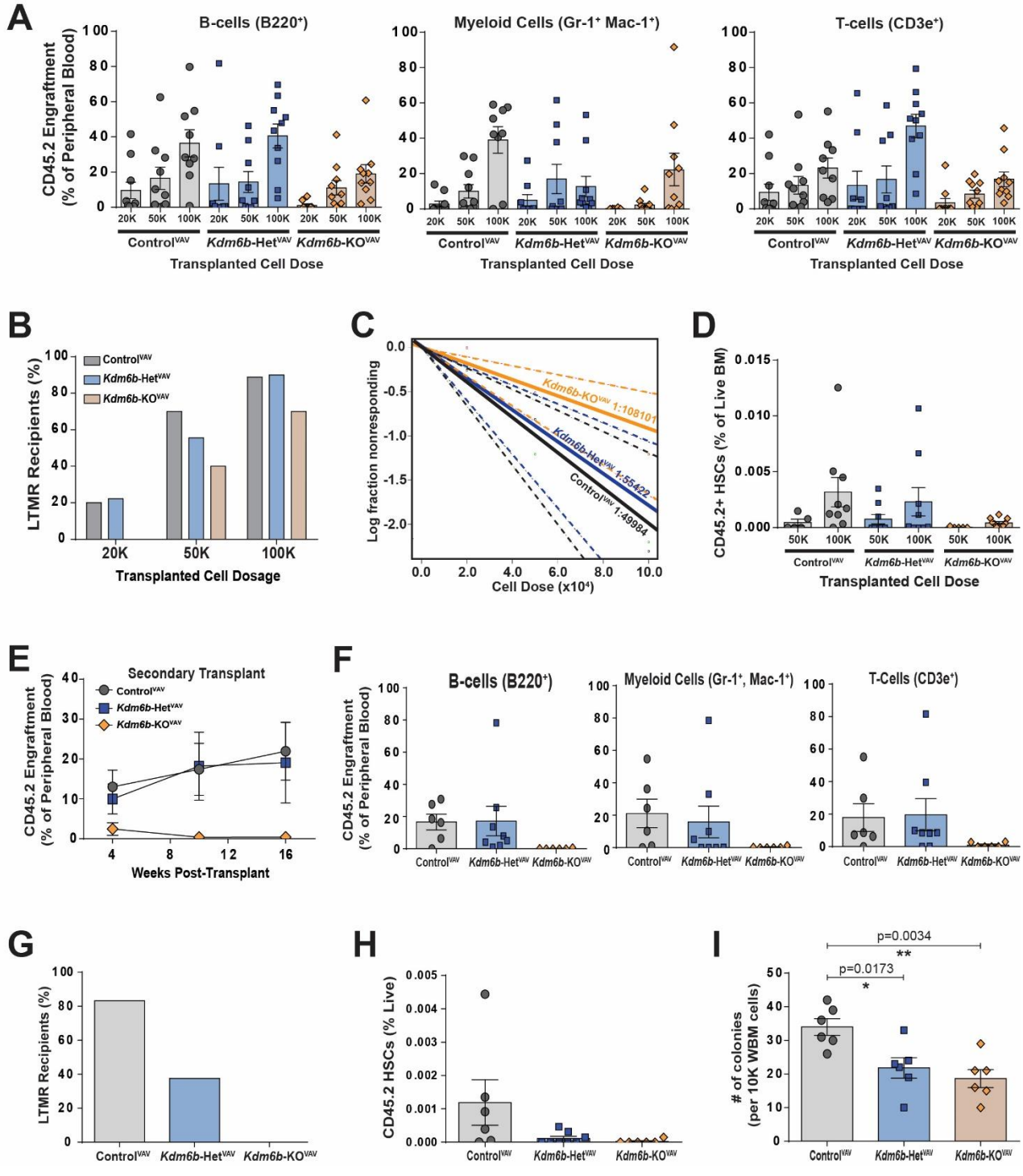
A
B-cells (B220+)
Myeloid Cells (Gr-1+ Mac-1+)
T-cells (CD3e+)
CD45.2 Engraftment (% of Peripheral Blood)
Transplanted Cell Dose
ControlVAV
Kdm6b-HetVAV
Kdm6b-KOVAV
B
LTMR Recipients (%)
Transplanted Cell Dosage
C
Log fraction nonresponding
Cell Dose (x10⁴)
Kdm6b-KOVAV 1:108101
Kdm6b-HetVAV 1:55422
ControlVAV 1:49964
D
CD45.2+ HSCs (% of Live BM)
E
Secondary Transplant
Weeks Post-Transplant
F
B-cells (B220+)
Myeloid Cells (Gr-1+, Mac-1+)
T-Cells (CD3e+)
G
LTMR Recipients (%)
H
CD45.2 HSCs (% Live)
I
# of colonies (per 10K WBM cells)
p=0.0034
**
p=0.0173
*

Figure 2.2: Loss of Kdm6b results in depletion of functional long-term repopulating HSCs.

(A) Donor-derived chimerism in B-cell, Myeloid and T-cell blood populations16-weeks post-transplant in mice transplanted with 20K, 50K, and 100K WBM cells from Control^{VAV}, *Kdm6b*-Het^{VAV}, and *Kdm6b*-KO^{VAV} (*n*=9-10) mice. **(B)** Proportion of long-term multi-lineage reconstituted (LTMR) recipient mice at each cell dose 16-weeks post-transplant. **(C)** Frequency of long-term repopulating cells using a maximum likelihood estimate with extreme limiting dilution analysis (ELDA) software. **(D)** Frequency of donor-derived (CD45.2+) HSCs in WBM of recipient mice 18-weeks post-transplant. **(E)** Peripheral blood engraftment in secondary transplants of 3.0x10^6 WBM from LTMR primary recipient mice. **(F)** Donor-derived chimerism in B-cell, Myeloid and T-cell blood populations 16-weeks post-transplant in secondary recipient mice. **(G)** Proportion of LTMR secondary recipient mice transplanted with Control^{VAV} (*n*=6), *Kdm6b*-Het^{VAV} (*n*=8), and *Kdm6b*-KO^{VAV} (*n*=6) primary WBM. **(H)** Frequency of donor-derived HSCs in WBM of secondary recipient mice 18-weeks post-transplant. **(I)** Number of colonies formed from 1x10^4 WBM cells (*n*=6 per genotype). Mean ± S.E.M. values are shown. **p*<0.05, ***p*<0.01.

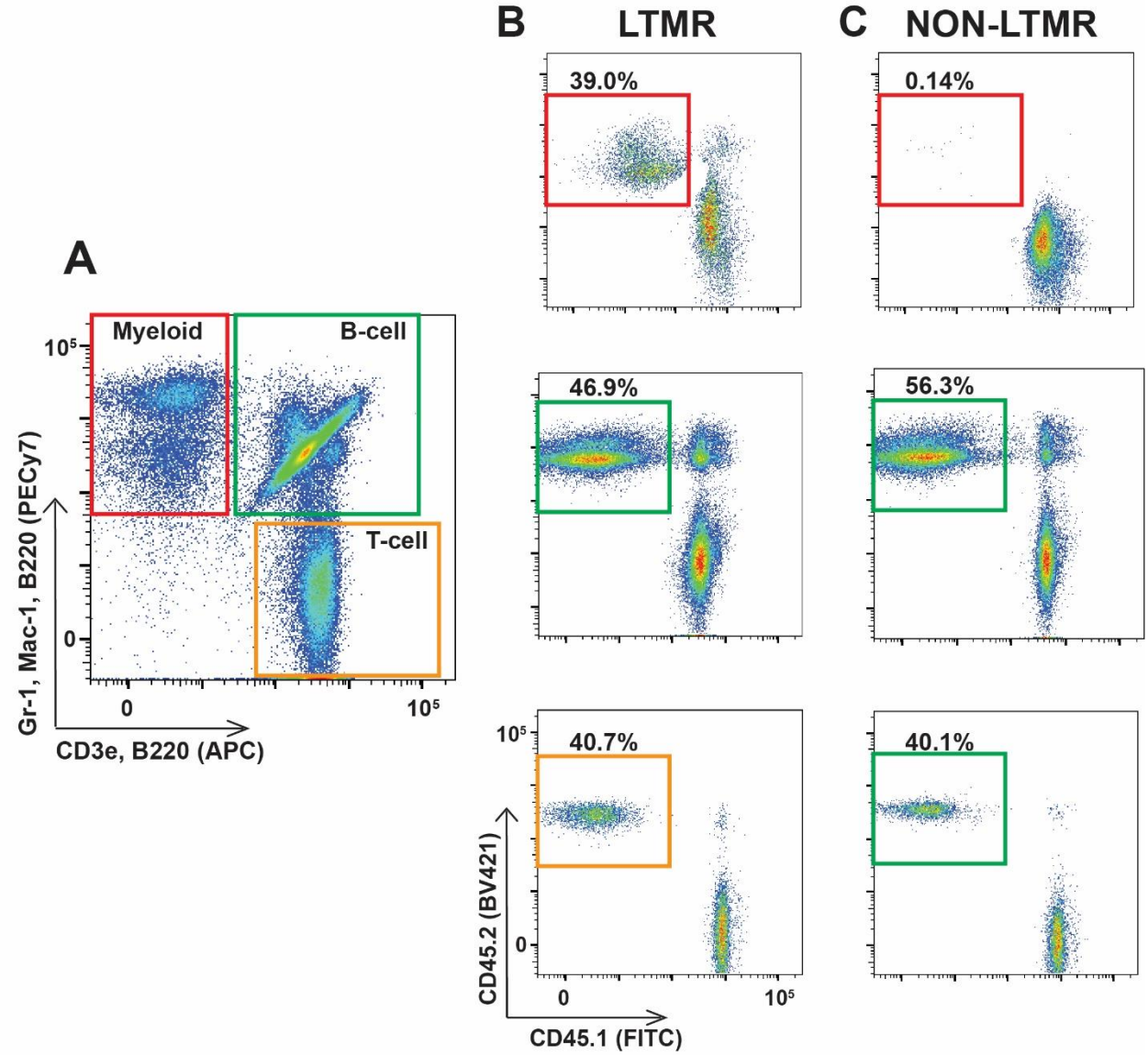

Supplementary Figure 2.2.1: Blood analysis to establish long-term multilineage reconstitution (LTMR).

(A) Flow cytometry gating scheme for analysis of blood trilineages (Myeloid: Mac-1$^+$, Gr-1$^+$, B-cells: B220$^+$, and T-cells: CD3e$^+$). **(B)** Representative flow cytometry plots of donor derived engraftment of all three lineages from a recipient mouse scored as LTMR. **(C)** Representative flow cytometry plots of donor derived engraftment of all three lineages from a recipient mouse scored as Non-LTMR.

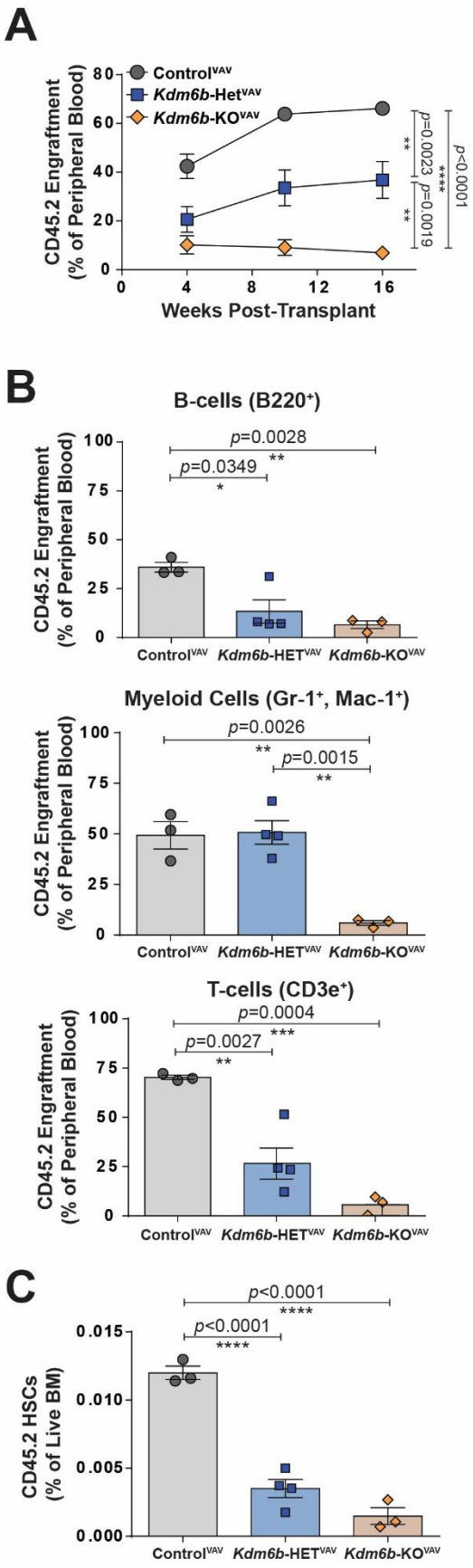
A
Control^VAV
Kdm6b-Het^VAV
Kdm6b-KO^VAV
CD45.2 Engraftment (% of Peripheral Blood)
Weeks Post-Transplant
p=0.0023
p=0.0019
p<0.0001
B
B-cells (B220+)
p=0.0028
p=0.0349
Myeloid Cells (Gr-1+, Mac-1+)
p=0.0026
p=0.0015
T-cells (CD3e+)
p=0.0004
p=0.0027
C
CD45.2 HSCs (% of Live BM)
p<0.0001
p<0.0001

Supplementary Figure 2.2.2: WBM from aged mice shows depletion of functional repopulating HSCs.

(A) Peripheral blood engraftment of primary recipients from transplantation of $5.0x10^5$ WBM from aged mice from Control^{VAV} (*n*=3), *Kdm6b*-Het^{VAV} (*n*=4), and *Kdm6b*-KO^{VAV} (*n*=3) mice. **(B)** Donor chimerism in B-cell, Myeloid and T-cell blood populations at 16-weeks post-transplant in recipient mice. **(C)** Frequency of donor-derived HSCs in WBM of recipient mice 18-weeks post-transplant. Mean ± S.E.M. values are shown. **p*<0.05, ***p*<0.01, ****p*<0.001, *****p*<0.0001.

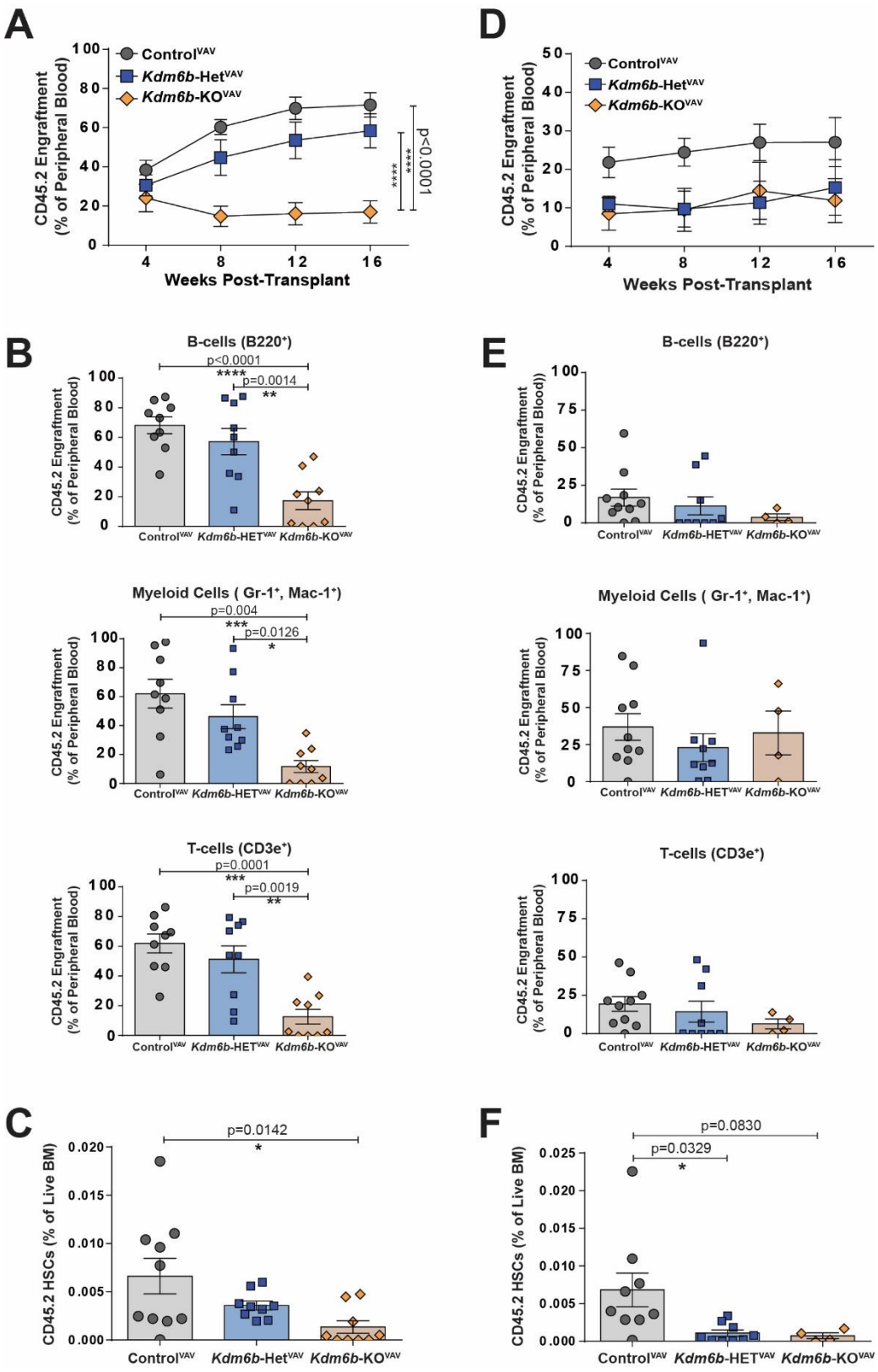
A
Control^VAV
Kdm6b-Het^VAV
Kdm6b-KO^VAV
CD45.2 Engraftment (% of Peripheral Blood)
Weeks Post-Transplant
p<0.0001
****
****
B
B-cells (B220+)
p<0.0001
****
p=0.0014
**
Myeloid Cells (Gr-1+, Mac-1+)
p=0.004
***
p=0.0126
*
T-cells (CD3e+)
p=0.0001
***
p=0.0019
**
C
CD45.2 HSCs (% of Live BM)
p=0.0142
*
D
E
F
p=0.0830
p=0.0329
*

Figure 2.3: Kdm6b is required for HSC self-renewal

(A) Peripheral blood engraftment of primary recipients from transplantation of 200 HSCs from Control^{VAV} (*n*=10), *Kdm6b*-Het^{VAV} (*n*=9), and *Kdm6b*-KO^{VAV} (*n*=9) mice. **(B)** Donor chimerism in B-cell, Myeloid and T-cell blood populations at 16-weeks post-transplant in recipient mice. **(C)** Frequency of donor-derived HSCs in WBM of recipient mice 18-weeks post-transplant. **(D)** Peripheral blood engraftment of secondary recipients transplanted with 200 HSCs from Control^{VAV} (*n*=9), *Kdm6b*-Het^{VAV} (*n*=9), and *Kdm6b*-KO^{VAV} (*n*=4) primary recipient mice. **(E)** Donor chimerism in B-cell, Myeloid and T-cell blood populations at 16-weeks post-transplant in secondary recipient mice. (F) Frequency of donor-derived HSCs in WBM of secondary recipient mice 18-weeks post-transplant. Mean ± S.E.M. values are shown. **p*<0.05, ***p*<0.01, ****p*<0.001, *****p*<0.0001.

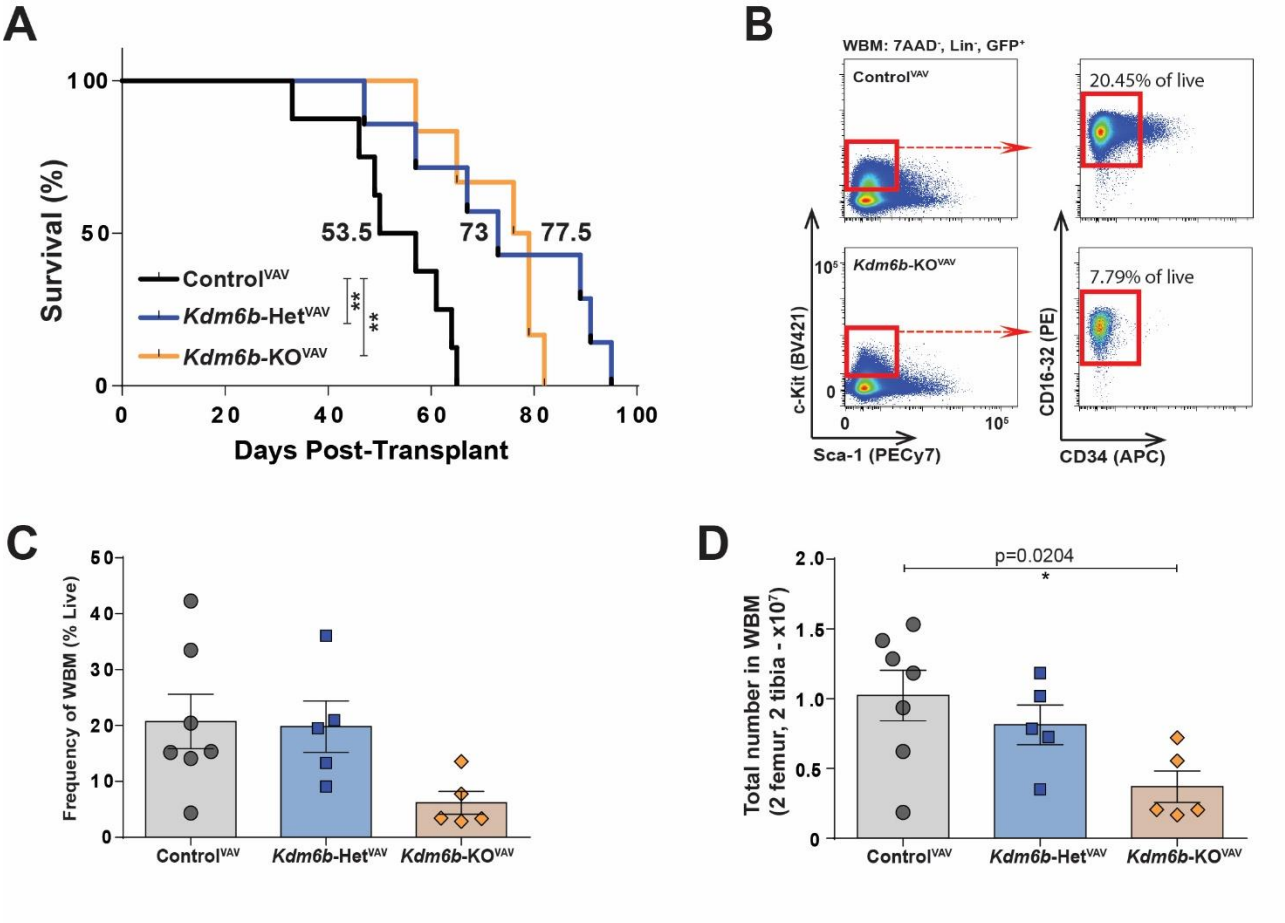

E

Genotype	No. of Cells transplanted	Type of Cells	No. of Animals Transplanted	No. of Animals with AML	Median Survival (days)	Frequency of Leukemic Stem Cell (Median and 95% CI)	P-value (Compared to Control)
Control^{VAV}	1000	GFP+ GMP	5	3	59	**1:7,232** (3328,15720)	NA
	5000	WBM	5	3	36		
	15000	WBM	5	3	36		
	50000	WBM	5	5	22		
Kdm6b-Het^{VAV}	1000	GFP+ GMP	5	2	Undefined	**1:22,286** (10372,47889)	0.0207
	5000	WBM	5	2	Undefined		
	15000	WBM	5	3	30		
	50000	WBM	5	3	22		
Kdm6b-KO^{VAV}	1000	GFP+ GMP	5	2	Undefined	**1:19,740** (9239,42175)	0.0359
	5000	WBM	5	3	44		
	15000	WBM	5	3	31		
	50000	WBM	5	3	36		

F

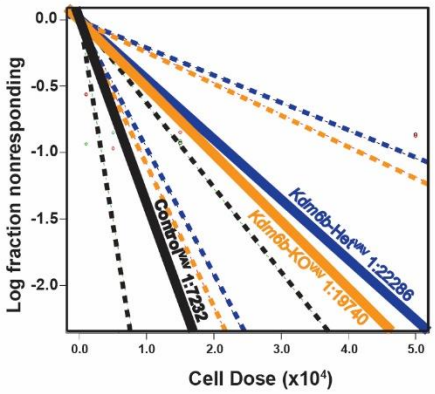

Figure 2.4: Kdm6b is required for self-renewal of leukemia-initiating cells.

(A) Kaplan-Meier survival curve comparing time to morbidity between recipient mice transplanted with Control^{VAV} (*n*=8), *Kdm6b*-Het^{VAV} (*n*=7), and *Kdm6b*-KO^{VAV} (*n*=6) c-Kit+ WBM cells transduced with the MLL-AF9 oncogene. **(B)** Flow cytometry gating scheme showing leukemic-initiating cells (GFP+ GMPs) in Control^{VAV} (top) and *Kdm6b*-KO^{VAV} (bottom) recipient mouse WBM. **(C)** Frequency and **(D)** absolute number of leukemic GMPs in WBM of moribund recipient mice. **(E)** Secondary limiting dilution transplantation response and **(F)** leukemic stem cell frequency estimates as calculated by a maximum likelihood estimate using extreme limiting dilution analysis (ELDA) software. Mean ± S.E.M. values are shown. **p*<0.05, ***p*<0.01.

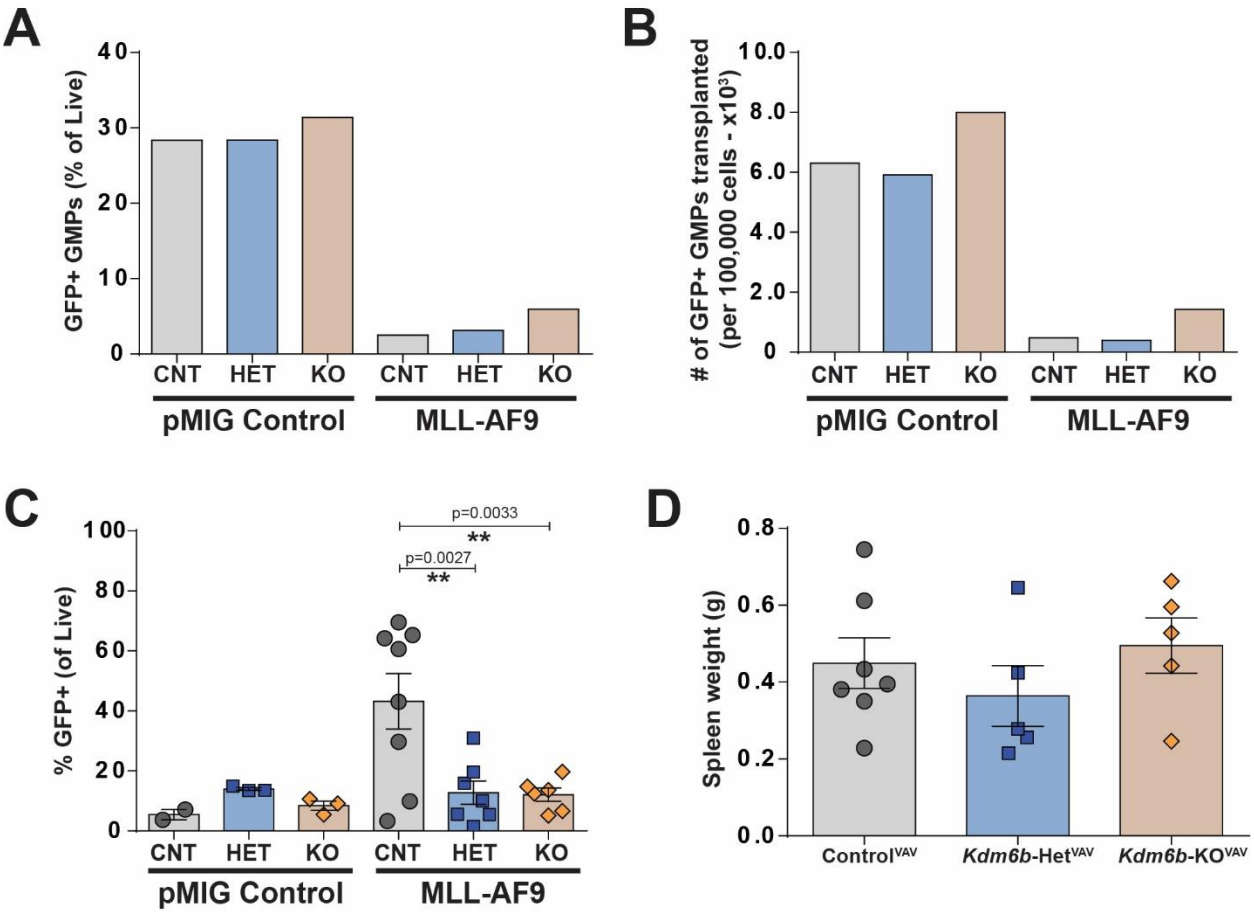

Supplementary Figure 2.4.1: *Kdm6b* is required for self-renewal of leukemia-initiating cells.

(A) Representative transduction efficiency from one experimental replicate showing frequency of GFP+ GMPs (Lin-, c-Kit+, Sca-1-, CD16-32+, CD34-) in c-Kit enriched Control^{VAV}, *Kdm6b*-Het^{VAV}, and *Kdm6b*-KO^{VAV} cells three-days post-transduction with empty vector (pMIG) control, or pMIG-MLL-AF9 retroviruses. **(B)** Representative number of GFP+ GMPs transplanted per 100K cells post-transduction. **(C)** Percentage of GFP+ blood cells four-weeks post-transplant. **(D)** Spleen weights from moribund primary MLL-AF9 recipient mice. Mean ± S.E.M. values are shown. ***p*<0.01.

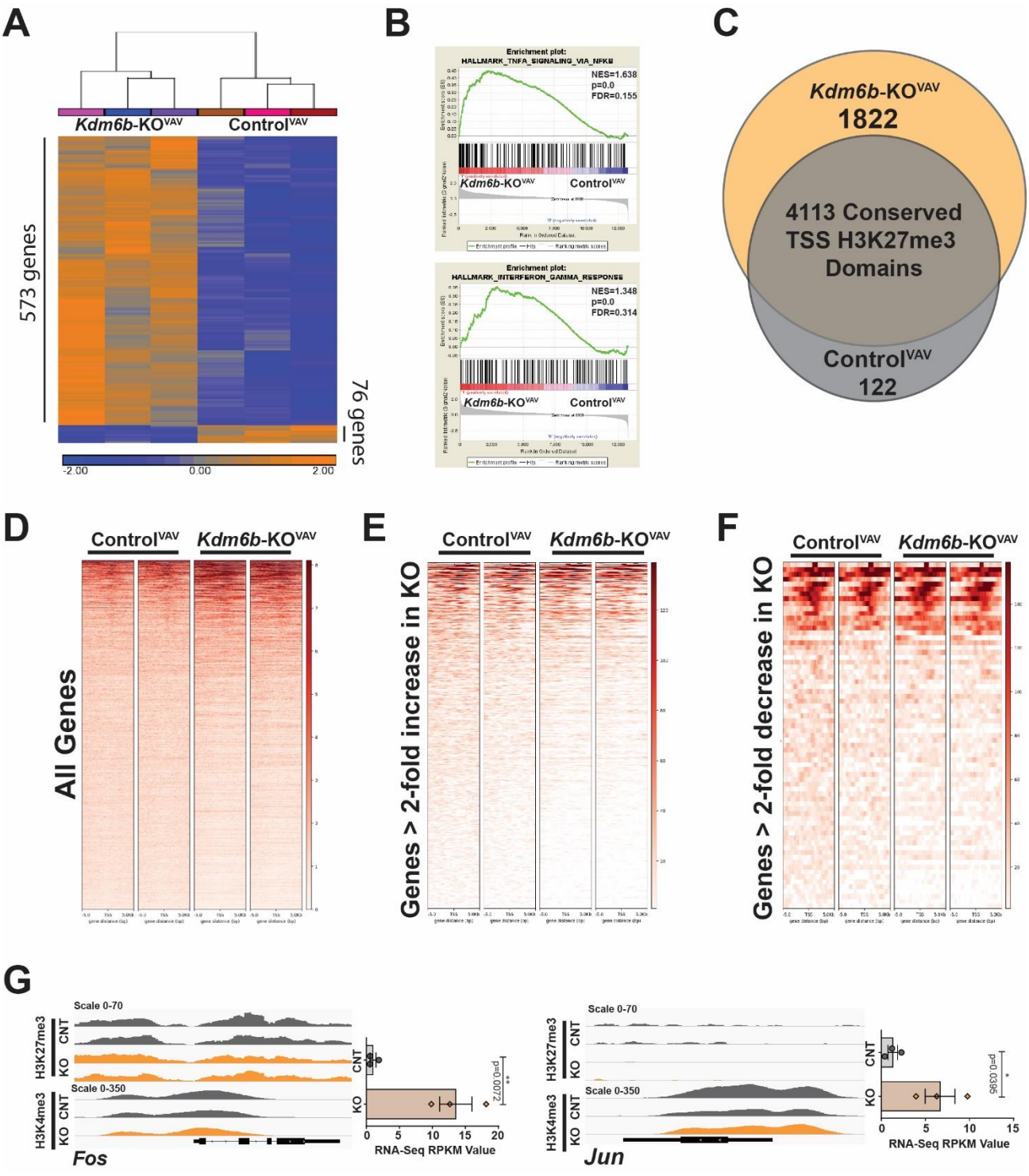
A
Kdm6b-KOVAV
ControlVAV
573 genes
76 genes
-2.00
0.00
2.00
B
Enrichment plot:
HALLMARK_TNFA_SIGNALING_VIA_NFKB
NES=1.638
p=0.0
FDR=0.155
Kdm6b-KOVAV
ControlVAV
Enrichment plot:
HALLMARK_INTERFERON_GAMMA_RESPONSE
NES=1.348
p=0.0
FDR=0.314
Kdm6b-KOVAV
ControlVAV
C
Kdm6b-KOVAV
1822
4113 Conserved
TSS H3K27me3
Domains
ControlVAV
122
D
ControlVAV
Kdm6b-KOVAV
All Genes
E
ControlVAV
Kdm6b-KOVAV
Genes > 2-fold increase in KO
F
ControlVAV
Kdm6b-KOVAV
Genes > 2-fold decrease in KO
G
Scale 0-70
H3K27me3
CNT
KO
Scale 0-350
H3K4me3
CNT
KO
Fos
CNT
KO
p=0.0072
**
0
5
10
15
20
RNA-Seq RPKM Value
Scale 0-70
H3K27me3
CNT
KO
Scale 0-350
H3K4me3
CNT
KO
Jun
CNT
KO
p=0.0396
*
0
5
10
15
RNA-Seq RPKM Value

Figure 2.5: Interferon response and NF-κB signaling are increased in *Kdm6b*-deficient HSCs.

(A) Hierarchical clustering of genes with >2-fold increased or decreased expression (adjusted *p*-value <0.05) in *Kdm6b*-KO^{VAV} HSCs compared to Control^{VAV} HSCs. **(B)** Gene Set Enrichment Analysis (GSEA) showing upregulation of NF-κB and interferon gamma response genes in *Kdm6b*-KO^{VAV} HSCs. **(C)** Venn diagram showing H3K27me3 domains overlapping >10% the transcriptional start site (TSS) ± 5kB. **(D)** Homer plot of H3K27me3 distribution ± 5Kb from transcriptional start sites (TSS) in all genes. **(E)** Homer plot of H3K27me3 distribution ± 5Kb from TSS in 573 genes that have > 2-fold increased expression in *Kdm6b*-KO^{VAV} HSCs. **(F)** Homer plot of H3K27me3 distribution in 76 genes that have > 2-fold decreased expression *Kdm6b*-KO^{VAV} HSCs. **(G)** H3K27me3 and H3K4me3 profiles (left) and RNA-seq expression values (right) of *Fos* and *Jun* showing no correlation between chromatin prolfile and gene expression. Statistics were calculated using a student *t*-test. Mean ± S.E.M. values are shown. **p*<0.05, ***p*<0.01.

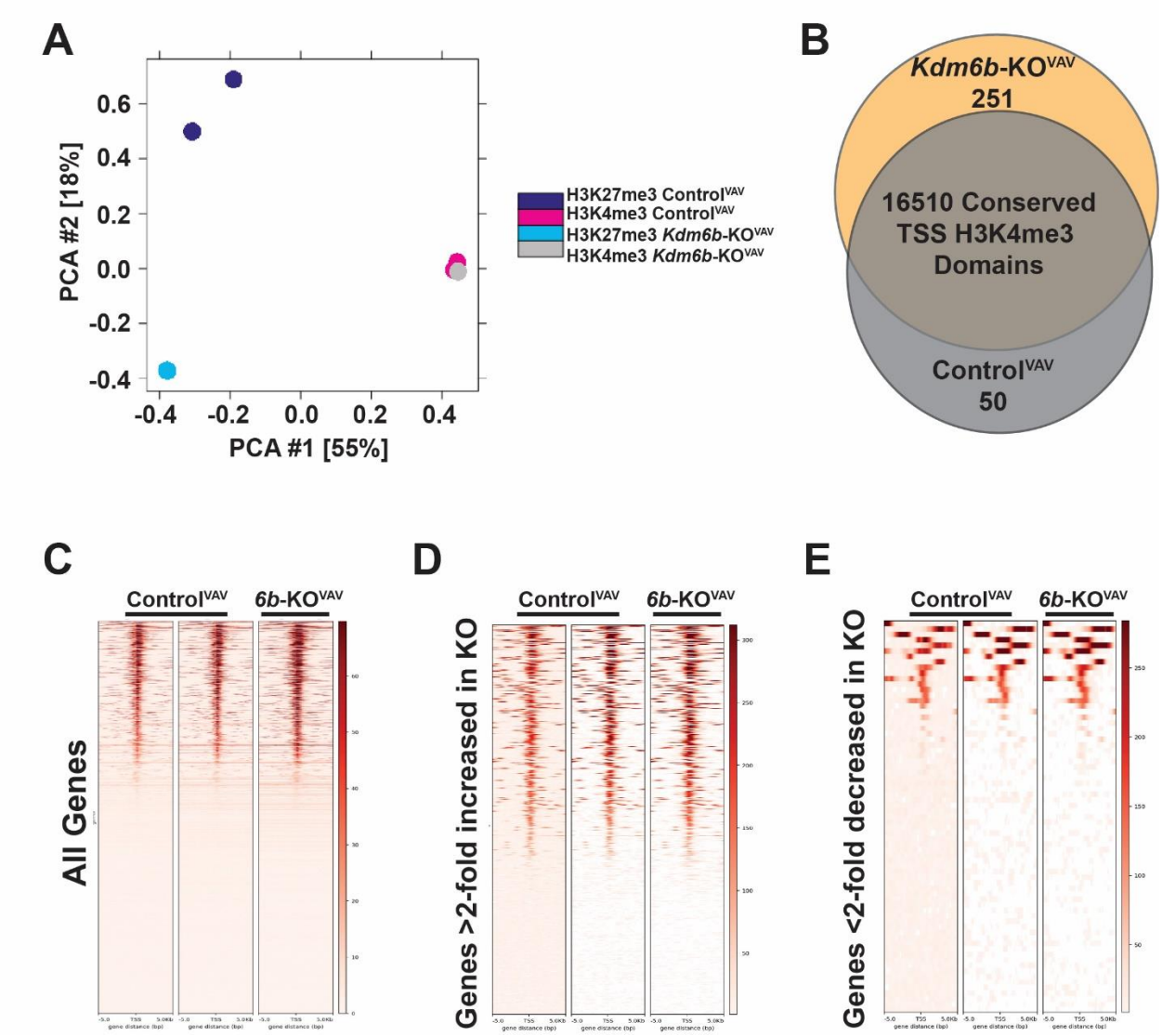

Supplementary Figure 2.5.1: Chromatin profile of *Kdm6b*-deficient HSCs

(A) Principal component analysis (PCA) of H3K27me3 and H3K4me3 ChIPmentation profiles between Control^{VAV} and *Kdm6b*-KO^{VAV} HSCs. **(B)** Venn diagram showing H3K4me3 domains overlapping >10% the transcriptional start site (TSS) ± 5kB. **(C)** Homer plot of H3K4me3 distribution ± 5Kb from transcriptional start sites (TSS) in all genes. **(D)** Homer plot of H3K4me3 distribution ± 5Kb from TSS in 573 genes with >2-fold increased expression in *Kdm6b*-KO^{VAV} HSCs. **(E)** Homer plot of H3K4me3 distribution in 76 genes with > 2-fold decreased expression *Kdm6b*-KO^{VAV} HSCs.

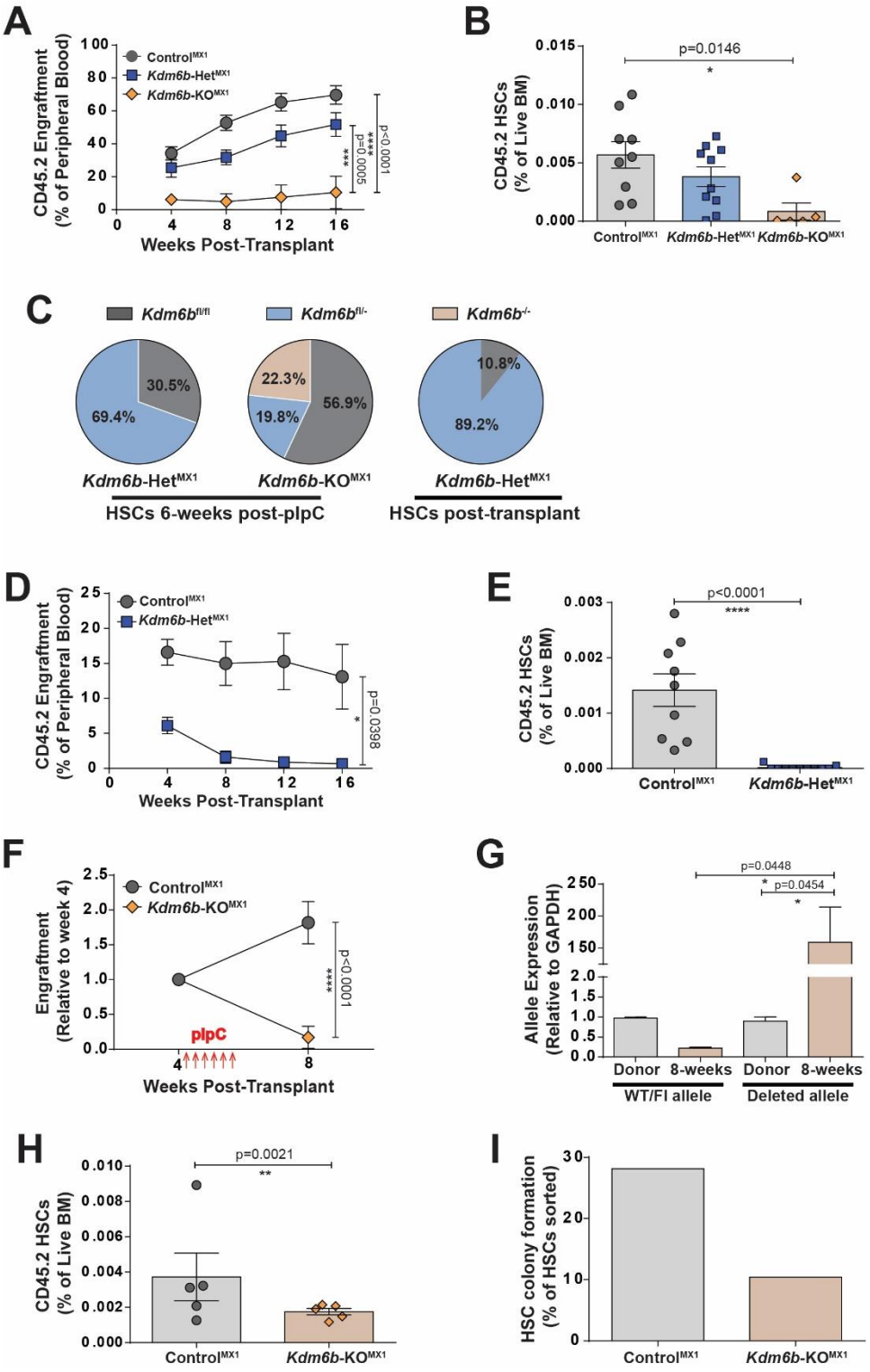
A
CD45.2 Engraftment (% of Peripheral Blood)
Control^MX1
Kdm6b-Het^MX1
Kdm6b-KO^MX1
p<0.0001
****
p=0.0005
***
Weeks Post-Transplant
B
CD45.2 HSCs (% of Live BM)
p=0.0146
*
Control^MX1
Kdm6b-Het^MX1
Kdm6b-KO^MX1
C
Kdm6b^fl/fl
Kdm6b^fl/-
Kdm6b^-/-
30.5%
69.4%
22.3%
19.8%
56.9%
10.8%
89.2%
Kdm6b-Het^MX1
Kdm6b-KO^MX1
Kdm6b-Het^MX1
HSCs 6-weeks post-pIpC
HSCs post-transplant
D
CD45.2 Engraftment (% of Peripheral Blood)
Control^MX1
Kdm6b-Het^MX1
p=0.0398
*
Weeks Post-Transplant
E
CD45.2 HSCs (% of Live BM)
p<0.0001
****
Control^MX1
Kdm6b-Het^MX1
F
Engraftment (Relative to week 4)
Control^MX1
Kdm6b-KO^MX1
p<0.0001
****
pIpC
Weeks Post-Transplant
G
Allele Expression (Relative to GAPDH)
p=0.0448
*
p=0.0454
*
Donor
8-weeks
Donor
8-weeks
WT/Fl allele
Deleted allele
H
CD45.2 HSCs (% of Live BM)
p=0.0021
**
Control^MX1
Kdm6b-KO^MX1
I
HSC colony formation (% of HSCs sorted)
Control^MX1
Kdm6b-KO^MX1

Figure 2.6: Inflammatory stress forces differentiation of *Kdm6b*-deficient HSCs without self-renewal.

(A) Peripheral blood engraftment of primary recipients transplanted with 200 HSCs from Control^{MX1} (*n*=9), *Kdm6b*-Het ^{MX1} (*n*=10), and *Kdm6b*-KO ^{MX1} (*n*=5) mice. **(B)** Frequency of donor-derived HSCs in WBM of primary recipient mice at 18-weeks post-transplant. **(C)** Efficiency of Mx1-CRE driven floxed allele recombination in HSCs from mice six-weeks post-pIpC treatment, as well as post-primary transplant in *Kdm6b*-Het ^{MX1} HSCs. **(D)** Peripheral blood engraftment of secondary recipients transplanted with 200 HSCs purified from primary recipient mice of Control ^{MX1} (*n*=9) and *Kdm6b*-Het^{MX1} (*n*=11) HSCs. **(E)** Frequency of donor-derived HSCs in WBM of secondary recipient mice 18-weeks post-transplant. **(F)** Relative peripheral blood chimerism of recipients transplanted with 200 ControlMX1 and *Kdm6b*-KO^{MX1} HSCs treated with pIpC four-weeks post-transplant (*n*=5). **(G)** Floxed allele recombination efficiency in macrophages from donors (pre-) and eight-week recipients (post-) pIpC treatment. **(H)** HSC frequency eight-weeks post-transplant (two-weeks post-pIpC treatment). **(I)** Colony-forming potential of HSCs purified from recipient mice two-weeks post-pIpC treatment. Mean ± S.E.M. values are shown. **p*<0.05, ***p*<0.01, ****p*<0.001, *****p*<0.0001.

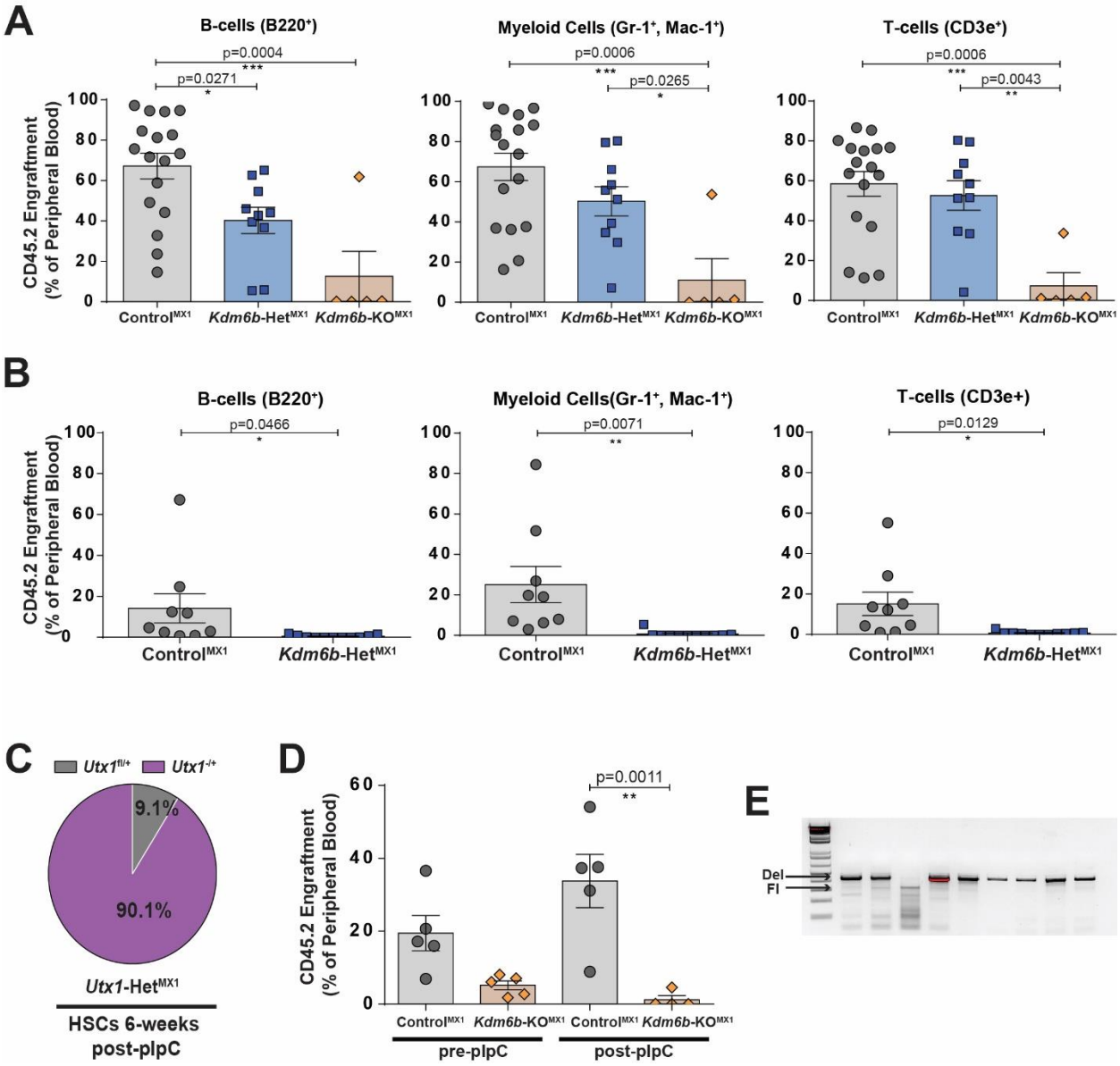
A
B-cells (B220+)
Myeloid Cells (Gr-1+, Mac-1+)
T-cells (CD3e+)
CD45.2 Engraftment (% of Peripheral Blood)
p=0.0004
p=0.0271
p=0.0006
p=0.0265
p=0.0006
p=0.0043
Control MX1
Kdm6b-Het MX1
Kdm6b-KO MX1
B
B-cells (B220+)
Myeloid Cells(Gr-1+, Mac-1+)
T-cells (CD3e+)
p=0.0466
p=0.0071
p=0.0129
C
Utx1fl/+
Utx1-/+
9.1%
90.1%
Utx1-Het MX1
HSCs 6-weeks post-plpC
D
p=0.0011
pre-plpC
post-plpC
E
Del
Fl

Supplementary Figure 2.6.1: Inflammatory stress forces differentiation of *Kdm6b*-deficient HSCs.

(A) Donor chimerism in B-cell, Myeloid and T-cell blood populations at 16-weeks post-transplant in primary recipient mice. **(B)** Donor chimerism in B-cell, Myeloid and T-cell blood populations at 16-weeks post-transplant in secondary recipient mice. **(C)** Floxed allele recombination efficiency in *Utx1*-HetMX1 HSCs six-weeks post-pIpC treatment. **(D)** Donor-cell engraftment in peripheral blood pre- and two-weeks post-pIpC treatment. **(E)** Floxed allele recombination efficiency in individual *Kdm6b*-KOMX1 HSCs two-weeks post-pIpC. Mean ± S.E.M. values are shown. *p<0.05, **p<0.01, ***p<0.001.

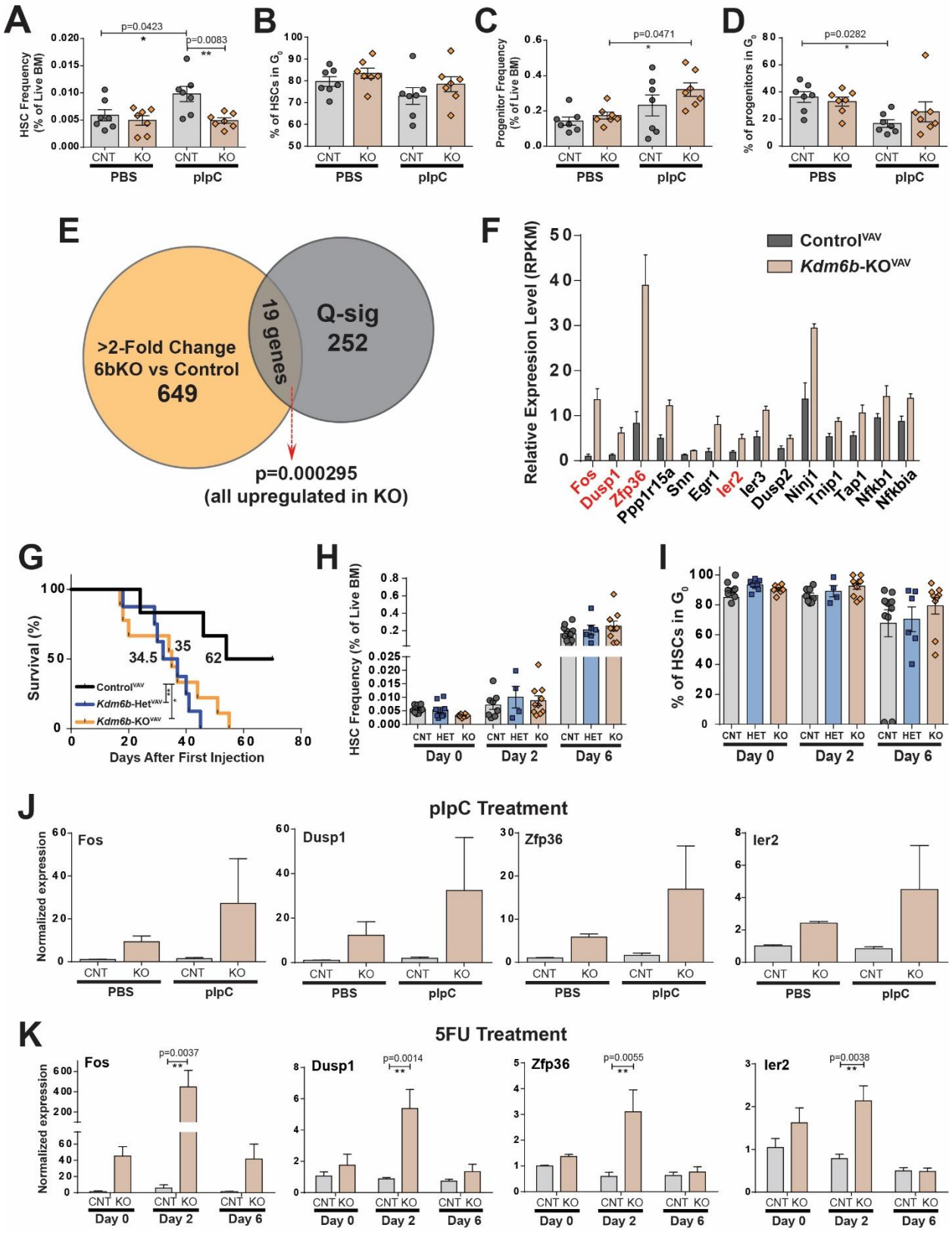
A
HSC Frequency (% of Live BM)
p=0.0423
p=0.0083
CNT KO CNT KO
PBS pIpC
B
% of HSCs in G0
C
Progenitor Frequency (% of Live BM)
p=0.0471
D
% of progenitors in G0
p=0.0282
E
>2-Fold Change 6bKO vs Control 649
19 genes
Q-sig 252
p=0.000295
(all upregulated in KO)
F
Control^VAV
Kdm6b-KO^VAV
Relative Expression Level (RPKM)
Fos Dusp1 Zfp36 Ppp1r15a Snn Egr1 Ier2 Ier3 Dusp2 Ninj1 Tnip1 Tap1 Nfkb1 Nfkbia
G
Survival (%)
34.5 35 62
Control^VAV
Kdm6b-Het^VAV
Kdm6b-KO^VAV
Days After First Injection
H
HSC Frequency (% of Live BM)
CNT HET KO
Day 0 Day 2 Day 6
I
% of HSCs in G0
J
pIpC Treatment
Fos Dusp1 Zfp36 Ier2
Normalized expression
K
5FU Treatment
p=0.0037
p=0.0014
p=0.0055
p=0.0038

Figure 2.7: Kdm6b is necessary for HSC maintenance in response to proliferative stress

(A) HSC frequency in WBM after two doses of either PBS (control) or pIpC in Control^{VAV} and *Kdm6b*-KO^{VAV} mice (*n*=7). **(B)** Proportion of quiescent HSCs (G_0) after two doses of either PBS (control) or pIpC in Control$_{VAV}$ and *Kdm6b*-KO^{VAV}mice (*n*=7). **(C)** Progenitor (Lineage- c-Kit$^+$ EPCR$^+$) frequency in WBM after two doses of either PBS (control) or pIpC in Control^{VAV} and *Kdm6b*-KO^{VAV} mice (*n*=7). **(D)** Proportion of quiescent progenitors (G_0) after two doses of either PBS (control) or pIpC in Control^{VAV} and *Kdm6b*-KO^{VAV} mice (*n*=7). **(E)** Overlap between genes with >two-fold increased or decreased expression with the Q-sig geneset previously identified. **(F)** NF-κB target genes with increased enrichment in *Kdm6b*-KO^{VAV} HSCs compared to Control$_{VAV}$ HSCs identified by GSEA with Q-sig genes highlighted in red. **(G)** Kaplan-Meier survival curve comparing time to morbidity of Control^{VAV} (*n*=8), *Kdm6b*-Het^{VAV} (*n*=8), and *Kdm6b*-KO^{VAV} (*n*=8) mice after serial 5-FU treatment. **(H)** HSC frequency in mice at day 0 (Control^{VAV} (*n*=11), *Kdm6b*-Het^{VAV} (*n*=9), and *Kdm6b*-KO^{VAV} (*n*=8)), two-days post-5FU treatment (Control^{VAV} (*n*=8), *Kdm6b*-Het^{VAV} (*n*=4), and *Kdm6b*-KO^{VAV} (*n*=10)), and six-days post-5FU treatment (Control^{VAV} (*n*=12), *Kdm6b*-Het^{VAV} (*n*=6), and *Kdm6b*-KO^{VAV} (*n*=9)). **(I)** Proportion of quiescent HSCs (G_0) at day 0, two-days post-5FU treatment and six-days post-5FU treatment. **(J)** Expression of genes involved in HSC quiescence after PBS (control) or two-doses of pIpC in Control^{VAV} HSCs (*n*=3) and *Kdm6b*-KO^{VAV}HSCs (*n*=3). **(K)** Expression of genes involved in HSC quiescence at baseline, two-days post-FU treatment, and six-days post-5FU treatment in Control^{VAV} HSCs (*n*=3, 3, and 5 respectively) and *Kdm6b*-KO^{VAV} HSCs (*n*=3, 5, and 5 respectively). Mean ± S.E.M. values are shown. *p<0.05, **p<0.01.

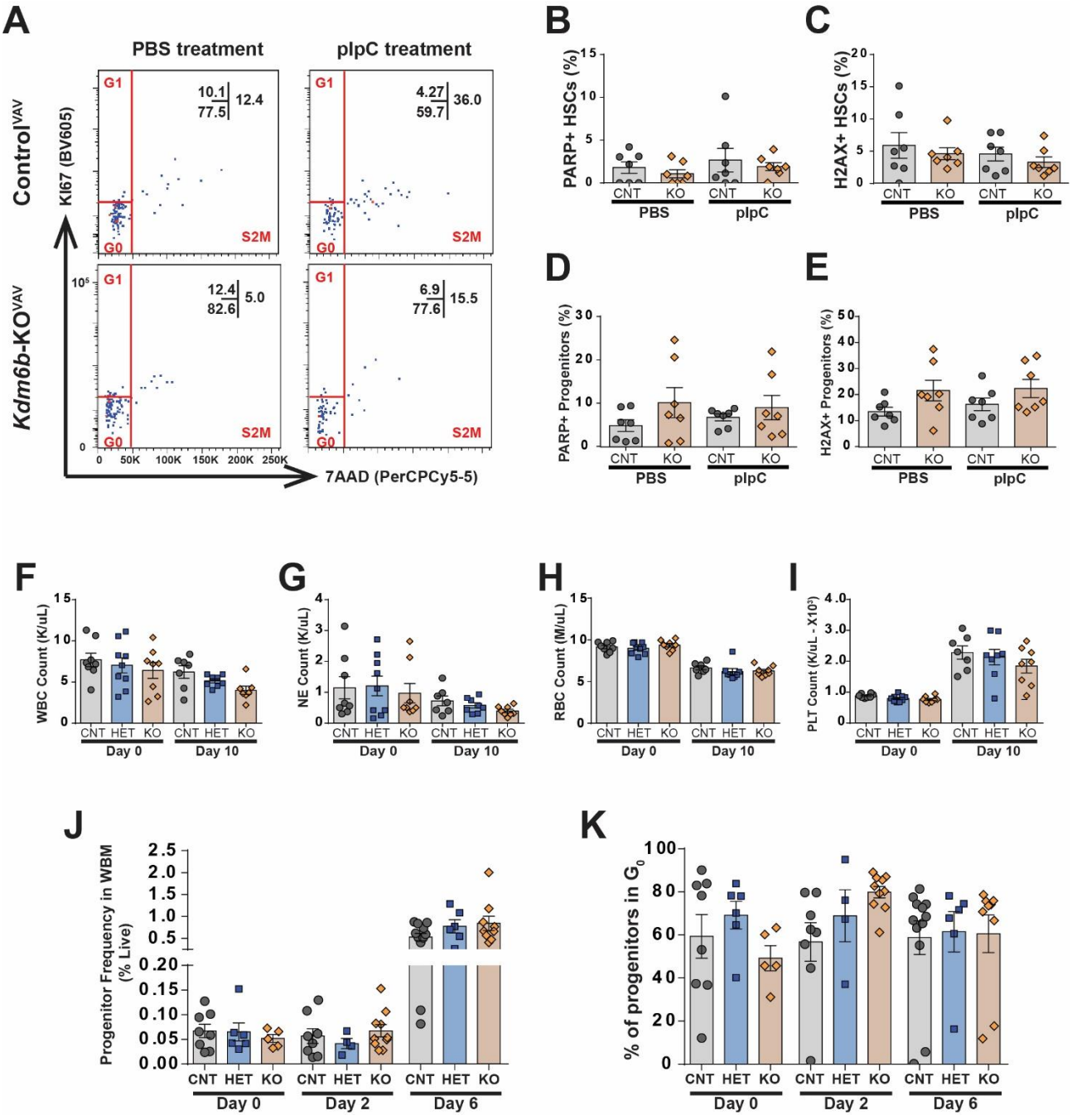
A
PBS treatment
pIpC treatment
Control^VAV
Kdm6b-KO^VAV
KI67 (BV605)
7AAD (PerCPCy5-5)
G1
G0
S2M
10.1
77.5
12.4
4.27
59.7
36.0
12.4
82.6
5.0
6.9
77.6
15.5
B
PARP+ HSCs (%)
C
H2AX+ HSCs (%)
D
PARP+ Progenitors (%)
E
H2AX+ Progenitors (%)
CNT
KO
PBS
pIpC
F
WBC Count (K/uL)
G
NE Count (K/uL)
H
RBC Count (M/uL)
I
PLT Count (K/uL - X10³)
CNT HET KO
Day 0
Day 10
J
Progenitor Frequency in WBM (% Live)
K
% of progenitors in G0
Day 0
Day 2
Day 6

Supplementary Figure 2.7.1: *Kdm6b* is necessary for HSC maintenance in response to proliferative stress.

(A) Flow cytometry gating scheme showing cell cycle analysis of HSCs from control^{VAV} and *Kdm6b*-KO^{VAV} mice after PBS (control) or pIpC treatment. **(B)** Frequency of HSCs after PBS (control) or pIpC treatment undergoing apoptosis as measured by flow cytometric analysis of cleaved PARP. **(C)** Frequency of HSCs after PBS (control) or pIpC treatment with DNA damage response measured by flow cytometric analysis of γH2AX. **(D)** Frequency of progenitors after PBS (control) or pIpC treatment undergoing apoptosis measured by cleaved PARP. **(E)** Frequency of progenitors after PBS (control) or pIpC treatment with DNA damage response as measured by γH2AX. **(F-I)** White blood cell (WBC), neutrophil (NE), red blood cell (RBC) and platelet (PLT) counts in blood of Control^{VAV} (*n*=7), *Kdm6b*-Het^{VAV} (*n*=9), and *Kdm6b*-KO^{VAV} (*n*=8) mice pre- and ten-days post-5-FU treatment. **(J)** Progenitor frequency in Control^{VAV}, *Kdm6b*-Het^{VAV}, and *Kdm6b*-KO^{VAV} mice 0, 2 and 6 days post-5-FU treatment. **(K)** Proportion Control^{VAV}, *Kdm6b*-Het^{VAV}, and *Kdm6b*-KO^{VAV} mice progenitors in G_0 0, 2 and 6 days post-5-FU treatment. Mean ± S.E.M. values are shown.

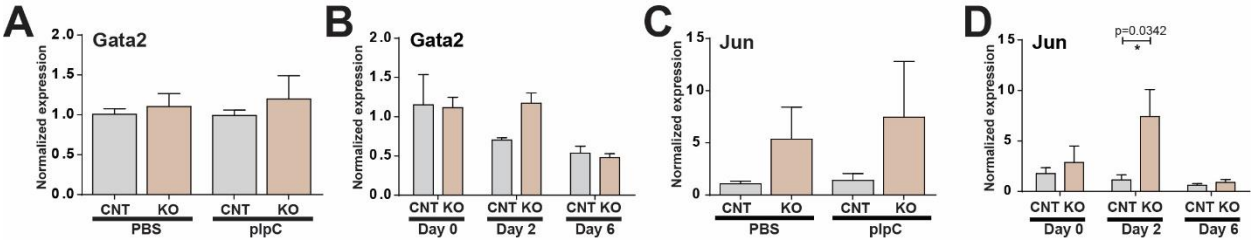

Supplementary Figure 2.7.2: *Kdm6b* is necessary to resolve expression of quiescence genes in HSCs

Expression profile of *Gata2* (a HSC quiescence signature gene not dysregulated in *Kdm6b*-KO^{VAV} HSCs) in HSCs after **(A)** pIpC and **(B)** 5-FU treatment. Expression profile of AP1 complex factor *Jun* in HSCs after **(C)** pIpC and **(D)** 5-FU treatment. Mean ± S.E.M. values are shown. *p<0.05.

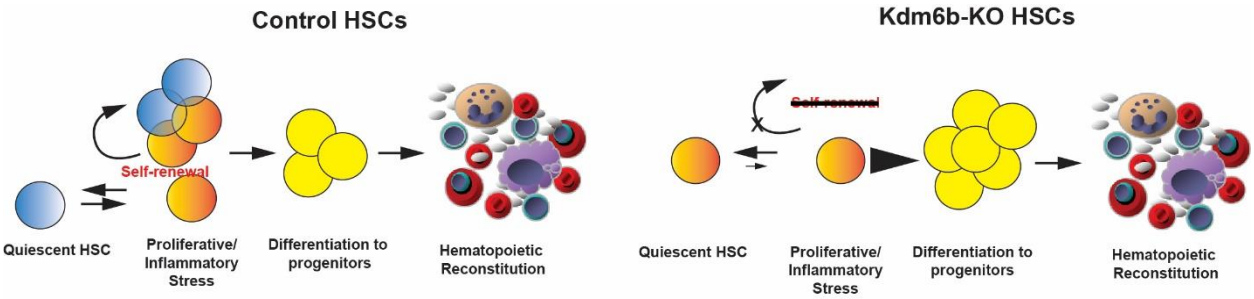

Figure 2.8 *Kdm6b*-deficient HSCs do not self-renew but rapidly differentiate more committed downstream progenitors

Schematic representation comparing HSC fate decisions between control^{VAV} and *Kdm6b*-KO^{VAV} HSCs after proliferative or inflammatory stress.

2.6 Tables

Table 2.1 Downregulated Genes in *Kdm6b*-KO^{VAV} HSCs (>2-Fold reduction, adjusted p<0.05)

Gene	Control Avg RPKM	SEM Control	6bKO Avg RPKM	SEM 6bKO	Fold Change	P-value
Gm8787	0.0625153	0.002609574	0.0205955	0.00170373	3.03539	0.000176732
2610507I01Rik	3.709333333	0.273591534	0.333587667	0.126721616	11.1195	0.000362367
Stxbp4	8.193396667	0.444633279	2.64112	0.227602304	3.10224	0.000372685
Ifit1bl1	1.89126	0.095795652	0.542378667	0.090378337	3.48697	0.000512282
Fndc9	0.061063733	0.003567587	0.0149676	0.003060886	4.07972	0.000606212
Lyrm7	1.273056667	0.020061187	0.464409333	0.091587182	2.74124	0.000993587
Synb	0.173734667	0.007252308	0.0483917	0.012970179	3.59017	0.00108192
Ypel4	0.136412	0.0137285	0.0175782	0.009334824	7.76028	0.00201603
Sh2d4a	0.774908	0.04397443	0.265330667	0.058810189	2.92054	0.00226474
1700125H03Rik	0.125205333	0.004431483	0.015784067	0.015784067	7.93239	0.00261916
Tbx4	0.113468	0.008595302	0.0186842	0.011688843	6.07293	0.00283647
0610043K17Rik	0.669269667	0.060223082	0.164948567	0.057754824	4.05745	0.00377982
A430085M09Rik	0.030123667	0.00393977	0.002432273	0.002432273	12.385	0.00392851
Med1	77.7309	11.46255012	14.18326667	1.06108486	5.48047	0.00525759
Gria3	2.244773333	0.171749515	1.075127333	0.130168561	2.08791	0.00558899
Rbm44	0.449686	0.043701075	0.165152667	0.032546649	2.72285	0.00641948
Gid4	8.94939	0.834536543	4.093176667	0.410474898	2.18641	0.00642023
Gm6981	0.311463667	0.032827862	0.104230133	0.023528216	2.98824	0.00683386
Sbspon	0.068623033	0.010607216	0.009503133	0.005089289	7.22109	0.00735895
Pla2g4c	0.499078333	0.043776061	0.196707667	0.041425795	2.53716	0.0074012
Pnpla1	0.0235867	0.004043493	0.001778907	0.001778907	13.2591	0.00783542
Cd300lb	0.190883	0.027536319	0.02397316	0.021300369	7.96237	0.0086832
Sema3c	0.010351363	0.001041775	0.001609453	0.001609453	6.43159	0.0103409
Nfia	30.99433333	3.331932319	15.10153333	1.037050287	2.05239	0.0103833
Spon2	0.392404667	0.046513566	0.069692667	0.056610442	5.63051	0.0116501
Rgs5	0.100181467	0.01008393	0.03161517	0.012941909	3.16878	0.0139276

Hist1h3g	0.1068421	0.010349625	0.0186386	0.0186386	5.7323	0.0144085
Cpa3	2.230573333	0.263061518	1.107607333	0.08819844	2.01387	0.0155089
Gm16793	0.101256467	0.023708539	0.004615067	0.004615067	21.9404	0.0161149
Rtl1	0.014205933	0.001725633	0.003945157	0.001973302	3.60086	0.0173314
Gm5779	1.313494333	0.301672018	0.125683767	0.034242789	10.4508	0.0173601
Nostrin	0.129872633	0.026423942	0.018865233	0.011509181	6.88423	0.0182786
Slc25a48	0.0538266	0.001905037	0.017433	0.009336044	3.08763	0.0187867
Gm15217	0.062120833	0.01205899	0.0077804	0.0077804	7.98429	0.019327
Zfp454	0.136019267	0.02842107	0.0187109	0.01332312	7.26952	0.020169
Cxcr6	0.131213133	0.03381617	0.005369733	0.005369733	24.4356	0.0212905
Slamf7	0.018416	0.004111653	0.00200524	0.00200524	9.18394	0.0230156
BC100451	0.055572633	0.014078295	0.004031767	0.004031767	13.7837	0.0244603
0610039H22Rik	2.908743333	0.733257609	0.319729	0.065045531	9.09754	0.0245157
4930447C04Rik	1.98163	0.254706146	0.899117	0.175559475	2.20398	0.0249105
Ermap	1.932366667	0.241866792	0.441870467	0.352349977	4.37315	0.0251786
Fpr2	0.257661333	0.01994297	0.055381	0.055381	4.65254	0.0263778
Kel	0.609217	0.050961991	0.185932	0.113625439	3.27656	0.0273013
Pde6a	0.047875233	0.013473344	0.001899677	0.001899677	25.2018	0.0278135
Hs6st2	0.0906533	0.009010389	0.03262813	0.014731955	2.77837	0.0283027
Olfr65	0.1582015	0.03704172	0.018965567	0.018965567	8.34152	0.0286797
Cmah	0.0320102	0.005129356	0.011518133	0.003365186	2.77912	0.0288266
Fbxl13	0.048582633	0.013268841	0.003135167	0.003135167	15.496	0.0290151
Fam46a	1.164166333	0.118018991	0.545954	0.144458296	2.13235	0.0295404
9530053A07Rik	0.0287659	0.007879747	0.00201334	0.00201334	14.2876	0.030232
Nxpe4	0.410090667	0.070279798	0.16575	0.024305342	2.47415	0.0303369
Adgre1	0.205100667	0.035484517	0.088387733	0.002175786	2.32047	0.0304157
Srsf2	372.7623333	82.952203	101.0621	8.006928465	3.68845	0.0310739
Tfpi2	0.396758	0.05686394	0.192101	0.026635058	2.06536	0.0311028
Padi3	0.0197889	0.004183804	0.004320437	0.002290216	4.58031	0.0315802
Ms4a7	0.359760667	0.079655123	0.0880748	0.028607583	4.08471	0.0325884
Asb10	0.055912467	0.016562776	0.002345347	0.002345347	23.8397	0.0328307
Adh1	0.290499667	0.033830917	0.112526567	0.044894368	2.58161	0.0339883
Nlrp1a	0.276917	0.072696584	0.047135067	0.007384599	5.87497	0.0346922
Fam186b	0.011172057	0.001191762	0.002502303	0.002502303	4.46471	0.0352513

Cacna1h	0.011881393	0.00251815	0.001945737	0.001945737	6.10637	0.0354521
Dnase1l3	0.1629461	0.03170082	0.0579235	0.011838332	2.81312	0.0360954
Pparg	0.1884508	0.054908561	0.0190596	0.003897714	9.88744	0.0370316
Gpr137b-ps	2.90479	0.300259155	1.429075333	0.392639172	2.03264	0.0405162
Bcas1os2	0.0383534	0.004968781	0.008658367	0.008658367	4.42963	0.0409566
4930478L05Rik	0.282499	0.065593869	0.074169533	0.02792058	3.80883	0.0431431
Snca	1.023752667	0.136095366	0.489096667	0.122969671	2.09315	0.0434645
Samd4	0.026411967	0.008225481	0.00187096	0.00187096	14.1168	0.0437122
Slc23a1	0.264689	0.037536263	0.128301633	0.028205579	2.06302	0.0439055
Slc45a3	0.1237583	0.030761967	0.021015013	0.01867203	5.88904	0.0461553
Slc38a5	1.930573333	0.419890857	0.424688433	0.321632246	4.54587	0.0465319
C4b	0.050184333	0.009385655	0.0232825	0.001503709	2.15545	0.0473366
Cpn1	0.1135452	0.035911416	0.008905467	0.008905467	12.7501	0.0474334
BC024386	0.022060333	0.002353241	0.00819009	0.004349308	2.69354	0.0485723
Ms4a2	0.277269	0.091727593	0.019438123	0.010094276	14.2642	0.0491127
Col5a1	0.081283133	0.01544602	0.018294723	0.01651326	4.44299	0.0495281

Table 2.2 Upregulated Genes in *Kdm6b*-KO^{VAV} HSCs (>2-Fold increase, adjusted p<0.05)

Gene	Control Avg RPKM	SEM Control	6bKO Avg RPKM	SEM 6bKO	Fold Change	P-value
Dhx40	0.423009333	0.038112613	2.32885	0.064933354	-5.50544	1.45E-05
Fam129b	0.526887333	0.025050149	1.100636667	0.027990893	-2.08894	0.000107151
Hdac11	1.136696667	0.087822894	2.49637	0.050737684	-2.19616	0.000179081
Arhgap33	0.211786667	0.007573768	0.450543	0.01657928	-2.12735	0.000196118
Dusp22	0.663596333	0.058913528	1.496203333	0.031933264	-2.25468	0.000241256
Fn3krp	0.274143667	0.162671357	5.974913333	0.43072318	-21.7948	0.000244554
Cuedc1	0.849794333	0.085633211	3.044526667	0.160026251	-3.58267	0.000268266
Socs2	4.239186667	0.26446176	10.65152333	0.482315443	-2.51263	0.000309535
Itm2c	1.78165	0.200374602	4.016836667	0.034421921	-2.25456	0.000389005
Tspan7	0.161131	0.022997806	0.461752	0.016616453	-2.86569	0.000449063
Rbm15b	0.155225	0.015909919	0.410896	0.019093522	-2.6471	0.000503593
Sspo	0.003623643	0.002093997	0.029612033	0.00144427	-8.1719	0.000517252
Plxnd1	0.186402667	0.018908729	0.645957	0.040984922	-3.46539	0.000524193

Luzp2	0.138562	0.005573331	0.522089667	0.037335201	-3.76792	0.000528484
Ap5b1	0.173386333	0.013590244	0.411751333	0.019828852	-2.37476	0.000580686
Zfp128	0.579838333	0.036511193	1.236023333	0.05557202	-2.13167	0.000591529
Pak6	0.047083633	0.014189519	0.281449	0.019604491	-5.97763	0.000636263
Per1	0.213605333	0.009746292	0.507551	0.029133254	-2.37612	0.000666498
Slc39a11	1.975896667	0.082942658	5.289816667	0.336795631	-2.67717	0.000670394
St6galnac1	0.019672467	0.010416942	0.327104333	0.030530214	-16.6275	0.000676867
Dlc1	0.012474197	0.002027051	0.0505757	0.003619861	-4.05442	0.000780704
Wtip	0.076079967	0.009241572	0.166553	0.003806384	-2.18918	0.000825338
Csf2rb	2.99018	0.16005133	6.095946667	0.314899512	-2.03865	0.000923007
Plekha4	0.002354907	0.002354907	0.0303155	0.002171206	-12.8733	0.000948794
Pomgnt2	0.994613667	0.162177122	2.45753	0.044920548	-2.47083	0.000964011
Gck	0.044946133	0.032163341	0.434841	0.031325607	-9.67469	0.000967839
Krt8	0.237767667	0.029576367	0.536149	0.018355395	-2.25493	0.00101726
Wfs1	0.071640533	0.013172799	0.269549	0.019126658	-3.76252	0.00104038
Nr6a1	0.039062467	0.005754275	0.127193333	0.008738393	-3.25615	0.00108765
Car5a	0.012598833	0.006671319	0.079600033	0.004532886	-6.31805	0.0011469
Micall2	0.270215	0.05887593	0.779315667	0.018131338	-2.88406	0.00116987
Bcam	0.122773467	0.045488369	0.524261	0.017455268	-4.27014	0.00118277
Epcam	0.136614033	0.019378766	0.451044333	0.033228266	-3.3016	0.00121966
Syde1	0.907371	0.139814052	2.14734	0.066423543	-2.36656	0.00131721
Pgm5	0.00196536	0.001040695	0.014033033	0.001106306	-7.1402	0.00135893
Dnaic1	0.068953367	0.007379507	0.155675333	0.008149661	-2.25769	0.00139682
Zfp579	0.245830667	0.020755417	0.503108667	0.026075007	-2.04657	0.00151582
Klhl42	1.443076667	0.272586963	6.23846	0.566197733	-4.32303	0.0015836
Npr2	0.953658333	0.07238169	1.910726667	0.102612102	-2.00358	0.00159097
Itgb4	0.070140167	0.009772283	0.249964667	0.021578727	-3.56379	0.00161529
Ctxn1	0.701444	0.099402266	1.611633333	0.069617289	-2.29759	0.00169075
Lrrc32	0.004924567	0.004924567	0.0533145	0.004309865	-10.8262	0.0017839
Ccser1	0.0404276	0.006019116	0.115578	0.008194017	-2.85888	0.00178654
AA465934	7.857686667	2.248747162	31.4181	2.267592579	-3.9984	0.00179932
C330021F23Rik	0.0259831	0.015389617	0.172857	0.012929679	-6.65266	0.00186551
Dxo	0.868801	0.096456703	1.778396667	0.079279127	-2.04696	0.00188671
Fscn1	0.368342667	0.022702516	0.828328	0.060461284	-2.2488	0.00205415
Zdhhc8	0.126728933	0.019343547	0.342570333	0.023821438	-2.70317	0.00215285
Pdxk-ps	0.096995867	0.018642683	0.287435667	0.020004751	-2.96338	0.0022344
Sytl1	0.604414	0.179648086	2.101663333	0.118171666	-3.47719	0.00223616
2810428I15Rik	4.463186667	0.921483427	11.11383333	0.287765485	-2.49012	0.00232701
Cdh10	0.001968153	0.001968153	0.0388466	0.005037695	-19.7376	0.00241841
Crtc2	2.243013333	0.394312397	5.3521	0.233791346	-2.38612	0.00246704
Plppr3	1.967716667	0.38590679	5.25195	0.293871712	-2.66906	0.0024828

Ager	0.104496467	0.025846439	0.303088333	0.013888568	-2.90046	0.00248628
1700037C18Rik	0.138370233	0.032551995	0.461256	0.035118412	-3.33349	0.00252117
Pacrgl	1.155256	0.157160799	2.620743333	0.151716877	-2.26854	0.00256945
BC029722	0.887579	0.198667403	2.300916667	0.072052365	-2.59236	0.00259949
Mxd4	0.357082667	0.037625397	0.834653	0.061427724	-2.33742	0.00268545
Pim2	2.65015	0.553959475	8.942656667	0.785961471	-3.37439	0.00281836
Rhbdf1	0.474124333	0.079911436	1.010115667	0.017970167	-2.13049	0.00281864
Nbeal2	0.687516667	0.096001534	1.630303333	0.108596151	-2.37129	0.00288283
Hbb-b2	5.538876667	1.178297203	16.2985	1.166132502	-2.94257	0.00290593
Hbb-bt	5.538876667	1.178297203	16.2985	1.166132502	-2.94257	0.00290593
Trim16	0.755176	0.085458859	3.33709	0.39034347	-4.41896	0.0029545
Nlrp1b	0.049862033	0.014172652	0.864582333	0.125531692	-17.3395	0.00297538
Mocs1	0.662081667	0.143404431	1.58091	0.016048459	-2.38779	0.00311914
Mcf2l	0.098545233	0.009287629	0.339370667	0.036730921	-3.4438	0.00313933
Pkdcc	0.010210333	0.010210333	0.133126333	0.016556651	-13.0384	0.00320866
Ikzf4	0.565255	0.14273054	1.559456667	0.078559723	-2.75886	0.00364896
Tgfbr3l	0.138265	0.045926213	0.43939	0.02149092	-3.17789	0.0040314
6030498E09Rik	1.360526667	0.137003315	2.886293333	0.220266452	-2.12145	0.00417531
Trpv4	0.0181748	0.009150895	0.0848782	0.006715596	-4.67011	0.00418925
Slc1a4	0.042971733	0.012014977	0.172579333	0.018545535	-4.01611	0.00421887
Stk38l	3.255873333	0.311206795	6.84161	0.526479702	-2.10131	0.00422464
Emp1	0.037814333	0.005305434	0.327030667	0.049171222	-8.64832	0.00426487
Arid5a	1.021930667	0.175413149	2.059873333	0.028027209	-2.01567	0.00427767
Cant1	0.905351667	0.172641374	3.217416667	0.362091346	-3.55378	0.0044963
Ccdc166	0.711257	0.160436103	1.732353333	0.080009001	-2.43563	0.00469494
6820408C15Rik	0.033142533	0.009254596	0.091078067	0.004365584	-2.74807	0.0047972
Slc5a2	0.1258928	0.051968334	0.666279333	0.080374086	-5.29244	0.00484634
Mvp	1.421673333	0.118546831	3.068113333	0.26667964	-2.1581	0.00486012
Nfkbib	1.218919	0.296693813	2.9821	0.103575351	-2.44652	0.0049577
Rrad	0.183365667	0.053356841	0.536055333	0.033353894	-2.92342	0.00497597
Chmp4c	0.0052634	0.0052634	0.036441533	0.001854269	-6.92357	0.00503431
Il20rb	0.011406167	0.011406167	0.0799855	0.004554813	-7.01249	0.00504496
Actn3	0.0728614	0.016187069	0.170465333	0.006676637	-2.33958	0.00507632
Arhgef10	0.552997667	0.083410374	1.114276667	0.057195045	-2.01497	0.00515766
Catsperg1	0.422413	0.047630803	1.093260667	0.111362387	-2.58813	0.00519503
Slc27a1	0.947949333	0.188319793	2.09026	0.084390205	-2.20504	0.00520597
Apobr	0.693869333	0.076745391	1.8039	0.185722923	-2.59977	0.00524586
Robo3	0.095301133	0.008877602	0.229466333	0.022658373	-2.4078	0.00528224
Ppargc1a	0.209158	0.023517331	0.445263333	0.035844287	-2.12884	0.00530227
Usp35	0.0202492	0.000716668	0.0490892	0.005208703	-2.42426	0.00538019
Ankrd50	0.369393333	0.073209077	0.840809667	0.048091908	-2.27619	0.00576111

N4bp3	0.066343367	0.007456307	0.200478	0.023788698	-3.02182	0.00576663
Alkbh2	0.200382	0.053778366	0.747902667	0.086599215	-3.73239	0.00580316
5031439G07Rik	0.162060667	0.025245528	0.399275	0.036253512	-2.46374	0.00580901
Cyp27a1	0.336269	0.092339351	1.094991333	0.106969858	-3.25629	0.0058107
Vmn2r46	0.001179646	0.001167893	0.037470533	0.006681338	-31.7643	0.00588343
Zc3h7b	0.906199667	0.239020758	2.46754	0.169126339	-2.72295	0.0059559
Jak3	0.563116333	0.156881321	1.684543333	0.14045703	-2.99146	0.00598271
Wls	14.14873333	1.740599064	28.51776667	2.06453346	-2.01557	0.00600073
Antxr2	0.913632667	0.127777821	1.941916667	0.144990233	-2.12549	0.00600268
Myo1e	0.0977176	0.03732688	0.376650667	0.036907759	-3.85448	0.00603089
2810429I04Rik	0.125197567	0.027952431	0.436077	0.052215645	-3.48311	0.0063016
Rnase4	1.614783333	0.206264847	3.405373333	0.274317219	-2.10887	0.00644004
Rabac1	10.96643667	1.92361175	22.0298	0.906817211	-2.00884	0.00650611
Ndrg4	0.303899	0.075807474	0.760378667	0.044624879	-2.50208	0.00656447
Plekhg6	0.265297333	0.040595302	0.881090333	0.111927558	-3.32114	0.00664249
Pcdhgb4	0.079867567	0.027666208	0.298491667	0.031992117	-3.73734	0.00665679
Ubl3	4.386566667	0.510696227	9.480423333	0.84457002	-2.16123	0.00669278
A430057M04Rik	0.093523267	0.028114778	0.240201	0.005332572	-2.56836	0.00685872
Akt1s1	0.361164667	0.015076045	1.20097	0.163357952	-3.32527	0.00689033
Pacsin1	0.004508167	0.004508167	0.0743657	0.0128942	-16.4958	0.00691405
Cbx8	0.312065333	0.035369103	0.737297	0.075294101	-2.36264	0.00692585
Ppp1r15a	4.98721	0.731368959	12.24926667	1.218111914	-2.45614	0.00692838
Foxp2	0.019791773	0.006692659	0.0544127	0.001221119	-2.74926	0.00703655
Fos	0.998012667	0.449878858	13.54475333	2.439594991	-13.5717	0.00719231
Ntng2	0.004896833	0.004896833	0.0651039	0.010916468	-13.2951	0.00732233
Ropn1l	0.966026667	0.189067429	2.148866667	0.139770729	-2.22444	0.00732941
Tmem86a	0.793568667	0.122674703	1.66543	0.123139946	-2.09866	0.00740665
Hmga1	2.84386	0.438173195	7.58733	0.841833806	-2.66797	0.00750009
BC018473	1.0232503	0.968333358	19.7004	3.611083231	-19.2528	0.00751338
Yipf3	2.083826667	0.356103562	4.574633333	0.349745054	-2.1953	0.00754216
Arrdc2	0.213781333	0.041029805	0.516808	0.044978748	-2.41746	0.00761166
Pitpnm1	0.558114333	0.037578491	1.466636667	0.178631974	-2.62784	0.0076129
Prx	0.0633828	0.024739957	0.251257667	0.028524072	-3.96413	0.0076205
Tgm5	0.374542	0.077861079	1.208299	0.149142949	-3.22607	0.00772996
Col4a6	0.002996367	0.001780941	0.026955533	0.004497682	-8.99608	0.0077455
Ubxn6	2.949456667	0.511551808	6.247926667	0.426534426	-2.11833	0.00774847
Gm17745	0.947168667	0.203242694	2.40827	0.214417192	-2.5426	0.00778569
Osgep	3.904063333	1.278637655	10.30631667	0.209003928	-2.63989	0.00780834
Ifi44l	0.017945	0.009414705	4.772526667	0.963153965	-265.953	0.00783779
Tgfbi	2.02981	0.336256939	6.392096667	0.817431143	-3.14911	0.00784293
Klc1	0.376422667	0.08177976	0.829579667	0.041795094	-2.20385	0.0078495

0610038B21Rik	0.004112967	0.004112967	0.080779167	0.015013034	-19.6401	0.00790002
9130008F23Rik	1.121753	0.162573918	2.38359	0.199711615	-2.12488	0.00804393
Creld1	0.782961667	0.094293812	2.090046667	0.250050259	-2.66941	0.00809565
Mzb1	0.1122292	0.035495147	0.559807	0.084570164	-4.98806	0.00816076
Slc39a3	0.232284667	0.022732411	0.578308667	0.067244249	-2.48966	0.00819142
Sbk2	0.0164988	0.0164988	0.132955667	0.017281959	-8.0585	0.0081953
Klrb1a	0.085552167	0.05172135	0.527375333	0.074627015	-6.16437	0.00824345
Slc25a47	0.047068467	0.00571749	0.22254	0.035641866	-4.728	0.00827302
Nr4a3	0.004701723	0.002357394	0.0196899	0.002008122	-4.18781	0.00840024
Pdpn	0.0086663	0.00458897	0.090673667	0.01636795	-10.4628	0.00849686
Dgkh	0.068762967	0.023703525	0.182805	0.000953099	-2.65847	0.00860241
Gm10406	0.006392667	0.006392667	0.070369167	0.011694935	-11.0078	0.00864736
Pcsk4	0.339648	0.095481826	0.917828333	0.074073622	-2.7023	0.00874698
Abca7	0.545889	0.112779963	1.111163333	0.035257242	-2.03551	0.00875068
Pycr2	2.435936667	0.616663753	5.542826667	0.20850831	-2.27544	0.008822
Serpinh1	0.873454333	0.052430028	2.65019	0.371085355	-3.03415	0.00903167
Rassf9	0.0108958	0.005716399	0.054320933	0.007190694	-4.9855	0.00912226
Igfbp4	3.536453333	1.099664446	9.3403	0.550907729	-2.64115	0.00917984
Ncdn	0.398379	0.073223991	0.840782333	0.058952953	-2.11051	0.00926642
Srcin1	0.001798723	0.001798723	0.0130836	0.001589681	-7.27382	0.00930141
Mfsd10	5.717826667	1.56625718	13.17803333	0.265269481	-2.30473	0.00933462
Eif4ebp1	6.357166667	1.531559341	14.71203333	0.906028716	-2.31424	0.00934204
Tnfrsf1a	6.886783333	1.666057084	14.97343333	0.448813567	-2.17423	0.00940073
Csnk1g2	1.014471667	0.147006306	2.30765	0.233922041	-2.27473	0.00944292
Shd	0.0471436	0.016857478	0.130994333	0.006230329	-2.77863	0.00954913
Tspan2	0.425516667	0.031111323	0.946856667	0.107375009	-2.2252	0.00956468
Dusp5	0.1078194	0.018577238	0.3716	0.053435971	-3.44651	0.00957051
Pgam2	0.088998033	0.003149832	0.219365333	0.027830347	-2.46483	0.00962812
Rap1gap	0.253696	0.018833079	0.543847	0.059612924	-2.14369	0.00972559
9030617O03Rik	0.517218	0.004875179	1.164144	0.139378382	-2.25078	0.00974349
Isyna1	2.943493333	0.930815693	7.415856667	0.258786925	-2.51941	0.0098131
Dctn1	0.777758667	0.151527782	1.757436667	0.148035362	-2.25962	0.00984636
S1pr4	2.007036667	0.326992213	5.310466667	0.636248372	-2.64593	0.00989686
Ap2a1	0.242731	0.072777662	0.580578667	0.009144129	-2.39186	0.00998577
Cfap45	0.059092833	0.032431439	0.249662333	0.025804434	-4.22491	0.0100449
Fam195a	0.987151	0.324784114	2.839	0.238804753	-2.87595	0.0100787
Fhod1	0.394418333	0.05089738	0.93464	0.106757909	-2.36966	0.0102786
Spr	1.590534667	0.395378939	5.60443	0.786034439	-3.52361	0.0103239
Habp2	0.0609394	0.012888552	0.126254333	0.006294131	-2.07181	0.0103885
Rapgefl1	0.139962733	0.038459344	1.028098667	0.191568895	-7.3455	0.0104539
Acvr1	0.460579333	0.106095883	0.952711	0.023005565	-2.06851	0.0105515

Rps6kb2	2.218486667	0.449017601	4.65213	0.295379783	-2.09698	0.0105933
Syne4	0.125009467	0.032588244	0.382222	0.046597719	-3.05755	0.0106304
Fam110a	4.396153333	1.023276815	9.053606667	0.119229342	-2.05944	0.0106508
Anapc7	1.555515667	0.375203716	3.34815	0.133230202	-2.15244	0.0108031
Prpf19	0.602152	0.16424439	1.60163	0.150125422	-2.65984	0.0108918
Ormdl3	5.17696	1.278010113	12.57833333	1.053104547	-2.42968	0.0110792
Ccdc86	0.846981	0.171764671	1.826206667	0.13663777	-2.15613	0.0111476
Arhgef10l	0.02576895	0.009591266	0.1180457	0.018366145	-4.58093	0.0112159
Ildr2	0.00355222	0.000777728	0.010093223	0.001246157	-2.84139	0.0112217
Josd2	2.029453333	0.570284623	5.23539	0.439790997	-2.5797	0.0112324
Nkx6-2	0.124179933	0.032731669	0.301258667	0.022737716	-2.42598	0.0113064
Acap1	13.60256667	2.51412225	29.9975	2.701754436	-2.20528	0.0113131
Gipc1	1.039609667	0.332525714	2.723076667	0.182040184	-2.61933	0.0113271
Speg	0.148107133	0.060595155	0.424767333	0.014580328	-2.86797	0.0113427
Ccdc64	0.0897459	0.042603406	0.436274	0.065518057	-4.86121	0.0113863
Syt14	0.0193461	0.004502389	0.060783533	0.008214162	-3.1419	0.011478
2010107G23Rik	0.188031667	0.061051341	0.501440333	0.036008077	-2.66679	0.0114954
5031434O11Rik	0.511774667	0.067698494	1.169991	0.132632639	-2.28614	0.0115092
Mink1	0.796622	0.085586539	1.896483333	0.234283637	-2.38066	0.0116046
Nox4	0.034155693	0.030474845	0.234500333	0.033826724	-6.86563	0.0116886
Arhgef40	0.561027667	0.064402341	1.327976667	0.162018363	-2.36704	0.0117005
Matk	4.612493333	1.193901391	10.29729667	0.494763049	-2.23248	0.0117023
Chchd2	15.03397	4.998046001	38.0728	1.59850214	-2.53245	0.0117783
Rab1b	3.992196667	0.955393056	8.526783333	0.396285311	-2.13586	0.0118367
Nectin1	0.118975367	0.01497338	0.270812333	0.031231418	-2.27621	0.0118392
Nectin2	0.082754633	0.025935308	0.263571	0.032081829	-3.18498	0.011847
Nr1d2	1.014303	0.235823559	2.068486667	0.050685174	-2.03932	0.0119643
Adora1	0.005713923	0.003572003	0.0359262	0.005928878	-6.28747	0.0120166
Slc15a3	0.058447567	0.013078842	0.196172	0.028742982	-3.35638	0.01205
Sart3	0.727451667	0.056576713	1.528033333	0.174809519	-2.10053	0.0120884
Lgi3	0.004931007	0.002611061	0.046918067	0.009282934	-9.51491	0.0121182
Lonrf2	0.008636667	0.008636667	0.054257733	0.005949057	-6.28225	0.0121559
Ltbp4	0.0497649	0.022940353	0.366372667	0.069449548	-7.36207	0.0123617
Als2cl	0.759714	0.020132116	1.531596667	0.177261906	-2.01602	0.0123822
Gnai1	0.0977782	0.015651688	0.234481667	0.027518269	-2.3981	0.0124656
Pdgfra	0.007647233	0.007647233	0.0472041	0.005046373	-6.1727	0.0124731
Homer1	0.265617667	0.064524615	0.656434	0.063634906	-2.47135	0.0125216
Gm20605	0.1334674	0.066935795	0.617791	0.090549156	-4.62877	0.0126342
Cxcr3	0.1639044	0.054351041	0.609519	0.088214007	-3.71874	0.0126383
Lama4	0.038935967	0.009343824	0.132484667	0.019655656	-3.40262	0.0126614
Ctbp1	3.633906667	0.850050357	7.61633	0.370560204	-2.09591	0.0126997

Tnfsf12	0.555146667	0.110261574	1.113966333	0.069788457	-2.00661	0.012823
Dmrtc1a	0.011771867	0.011771867	0.066270833	0.004872074	-5.6296	0.0128711
Lin28b	0.050335967	0.017851445	0.13721	0.009754187	-2.72588	0.0129443
Abr	0.844857667	0.192669734	2.262706667	0.271009847	-2.6782	0.0130123
Iba57	0.1291109	0.047818378	0.336961	0.009735063	-2.60986	0.0130609
Chpf2	0.416868	0.187363722	1.370263333	0.12273075	-3.28704	0.0130893
Cc2d1a	0.602065	0.148004272	1.249926667	0.037203851	-2.07606	0.0132081
Ninj1	13.69235333	3.575939849	29.42513333	0.97420154	-2.14902	0.0132117
Llgl2	0.0618692	0.007124818	0.125014333	0.013063636	-2.02063	0.0132254
Ooep	0.063253567	0.023166631	0.177426667	0.013694122	-2.805	0.0132366
Plpp7	0.297023	0.114221837	0.832968667	0.055204716	-2.80439	0.0134279
Zfp36	8.31855	2.573426921	38.933	6.800684618	-4.68026	0.0135827
Ddx54	0.490287	0.151296703	1.129616667	0.016572014	-2.304	0.0136897
Rps10	73.6621	14.4877046	149.5	10.82877585	-2.02954	0.0137747
Rbck1	2.28045	0.569053983	4.734306667	0.13755778	-2.07604	0.0137903
Sema7a	0.063891657	0.032300704	0.209551333	0.01285341	-3.27978	0.0138074
Actr1b	4.308726667	0.649417421	8.814836667	0.864505493	-2.04581	0.0140601
4930404N11Rik	0.411395667	0.086155608	1.057733667	0.129176538	-2.57109	0.0141152
9330151L19Rik	0.35659	0.033613451	0.724621	0.081795594	-2.03208	0.0141257
Cltb	1.693653333	0.291028488	3.799183333	0.414696299	-2.24319	0.0141914
Ddah2	5.069463333	0.819683192	11.39647667	1.284108259	-2.24806	0.0142238
Sars2	0.848881333	0.093459817	1.765893333	0.200286361	-2.08026	0.0142717
Plekhf1	0.477408	0.078055913	1.097690333	0.127553119	-2.29927	0.0142847
Klrb1b	0.0058385	0.0058385	0.102910067	0.022697562	-17.6261	0.0143541
Med25	0.401475	0.092037224	0.809879667	0.035491365	-2.01726	0.014374
Osbpl5	0.447100333	0.04213013	1.063348	0.143054495	-2.37832	0.0144672
Ephb4	0.314247	0.074951667	0.902001333	0.121386382	-2.87035	0.0146133
Ydjc	0.250072333	0.061219053	0.549812667	0.039378177	-2.19862	0.0146377
Ctsf	3.070153333	0.704543228	6.534886667	0.460980932	-2.12852	0.0146707
Ldb1	2.753656667	0.51192006	6.129093333	0.641409077	-2.2258	0.0146946
Hyls1	0.468588	0.133158977	1.051751667	0.048854824	-2.24452	0.0147145
Hist1h2bc	3.226696667	0.401391881	8.764876667	1.286692971	-2.71637	0.0147455
Sh3rf3	0.01286424	0.001562644	0.028842767	0.003561087	-2.24209	0.0147464
Swsap1	0.607752667	0.073331051	1.250773333	0.13870691	-2.05803	0.0148734
Tpd52l1	0.1919089	0.069094164	0.602528	0.0726624	-3.13966	0.0149117
Kazn	0.289347333	0.070564683	0.816500667	0.107778704	-2.82188	0.0149503
Dagla	0.00222366	0.00222366	0.019840267	0.003689852	-8.92235	0.0149852
Gchfr	4.31352	0.611510177	10.14852667	1.290594205	-2.35272	0.0150276
Mrpl38	1.432590333	0.334249014	3.721833333	0.45038817	-2.59797	0.0150783
Cox5b	18.81763333	4.604065158	40.8317	2.820884703	-2.16986	0.0151352
Ercc2	0.347670333	0.023848501	1.235740333	0.21684086	-3.55435	0.0152112

Ube2e2	1.162501333	0.158855993	2.61364	0.319136467	-2.24829	0.0152147
Pla2g1b	0.022695833	0.022695833	0.118171	0.006013084	-5.20672	0.0152677
Cystm1	0.042196667	0.027934713	0.171147333	0.015015725	-4.05595	0.0152734
Ctu2	0.543544	0.143063885	1.54188	0.199692935	-2.83672	0.0152975
5730559C18Rik	0.002079007	0.002079007	0.0224837	0.004597919	-10.8146	0.015557
Pik3r6	0.031319	0.016327018	0.530735667	0.122482414	-16.9461	0.015582
1700052K11Rik	0.117972633	0.01686239	0.237416	0.024272513	-2.01247	0.015586
Dusp1	1.266375	0.283255003	6.15678	1.177071749	-4.86174	0.0156116
Fndc7	0.006415333	0.006415333	0.034108767	0.002425005	-5.31677	0.0156308
Arhgap27	1.066471	0.219586741	2.301116667	0.213739821	-2.15769	0.0157464
Hmga1-rs1	6.7367	2.278042051	19.25726667	2.114722373	-2.85856	0.0157584
Ap2s1	5.335403333	1.130528859	11.73806333	1.120873197	-2.20003	0.015841
Piezo1	0.1731288	0.066846906	0.558983	0.068933388	-3.22871	0.0158857
Apba3	0.234391333	0.072229523	0.578672667	0.046153684	-2.46883	0.0159102
Zfp213	0.258436667	0.023786722	0.901392667	0.158318844	-3.48787	0.0159164
Gramd1a	1.874383333	0.199546038	3.949203333	0.477069015	-2.10694	0.0159664
Hsd17b14	0.183401567	0.077580235	0.632191	0.080747759	-3.44703	0.0160249
Slc6a9	0.1144772	0.03191112	0.37069	0.055427267	-3.23811	0.0160496
LOC105246506	0.311938667	0.070027076	0.705764	0.069101172	-2.26251	0.0160888
Akna	0.57413	0.100486602	1.203431333	0.121143674	-2.09609	0.0161541
Map3k6	0.025328367	0.013039165	0.100462833	0.013539384	-3.96642	0.0161692
Ppp1r37	0.1405475	0.032039739	0.384254333	0.051897108	-2.73398	0.0161865
Gramd4	0.732592	0.07526533	2.25635	0.373912268	-3.07995	0.0161969
Igsf9	0.0468321	0.009746211	0.116214233	0.014399751	-2.48151	0.0162618
Gm5129	0.098729367	0.076499012	0.461355333	0.049219797	-4.67292	0.0163136
Slco3a1	1.43077	0.221002678	2.90937	0.298630612	-2.03343	0.0164019
Bmp8a	0.0890998	0.010262219	0.338454	0.062089424	-3.7986	0.0166454
Fam219a	0.047198867	0.024019524	0.157688333	0.014338698	-3.34094	0.0168214
Csf2rb2	1.021685	0.17516212	2.051296667	0.193194766	-2.00776	0.0168432
Rcl1	3.700123333	0.907099763	8.011343333	0.610394738	-2.16516	0.0169154
Rilpl2	2.389436667	0.390552902	5.318046667	0.632149299	-2.22565	0.016942
Tmem17	0.287236333	0.040136539	0.644322667	0.081316618	-2.24318	0.0169917
Ppcs	2.208613333	0.53593801	4.773956667	0.370630512	-2.16151	0.0170038
Zfp85os	0.154240633	0.036920404	0.328996667	0.024693994	-2.13301	0.0170398
Axl	1.163254	0.213338257	2.53546	0.276161715	-2.17963	0.0170715
Edn3	0.012419633	0.006970997	0.042557167	0.003231834	-3.42661	0.0172148
2410004P03Rik	0.1809276	0.106237791	0.632336333	0.044456505	-3.49497	0.0172523
Itga3	0.1195369	0.039596625	0.297697	0.022419398	-2.49042	0.0173154
Ptprf	0.025868857	0.011429918	0.089794733	0.011659665	-3.47115	0.0173176
Cnn3	0.290046	0.024146411	0.899349	0.153772578	-3.10071	0.0173293

Palm	0.100978433	0.018567257	0.323998	0.053923842	-3.20859	0.0173863
Hist1h1c	1.030044	0.413932684	2.874066667	0.227833175	-2.79024	0.0175003
C2cd2l	0.149037967	0.030530735	0.406286667	0.058543278	-2.72606	0.0175986
Sbf1	0.671631667	0.13089694	1.787343333	0.255564435	-2.6612	0.0177561
Zfp618	0.200050667	0.013102435	0.453612333	0.063952771	-2.26749	0.0177785
Prodh	3.829136667	0.764066647	8.52968	0.939204051	-2.22757	0.0178053
Tox3	0.0039236	0.0039236	0.076584967	0.018312966	-19.519	0.0178458
Spsb4	0.062417033	0.006626427	0.165065667	0.02563388	-2.64456	0.0178872
Plxna3	0.383510667	0.04650308	0.774	0.089383048	-2.0182	0.0179084
Fzd2	0.00259688	0.00259688	0.0301777	0.00664189	-11.6207	0.0180324
Ier3	5.315423333	1.264931403	11.22464667	0.860324813	-2.11171	0.018104
Hbegf	0.562839333	0.089602627	1.160595	0.126195596	-2.06204	0.018113
AI467606	6.251883333	1.323362059	12.59283333	0.971934842	-2.01425	0.0181185
Csrnp1	1.75316	0.351353125	3.540573333	0.302052914	-2.01954	0.0181833
Ptpn18	5.891523333	1.410828681	11.90686667	0.667460751	-2.02102	0.018238
Vars	1.57608	0.598130464	4.63813	0.526599213	-2.94283	0.0184218
Gli1	0.033760033	0.00569679	0.097891633	0.015700947	-2.89963	0.0184652
Tjap1	0.753126333	0.237541024	1.70026	0.068273935	-2.25761	0.0185842
Cdh15	0.173166667	0.018395188	0.558383667	0.098845385	-3.22455	0.0185961
Nrbp2	0.243588667	0.083556236	0.751075667	0.102884811	-3.08337	0.0186353
Tmcc3	0.107290667	0.011540489	0.219394333	0.026955493	-2.04486	0.0187269
Rn45s	40.1307	9.8452222	83.4362	5.603334637	-2.07911	0.0187327
Sdsl	2.28522	0.472119522	4.63699	0.394423322	-2.02912	0.0187333
Cox4i2	2.26057	0.337300506	7.883236667	1.438012321	-3.48727	0.0189934
Zc3h12a	0.0577953	0.019008379	0.146227333	0.01339867	-2.53009	0.0190615
Shb	0.0919995	0.011765513	0.341726333	0.064620273	-3.71445	0.0190705
Hopx	0.005080333	0.005080333	0.042597667	0.008474774	-8.38482	0.0191536
Sv2a	0.0668411	0.003271014	0.232057667	0.043401844	-3.47178	0.0191714
Gfod2	0.806866	0.196664526	1.89332	0.208552592	-2.34651	0.019267
5430416N02Rik	4.084133333	0.581628571	8.232483333	0.931339927	-2.01573	0.0194705
Ccdc107	3.963153333	1.472821389	9.531103333	0.101522237	-2.40493	0.0195788
Fuz	0.710834	0.15096398	1.42789	0.115656342	-2.00876	0.0195954
Cmtm8	0.797993667	0.126874827	1.82888	0.242184737	-2.29184	0.0195956
AI661453	0.0376995	0.010181231	0.095002	0.011295172	-2.51998	0.0196337
Il17re	0.704684333	0.240602032	2.59543	0.440775773	-3.68311	0.0196869
Atp5d	14.11860667	5.115053191	33.96246667	1.418600538	-2.40551	0.0201494
Coro1a	43.42803333	8.914485352	90.4071	8.914651076	-2.08177	0.0203606
Tmbim7	0.033284367	0.009685259	0.082810667	0.009192607	-2.48798	0.0206731
Fbxw4	0.979474333	0.056144875	1.976056667	0.263499197	-2.01746	0.0208531
Dennd2a	0.207481667	0.023751721	0.568415	0.094871179	-2.73959	0.0210084
Dhrs11	1.754946667	0.297874627	3.88785	0.496433782	-2.21537	0.0211271

Kdf1	0.040131233	0.012484761	0.1273811	0.020124723	-3.17411	0.0211277
Slc3a2	4.63746	0.500011096	9.444576667	1.207895353	-2.03659	0.0212576
Kctd13	0.419219	0.102993781	0.990992	0.116971003	-2.36389	0.0214159
Gbp2b	0.081084467	0.026977639	2.736186667	0.723770812	-33.7449	0.0214689
Arrb2	1.030261667	0.233971065	2.134973333	0.192332012	-2.07227	0.0218209
Il3ra	0.136733333	0.007837811	0.375769	0.065217778	-2.7482	0.0219837
Actr1a	6.837883333	1.174951453	16.89003333	2.504799956	-2.47007	0.0220952
Klhl11	0.0764445	0.033699651	0.198973333	0.001274449	-2.60284	0.0220952
Tnfrsf13c	1.647383333	0.357019108	4.123266667	0.581446473	-2.50292	0.0221856
St3gal2	1.096093667	0.184814475	2.305953333	0.278788237	-2.10379	0.0224148
St6galnac2	0.202008567	0.114233073	2.562063333	0.642887359	-12.6829	0.0224684
Adam11	0.425179667	0.054319989	1.72806	0.356425964	-4.06431	0.0224832
Cog8	0.1560078	0.074634291	0.475682333	0.047897192	-3.0491	0.0226622
S100a2	0.019885867	0.019885867	0.116198733	0.01787371	-5.84328	0.0227155
Prex1	0.664112333	0.128983235	1.500613333	0.193156914	-2.25958	0.022727
Trim46	0.439176333	0.069092271	0.972915	0.131226717	-2.21532	0.0227795
Tmcc2	0.482471	0.10709657	1.006408	0.098717372	-2.08594	0.0228157
Nr1d1	1.028071667	0.094535753	2.111276667	0.286201224	-2.05363	0.0228838
Enkur	0.91934	0.190048296	2.32171	0.341725138	-2.5254	0.0230344
Med16	0.571185333	0.075288669	1.233495667	0.168796939	-2.15954	0.0230966
Jag2	0.083637467	0.0132743	0.210892667	0.032958553	-2.52151	0.0231364
Sfxn2	2.866673333	0.123921828	5.935563333	0.848211787	-2.07054	0.0231662
Mpst	0.139135533	0.050030989	1.339588667	0.332378336	-9.62794	0.0233451
Nle1	3.55372	0.458710427	7.897536667	1.126569626	-2.22233	0.023353
Smg9	0.687807333	0.177054107	1.48776	0.137633939	-2.16304	0.0234363
Arhgef17	0.084385367	0.028409672	0.239278	0.032917874	-2.83554	0.0235394
Cd248	0.1051939	0.062649776	0.332402333	0.012126583	-3.1599	0.0235743
Mfsd4b4	0.0942904	0.061743172	0.323737333	0.018473403	-3.4334	0.0235818
Fam131a	0.285012	0.020465809	0.913094	0.175867324	-3.2037	0.0238538
Vps4a	2.750623333	0.481561955	5.58385	0.638548622	-2.03003	0.0239592
Xrcc1	1.346107667	0.350911878	2.87349	0.250797236	-2.13467	0.023988
Ear12	0.001324285	0.001324273	0.1078603	0.030093417	-81.448	0.0240835
Ear3	0.001324285	0.001324273	0.1078603	0.030093417	-81.448	0.0240835
Fasn	0.670196667	0.174727275	1.39532	0.108015458	-2.08196	0.0242317
Rcor2	0.250365667	0.071005708	0.616969	0.076204847	-2.46427	0.0244574
Guk1	6.10286	1.485784062	13.67083333	1.560774231	-2.24007	0.0246276
Dmap1	1.979743333	0.538199332	4.05105	0.243882667	-2.04625	0.0247732
Dlk1	0.047821467	0.00435456	0.104988833	0.015748963	-2.19543	0.024927
Arhgap20os	0.040877033	0.01772408	0.1190613	0.013655451	-2.91267	0.0250237
Skint3	0.458962333	0.054118335	0.933059667	0.124425712	-2.03298	0.0250297
Syt3	0.075596867	0.024391517	0.190738667	0.022295328	-2.5231	0.0252535

Sox13	0.252573667	0.078908714	0.54087	0.024921174	-2.14143	0.0252618
Lrrc61	0.401493667	0.098663381	1.036286333	0.153981906	-2.58107	0.0255581
Gna15	1.478567333	0.461951312	3.590053333	0.39612847	-2.42807	0.0255886
Fkbp10	0.384346667	0.12160053	1.029982333	0.14163932	-2.67983	0.0258515
Sbno2	1.455126333	0.445219169	3.71239	0.478031203	-2.55125	0.0259253
Shf	0.024156033	0.01207805	0.090120633	0.014846402	-3.73077	0.0261346
Mier2	0.342641	0.15465346	1.037982667	0.129610572	-3.02936	0.0261505
Bzrap1	0.013765403	0.004817022	0.0424097	0.006775537	-3.08089	0.0261598
Pigt	0.918496667	0.283048844	2.198133333	0.242179594	-2.39319	0.0264111
Scarf1	5.40991	1.142927495	12.20925667	1.617221846	-2.25683	0.026452
Slc7a3	0.0114649	0.005748377	0.105203367	0.026776994	-9.17614	0.0267133
Ptgfrn	0.002710947	0.001435496	0.0411714	0.01116713	-15.1871	0.0268797
Depdc1b	0.587025333	0.112159014	1.531686667	0.253481974	-2.60924	0.0270766
Sntb1	0.00290945	0.00290945	0.043845233	0.011657232	-15.0699	0.0270993
Slc9a1	0.976814	0.11423339	2.386446667	0.398051208	-2.44309	0.027179
Skap1	0.191146	0.030591446	0.480052667	0.079277117	-2.51144	0.0272796
Rab4a	2.933636667	0.632164015	6.337033333	0.77642828	-2.16013	0.0272977
Plod3	0.801357667	0.204448293	1.66378	0.150292969	-2.0762	0.0273086
Retn	0.010762967	0.010762967	0.1271686	0.032550853	-11.8154	0.0273951
1110004E09Rik	2.390666667	0.719571439	4.92496	0.212645414	-2.06008	0.0278485
Ap1m2	0.090029867	0.034365042	0.224465	0.020085667	-2.49322	0.0278529
Rbfa	0.539155667	0.131652165	1.186113667	0.139651358	-2.19995	0.0280202
4430402I18Rik	0.223297	0.028971028	0.566979667	0.097776409	-2.53913	0.0280397
Sertad1	2.287246667	0.843580904	6.359443333	0.868877572	-2.78039	0.0282366
Dctn2	4.866363333	0.804290098	10.10233333	1.333807325	-2.07595	0.0282608
Zfp777	0.236993667	0.088775965	0.596568	0.060054599	-2.51723	0.0284409
Clcn2	0.188677	0.019093275	0.501410333	0.091309365	-2.65751	0.0285032
Ifi204	0.898118333	0.705646258	4.464303333	0.797146693	-4.97073	0.0285746
S1pr3	0.217457667	0.058648291	0.481747333	0.052987733	-2.21536	0.0287355
Thy1	0.208380333	0.083443494	0.557137333	0.062592392	-2.67366	0.028743
Gm12709	0.003276177	0.003276177	0.014972667	0.001238604	-4.57016	0.0288498
Pnmal2	0.006054267	0.004008	0.037150267	0.008420147	-6.13622	0.0289823
Tnfsf8	0.0295551	0.015215101	0.087687567	0.008542124	-2.96692	0.0290631
Aoc2	0.179636333	0.007761101	1.573125	0.418352636	-8.75728	0.0290969
Brinp2	0.006109767	0.006109767	0.0361564	0.0066598	-5.91779	0.0292541
Padi4	2.51948	0.728622975	5.116	0.283810435	-2.03058	0.0293624
Eng	2.07934	0.648322603	4.389993333	0.25641737	-2.11124	0.0295372
Atp13a2	1.126154333	0.089893583	2.55249	0.421674429	-2.26655	0.0297039
Carmil2	0.283287	0.075244774	0.587751667	0.053210485	-2.07476	0.0298292
Apof	0.069379467	0.019429192	0.139211333	0.00834186	-2.00653	0.0298581
Crat	0.618759	0.145712529	1.23837	0.119489973	-2.00138	0.0302697

Agpat3	0.475228667	0.113266244	1.015573333	0.119289679	-2.13702	0.0303628
Alox12	0.1194261	0.029542944	0.331985	0.057690451	-2.77984	0.0305159
Lrp10	1.995173333	0.543736282	4.740686667	0.638647009	-2.37608	0.0306937
Atp8b5	0.329571333	0.048822923	0.780222667	0.128938317	-2.36739	0.0308293
Gm13032	0.643332333	0.085944678	1.323182	0.190051566	-2.05677	0.0310984
Itpr3	0.264297667	0.0348777	0.540877333	0.077360205	-2.04647	0.0311019
Rhobtb2	0.553912333	0.059497068	1.132385333	0.16723972	-2.04434	0.0311144
Ptprcap	14.76837667	4.857788901	36.3038	4.484281223	-2.45821	0.0311557
Tecpr1	0.572600667	0.07119735	1.151356	0.162887423	-2.01075	0.0312073
Rarg	0.231730333	0.052810114	0.465601333	0.048707496	-2.00924	0.0312181
Abcb10	0.943580333	0.157249997	2.192726667	0.350058229	-2.32383	0.0312266
Trpm5	0.0498963	0.018853535	0.140926333	0.020743233	-2.82439	0.0314511
Mrpl54	7.12604	3.080496351	17.52076667	0.894933518	-2.4587	0.0316622
Gltscr2	7.856193333	1.419109917	16.37106667	2.213834476	-2.08385	0.0317325
Pde1b	0.553770333	0.0855416	1.160881	0.166998502	-2.09632	0.0318047
Abcc3	0.201875667	0.04390105	0.527297333	0.09098231	-2.61199	0.0322392
Arhgap27os3	0.430301	0.066455843	1.785856667	0.416377394	-4.15025	0.0324373
Gaa	6.59004	0.674459541	13.3889	2.00604893	-2.03169	0.0325117
Tnfrsf25	0.236425	0.051111688	1.190326667	0.292823936	-5.03468	0.0326176
Gas2l1	0.096061833	0.018299119	0.215584333	0.03248773	-2.24422	0.0327293
Gpr165	0.031732167	0.025588274	0.115731667	0.005694155	-3.64715	0.0327643
9430065F17Rik	0.2022118	0.088787033	0.492177333	0.01758054	-2.43397	0.0327865
Tmem160	0.250288333	0.072751497	0.726931	0.129975178	-2.90437	0.0329008
Gtf2h4	3.14329	0.745500609	6.374566667	0.683568882	-2.02799	0.033068
Tymp	0.132260667	0.029541251	0.333190667	0.055546462	-2.51919	0.0330974
Tjp3	0.0457043	0.00503483	0.138543667	0.028666151	-3.03131	0.0332222
Fads3	0.415832	0.082392948	0.962359	0.150349411	-2.3143	0.0332873
Klhl32	0.0118869	0.0118869	0.10727	0.027501548	-9.02421	0.033419
Dohh	0.438886667	0.183989342	1.171032667	0.138556982	-2.66819	0.0335758
Jam3	3.2107	0.377817498	6.882506667	1.091608264	-2.14362	0.0335781
Itprip	1.153834333	0.212467853	2.33146	0.303870532	-2.02062	0.0336616
Pnpla2	6.97133	1.883993747	14.1243	1.241030737	-2.02606	0.0338374
Ppp1r9b	2.350596667	0.475515034	4.79834	0.608566566	-2.04133	0.0338781
Ryr2	0.004292133	0.002428115	0.012700733	0.001076564	-2.95907	0.0339943
Gm16287	0.045008533	0.030142132	0.142719667	0.006706962	-3.17095	0.0340436
Gtpbp6	0.461381	0.104286816	0.943702667	0.11133209	-2.04539	0.0341257
Zfp995	0.073510867	0.024096244	0.176478	0.022020219	-2.40071	0.0343677
Dzip1l	0.0188312	0.009433715	0.0976987	0.023215813	-5.18813	0.0346061
Znhit2	0.1047139	0.048226088	0.368558333	0.068586992	-3.51967	0.0346196
Acsbg1	0.0860138	0.013696781	0.230920667	0.043971289	-2.68469	0.0346348
A230056J06Rik	0.0650326	0.012181395	0.14672	0.022929018	-2.2561	0.0346413

Lrguk	0.00821028	0.005435306	0.060880333	0.015858503	-7.41514	0.034786
Plekha7	0.157631767	0.062537056	0.360629	0.017178494	-2.28779	0.0351825
Qprt	0.168718	0.041592955	0.574049	0.123300572	-3.40242	0.0357024
BC037034	0.272138667	0.089265792	0.555513	0.017813032	-2.04129	0.0357635
Agbl1	0.039492667	0.006114671	0.0974262	0.017586839	-2.46695	0.0358221
1700067G17Rik	0.0713055	0.032603647	0.562312333	0.154563652	-7.88598	0.03593
Treml1	0.949284667	0.162500149	2.025353333	0.305756681	-2.13355	0.0359508
E230013L22Rik	0.124068267	0.018856351	0.282096	0.047373072	-2.27372	0.0362456
Gem	1.834093333	0.212528901	3.879716667	0.625487795	-2.11533	0.0363418
Dab1	0.007275307	0.004970059	0.0231325	0.001256571	-3.17959	0.0364605
Gpr173	0.0191817	0.012153375	0.071685033	0.011908434	-3.73716	0.0367279
Fam135a	0.159568333	0.028051701	0.382518667	0.066592425	-2.3972	0.0367383
Tmem189	0.570634	0.055650484	1.283563333	0.224526358	-2.24937	0.0368593
Ckb	0.488838667	0.207836028	1.13405	0.027703737	-2.31988	0.0370329
Hexim2	0.216845	0.03462946	0.537898333	0.098490916	-2.48056	0.0371053
Cntn3	0.001208577	0.001208577	0.014061763	0.004002472	-11.635	0.0371401
Hist1h2bp	0.140177867	0.041311215	0.511851	0.114071056	-3.65144	0.0375284
Smoc1	0.0711903	0.029242437	0.212768333	0.035786147	-2.98873	0.0375297
Sesn2	0.325877	0.161124338	0.916585	0.107029572	-2.81267	0.0378868
Lmnb2	0.824516	0.216573603	1.657753333	0.166176302	-2.01058	0.0379399
Usf2	1.213154333	0.293035721	2.562323333	0.331067456	-2.11212	0.0379708
Cxx1a	0.127989557	0.085989928	1.157968667	0.326890878	-9.04738	0.0381338
Rasd1	0.7922	0.153753973	1.88145	0.322839258	-2.37497	0.0381719
Agpat9	0.066330033	0.025610218	0.269707333	0.061796044	-4.06615	0.038389
Gpr4	0.199165633	0.073759922	0.826804333	0.192826234	-4.15134	0.038398
Akr1c14	0.041914167	0.026954384	0.272268	0.070854408	-6.49585	0.0384534
Entpd3	0.197839333	0.037594718	0.425365	0.064796042	-2.15006	0.0385068
Cpe	0.0289835	0.017613764	0.093045733	0.011609056	-3.2103	0.0385232
Plekhg1	0.180521667	0.027145404	0.371080667	0.056653871	-2.0556	0.0386533
Phc2	1.264682	0.342979999	3.111313333	0.503136964	-2.46016	0.0386799
Klrb1c	0.957277	0.082700421	2.21068	0.405587746	-2.30934	0.0388563
Tctn2	0.446286	0.151628727	1.061549333	0.135360775	-2.37864	0.0388947
Clip2	0.194953667	0.017722886	0.423597667	0.073431583	-2.17281	0.0389029
Ccdc103	0.033826233	0.028764504	0.164748667	0.032464098	-4.87044	0.039223
1110008P14Rik	0.288321333	0.056928502	0.943114	0.209349111	-3.27105	0.0392342
Git1	0.987949	0.089308346	2.64485	0.542188798	-2.67711	0.0393438
Ccdc120	0.152074	0.020152392	0.3075	0.04745593	-2.02204	0.0393718
Gadd45g	0.664067333	0.099200479	2.362773333	0.554860789	-3.55803	0.0394063
Agap3	0.452156333	0.070569855	1.188596333	0.234085138	-2.62873	0.0394676
Jun	1.298306667	0.542993297	6.66715	1.697985213	-5.13527	0.0394863
Camk2n1	0.038766833	0.028198376	0.126081	0.00687478	-3.25229	0.0396159

Boc	0.1087929	0.035322298	0.264007667	0.037690363	-2.4267	0.0397517
Egr1	2.021918333	0.713394456	8.03635	1.873387801	-3.97463	0.0399313
Rara	0.064549367	0.01911577	0.252864333	0.059791462	-3.91738	0.0399442
Ccm2l	0.846652	0.13408799	1.985413333	0.355320469	-2.34502	0.0400017
Bcar3	0.0291718	0.008488545	0.079035133	0.014311822	-2.7093	0.0400752
Anks1	1.454817	0.324914244	3.09852	0.44222053	-2.12984	0.0401258
Asic1	0.031068063	0.013186444	0.106170467	0.021346137	-3.41734	0.040209
Ifi211	0.441594	0.194900402	1.35595	0.23527553	-3.07058	0.0402264
Rnpepl1	0.710759333	0.16353501	1.754006667	0.308047766	-2.46779	0.0402882
Ccdc116	0.062012633	0.024744778	0.196072333	0.037406286	-3.16181	0.0403755
Rell2	0.545471333	0.131962172	1.383736667	0.247559234	-2.53677	0.0404146
Smurf1	0.405169667	0.09134364	0.853577	0.11928753	-2.10672	0.0405571
Ier2	1.914716667	0.319216165	4.903293333	0.951970586	-2.56084	0.040881
Rtbdn	0.0049379	0.0049379	0.028690967	0.006314661	-5.81037	0.0414236
P2ry10	0.562403333	0.172457083	1.139546667	0.091084282	-2.02621	0.0415881
Rasgrp3	0.179773667	0.021276631	0.440880667	0.085680428	-2.45242	0.0416524
Lrch2	0.239596667	0.046444661	0.535351333	0.088879284	-2.23439	0.0420023
Cracr2b	0.467935667	0.030398763	1.056253667	0.197362256	-2.25726	0.0421294
Scimp	0.205343333	0.096105666	1.004348	0.253690711	-4.89106	0.0421672
Magee1	0.347435	0.091562547	0.710094	0.082707334	-2.04382	0.0424224
Rapgef3	0.270549	0.023012612	0.690636333	0.141154302	-2.55272	0.0425029
Uchl1	0.279291	0.080742855	0.696288	0.117216994	-2.49306	0.0428272
Gm16675	0.129234467	0.049248545	0.444534333	0.095693345	-3.43975	0.0428274
Pcdhgb6	0.271277	0.095833996	0.611251333	0.065638613	-2.25324	0.0429494
Bmp1	0.825521	0.07068801	1.716603333	0.29623582	-2.07942	0.0429904
Gnb2	2.475576667	0.476402989	4.964303333	0.7059599	-2.00531	0.0431495
Ext2	1.336978667	0.355804863	3.130953333	0.501057644	-2.34182	0.0432761
Id1	0.146931833	0.046371617	1.000955333	0.289310898	-6.81237	0.0434723
Lrig3	0.0258732	0.007766843	0.074277133	0.014713731	-2.87082	0.0437101
Arhgef16	0.132827167	0.044224052	0.336867333	0.054521309	-2.53613	0.043833
Vps18	1.118062667	0.318328824	2.271316667	0.2378395	-2.03147	0.0440194
Camkk1	0.536730333	0.090292375	2.115743333	0.537306663	-3.94191	0.0442009
Zfp219	0.235465	0.061985251	0.476084	0.055243486	-2.02189	0.0442078
Acbd4	0.571641333	0.111107103	1.441013333	0.278666451	-2.52084	0.0442098
6720468P15Rik	0.045236	0.019614105	0.136553067	0.024733836	-3.01868	0.0444376
Nab2	0.346081	0.036210664	1.105848667	0.260281048	-3.19535	0.04451
Emp2	0.075752267	0.021365758	0.157316667	0.018432033	-2.07673	0.0445379
Npepl1	2.664	0.400419357	6.044606667	1.100934452	-2.269	0.0447548
Slc7a8	3.37125	1.289559406	8.191066667	1.068823908	-2.42968	0.0451199
Tbc1d16	0.530487667	0.066321796	1.062001333	0.172492556	-2.00193	0.0451904
S1pr2	0.403628667	0.047086806	0.901655	0.166869446	-2.23388	0.0453609

Dcxr	1.477703	0.533433299	3.781873333	0.604437879	-2.55929	0.0460133
Plcxd1	0.252671333	0.068421335	0.593477333	0.097673803	-2.34881	0.0460315
Adamts10	2.189146667	0.398936574	4.395423333	0.66363638	-2.00783	0.0464269
Pnldc1	0.034744033	0.007606913	0.239081	0.071346524	-6.88122	0.0464963
Rhbdl3	0.020267333	0.00742295	0.076540467	0.018325571	-3.77654	0.046578
Bmf	0.109213367	0.041596344	0.241063667	0.02045354	-2.20727	0.0466557
Fosb	0.0901801	0.02023592	0.557517667	0.163134742	-6.18226	0.0467281
Thop1	0.243245667	0.090000303	0.675569667	0.122788091	-2.77731	0.0468793
Exoc3l	0.699345	0.173667013	1.566436667	0.251204059	-2.23986	0.0469006
Pcsk9	0.020261933	0.010920858	0.073802167	0.015380832	-3.64241	0.0469495
Crtc1	0.639868667	0.163663243	1.535896667	0.270200515	-2.40033	0.0470387
Mir5121	0.127317333	0.127317333	0.636358667	0.126625167	-4.99821	0.0471125
Acsf2	0.377635667	0.058366519	1.191637333	0.281304814	-3.15552	0.0471854
Mesp2	0.0896901	0.053299256	0.272647333	0.036684767	-3.03988	0.0474601
Dnmt3aos	0.027987567	0.007905636	0.080474567	0.016827384	-2.87536	0.047677
Kcnd1	0.251367	0.089683167	0.578410333	0.073350868	-2.30106	0.0476942
Majin	0.098611167	0.02599177	0.214736	0.031915442	-2.1776	0.0477665
Tmem132a	0.037861267	0.016586677	0.101189933	0.015129659	-2.67265	0.0477886
Klc4	1.223043333	0.143745627	2.531583333	0.441511425	-2.06991	0.0479167
Tspan9	0.277069333	0.087714947	0.748571667	0.142673346	-2.70175	0.0480589
Gpr162	0.120073867	0.049062241	0.268409667	0.019718883	-2.23537	0.0485478
Gm5820	0.005728433	0.005728433	0.0486652	0.014219787	-8.49537	0.0487728
Dhrs13	0.234833333	0.041384683	0.481983667	0.078163736	-2.05245	0.0490891
Rgs14	0.991107667	0.069667347	2.312416667	0.468153648	-2.33317	0.0492288
Polm	0.192991	0.030342036	0.613705333	0.147983046	-3.17997	0.0495621
Irak4	4.985333333	0.401397089	12.31314333	2.600468399	-2.46987	0.0495692
Fam220a	0.632410333	0.141130309	1.266347667	0.178805959	-2.00241	0.0496679
Sh3bp1	1.375672333	0.403049047	2.81553	0.326171467	-2.04666	0.0499724

Table 2.3 Differentially Expressed Genes with Changes in TSS H3K27me3

Gene	Control Avg RPKM	6bKO Avg RPKM	Change in gene expression (6bKO compared to Control)	Change in H3K27me3 (6bKO compared to Control)
Nlrp1b	0.049862033	0.864582333	Increased	Decreased
Id1	0.146931833	1.000955333	Increased	Decreased
Dhx40	0.423009333	2.32885	Increased	Decreased
Rara	0.064549367	0.252864333	Increased	Decreased
Kdf1	0.040131233	0.1273811	Increased	Decreased
Dgkh	0.068762967	0.182805	Increased	Decreased
Arhgef16	0.132827167	0.336867333	Increased	Decreased
Fscn1	0.368342667	0.828328	Increased	Decreased
Wtip	0.076079967	0.166553	Increased	Decreased
Ear12	0.001324285	0.1078603	Increased	Increased
Slc7a3	0.0114649	0.105203367	Increased	Increased
Col4a6	0.002996367	0.026955533	Increased	Increased
Hopx	0.005080333	0.042597667	Increased	Increased
Rapgefl1	0.139962733	1.028098667	Increased	Increased
Chmp4c	0.0052634	0.036441533	Increased	Increased
Dmrtc1a	0.011771867	0.066270833	Increased	Increased
Slc1a4	0.042971733	0.172579333	Increased	Increased
Gpr173	0.0191817	0.071685033	Increased	Increased
Cxcr3	0.1639044	0.609519	Increased	Increased
Hist1h2bp	0.140177867	0.511851	Increased	Increased
Gpr165	0.031732167	0.115731667	Increased	Increased
Edn3	0.012419633	0.042557167	Increased	Increased
Tspan7	0.161131	0.461752	Increased	Increased
Ooep	0.063253567	0.177426667	Increased	Increased
Chchd2	15.03397	38.0728	Increased	Increased
Syt3	0.075596867	0.190738667	Increased	Increased
Acbd4	0.571641333	1.441013333	Increased	Increased
Boc	0.1087929	0.264007667	Increased	Increased
Ap5b1	0.173386333	0.411751333	Increased	Increased
Actn3	0.0728614	0.170465333	Increased	Increased
Plekhf1	0.477408	1.097690333	Increased	Increased
Pacrgl	1.155256	2.620743333	Increased	Increased
Guk1	6.10286	13.67083333	Increased	Increased
Nle1	3.55372	7.897536667	Increased	Increased
S1pr3	0.217457667	0.481747333	Increased	Increased
Magee1	0.347435	0.710094	Increased	Increased
P2ry10	0.562403333	1.139546667	Increased	Increased
Rarg	0.231730333	0.465601333	Increased	Increased
Tbc1d16	0.530487667	1.062001333	Increased	Increased
Gria3	2.244773333	1.075127333	Decreased	Increased
Nlrp1a	0.276917	0.047135067	Decreased	Increased
Nostrin	0.129872633	0.018865233	Decreased	Increased
Sbspon	0.068623033	0.009503133	Decreased	Increased
Zfp454	0.136019267	0.0187109	Decreased	Increased

Table 2.4: Genotyping Primers

Gene	Primer Sequence
Kdm6b WT/Fl Universal Forward	GCGAGAGACCTGAGGCATGA
Kdm6b WT Reverse	CTCGCCTCCACCAGAGTCTT
Kdm6b Fl/KO Reverse	AGGGGGAAGAGCTTGCACAC
GAPDH Forward (RT-PCR)	AATTTGCCGTGAGTGGAGTC
GAPDH Reverse (RT-PCR)	TGGCAAAGTGGAGATTGTTG
Vav-CRE Forward	AGATGCCAGGACATCAGGAACCTG
Vav-CRE Reverse	ATCAGCCACACCAGACACAGAGATC
Mx-1 CRE Forward	CTGGGGATTGCTTATAACACCC
Mx-1 CRE Reverse	TCATCAGCTACACCAGAGACGG
GAPDH Forward (Cre genotyping)	GCAAGGTCATCCCAGAGC
GAPDH Reverse (Cre genotyping)	TGCAGCGAACTTTATTGATGGTATT
Utx1 Forward	GAGAAAGGAAATGTGAGAGC
Utx1 Reverse	CAGCATAAATGTCTTTCCC

Table 2.5: Flow Cytometry Panels

Cell Type	Tissue	Immunophenotype
Lineage - Myeloid	Blood, WBM, Spleen	CD45.2+, Mac-1+, Gr-1+
Lineage – B-cells	Blood, WBM, Spleen	CD45.2+, B220+
Lineage – T-cells	Blood, WBM, Spleen	CD45.2, CD3e+
Hematopoietic stem cells (HSC) (Naïve)	WBM, Spleen	Lineage- (Mac-1, Gr-1, B220, CD3e, Ter119), CD48-, EPCR+, c-Kit+, Sca-1+, CD150+
Hematopoietic stem cells (HSC) (post-pIpC)	WBM	Lineage- (Mac-1, Gr-1, B220, CD3e, Ter119), CD48-, EPCR+, c-Kit+, CD150+
Hematopoietic stem cells (HSC) (post-5-FU)	WBM	Lineage- (Gr-1, B220, CD3e, Ter119), CD48-, EPCR+, Sca-1+, CD150+
Multipotent Progenitors (MPP)	WBM, Spleen	Lineage- (Mac-1, Gr-1, B220, CD3e, Ter119), CD48-, EPCR+, c-Kit+, Sca-1+, CD150-
Restricted Progenitors (RP)	WBM	Lineage- (Mac-1, Gr-1, B220, CD3e, Ter119), CD48+, EPCR+, c-Kit+, Sca-1+, CD150-
Total Common Lymphoid Progenitors (CLP)	WBM	Lineage- (CD3e, B220, Mac-1, Gr-1, Ter119), c-Kit+, Sca-1^{low}, Flk2+, IL7RA+
Common B-cell lymphoid progenitors (CLP-B)	WBM	Lineage- (CD3e, B220, Mac-1, Gr-1, Ter119), c-Kit+, Sca-1^{low}, Flk2+, IL7rα+, Ly6D+
Immature B-cells	WBM	B220+, IgM+
Pre-Pro-B-cells	WBM	B220+, IgM-, CD43+, CD19-
Pro-B-cells	WBM	B220+, IgM-, CD43+, CD19+
Pre-B-cells	WBM	B220+, IgM-, CD43-, CD19+
Early thymic progenitor (ETP)	Thymus	CD4- CD8a- Lineage- (Mac-1, Gr-1, B220, NK1.1, CD11c, Ter119, CD3e), CD25- c-Kit+
Double negative 1 (DN1)	Thymus	CD4- CD8a- Lineage- (Mac-1, Gr-1, B220, NK1.1, CD11c, Ter119, CD3e), CD25- CD44+
Double negative 2 (DN2)	Thymus	CD4- CD8a- Lineage- (Mac-1, Gr-1, B220, NK1.1, CD11c, Ter119, CD3e), CD25+ c-Kit+
Double negative 3 (DN3)	Thymus	CD4- CD8a- Lineage- (Mac-1, Gr-1, B220, NK1.1, CD11c, Ter119, CD3e), CD25+ c-Kit-
Proerythroblasts	Spleen	Lineage- (CD3e, B220, Gr-1, Mac-1), CD71+, Ter119^{low}
Maturing Erythroblasts	Spleen	Lineage- (CD3e, B220, Gr-1, Mac-1), CD71+, Ter119+
Mature Erythroblasts	Spleen	Lineage- (CD3e, B220, Gr-1, Mac-1), CD71-, Ter119+

Table 2.6: Flow Antibodies

Antigen	Conjugate	Company	Clone Number	Product Number	Staining Ratio
CD45.1	FITC	BioLegend	A20	110706	1:100
CD45.2	BV421	BioLegend	104	84208	1:100
CD45.2	BV605	BioLegend	104	109841	1:100
CD45.2	PE	BioLegend	104	109808	1:100
B220	PECy7	BioLegend	RA3-6B2	103222	1:100
B220	APC	BioLegend	RA3-6B2	103212	1:100
B220	APCCy7	BioLegend	RA3-6B2	103224	1:100
Gr-1	PECy7	BioLegend	RB6-8C5	108416	1:100
Gr-1	APCCy7	BioLegend	RB6-8C5	108424	1:100
Mac-1	PECy7	BioLegend	M1/70	101216	1:100
Mac-1	APCCy7	BioLegend	M1/70	101226	1:100
CD3e	APC	BioLegend	145-2C11	100312	1:100
CD3e	APCCy7	BioLegend	145-2C11	100330	1:100
Ter119	APCCy7	BioLegend	TER-119	116223	1:100
NK1.1	Biotin	eBiosciences	PK136	13-5941-85	1:100
CD11c	Biotin	eBiosciences	N418	13-0114-82	1:100
Streptavidin	APCCy7	BD Biosciences		554063	1:100
CD48	PECy7	BioLegend	HM48-1	103424	1:100
CD150	PE	BioLegend	TC15-12F12.2	115904	1:100
CD150	BV421	BioLegend	TC15-12F12.2	115925	1:100
EPCR	APC	BioLegend	RCR-16	141506	1:100
EPCR	PerCP-eFlour 710	eBioscience	eBio1560	46-2012-80	1:100
c-Kit	BV421	BioLegend	2B8	84158	1:100
c-Kit	APC	BD Biosciences	2B8	561074	1:100
c-Kit	FITC	BD Biosciences	2B8	561680	1:100
Sca-1	FITC	BD Biosciences	E13-161.7	553335	1:100
Sca-1	APC	BioLegend	E13-161.7	122512	1:100
Flk2	PE	BD Biosciences	A2F10.1	553842	1:50
IL7rα	APC	BioLegend	A7R34	135012	1:50
Ly6D	FITC	BD Biosciences	49-H4	561148	1:100
CD16/32	PE	eBiosciences	93	12-0161-82	1:50
CD34	FITC	BD Biosciences	RAM34	560238	1:50

CD34	APC	BioLegend	MEC14.7	119310	1:50
IgM	PECy7	eBiosciences	II/41	25-5790-82	1:100
CD43	PE	eBiosciences	EBioR2/60	12-0431-83	1:100
CD19	FITC	eBiosciences	eBio1D3	11-0193-85	1:100
CD4	APC	eBiosciences	GK1.5	17-0041-81	1:100
CD8a	PECy7	BD Biosciences	53-6.7	552877	1:100
CD44	BV421	BioLegend	IM7	103039	1:100
CD25	PE	eBiosciences	PC61.5	12-0251-83	1:100
CD71	APC	eBiosciences	R17217	17-0711-82	1:100
H2AX	Alexa Fluor 647	BioLegend	2F3	613408	1:10
Anti-Cleaved PARP	PE	BD Pharmingen	F21-852	552933	2:5
Ki67	BV605	BioLegend	16A8	652413	1:10

Table 2.7: TaqMan Gene Specific Probes for qRT-PCR

Gene AOD	**Assay ID**
Kdm6b	Mm01332680_m1
Fos	Mm00487425_m1
Jun	Mm00495062_s1
Gata2	Mm00492301_m1
Dusp1	Mm00457274_g1
Ier2	Mm00494886_s1
Zfp36	Mm00457144_m1

Chapter 3: Discussion

3.1 Conclusions

3.1.1 Introduction

The balance between self-renewal and differentiation is critical for HSCs in normal hematopoiesis as well as HSCs undergoing proliferative, oncogenic, and inflammatory stress. Epigenetic modifiers with varied functions have been identified as being frequently mutated in numerous different leukemias and blood disorders including enzymes involved in DNA methylation, *DNMT3A* and *TET2,* and enzymes involved in H3K27me3 methylation, *UTX,* and *EZH2*[115–117]. Research driven to elucidate the function of such genes have shown that in normal hematopoiesis aberrant expression can result in an imbalance of HSC fate decisions. Loss of *Dnmt3a* results in an increase in self-renewal and diminishes differentiation[157]. Competitive transplants of *Tet2*-KO HSCs from both adult WBM and fetal liver cells showed increased repopulating capacity, expansion of progenitors, and altered hematopoietic differentiation skewed toward myeloid lineages[158–160]. Conversely, loss of *Ezh2,* has been shown to alter fetal and adult hematopoiesis in different ways, with it being essential in embryonic hematopoiesis and redundant with *Ezh1* in adult WBM[124].

In addition to being mutated, epigenetic modifiers have also been identified as being dysregulated including KDM2B, which is the H3K36me2 demethylase, and is upregulated in T-cell lymphomas and AML[161]. Analysis of *Kdm2b* deficient mice indicate

that not only is *Kdm2b* necessary for leukemia initiation and maintenance of disease[161], but that loss of *Kdm2b* leads to a loss in HSCs and progenitors and skews differentiation to myeloid bias[162]. Given that *KDM6B* is also seen to be overexpressed in blood cancers but rarely mutated[92,120–122], we aimed to elucidate the role that *KDM6B* plays in normal and malignant hematopoiesis.

3.1.2 Kdm6b in Stem Cell Fate Decisions

Similar to what has been seen in other mouse models, the loss of Kdm6b drastically influences that stem cell fate decisions between self-renewal and differentiation. Here we show that loss of *Kdm6b* leads to a reduction in phenotypic and functional HSCs and MPPs. Additionally, we showed that while complete ablation of Kdm6b leads to this phenotype quickly, it acts in a dose dependent manner, with *Kdm6b*-Het^{VAV} eventually losing phenotypic HSCs and MPPs with age, or with serial transplants. Transplantation of HSCs with reduced expression of *Kdm6b* showed that they are capable of making all three lineages, but not to sustain the progenitor compartment. Taken together, our data suggests that *Kdm6b* is necessary for the self-renewal of HSCs, and one of the reasons that deletions may not be seen in leukemia is due to the fact that HSCs with mutated *KDM6B* are rapidly outcompeted and lost in the HSC pool.

We also observed that loss of *Kdm6b* leads to a phenotype that is very similar to that of aged HSCs. This may suggest that as people age, *KDM6B* is not capable of responding to environmental queues either inflammatory or proliferative, or that it has decreased expression in HSCs. Interestingly, Kristina Kirschner et al recently studied aging HSCs to identify a molecular signature that characterizes the population and many

of the genes they identified are significantly upregulated in *Kdm6b*-KO^{VAV} HSCs[163] (p=3.8655x10^{-8}) **(Figure 3.1, Table 3.1)** and are related to stress response.

3.1.3 Regulation of Stress Response in Hematopoiesis Requires Kdm6b

While we did see a significant reduction HSCs and MPPs in non-manipulated mice, aging mice did not lead to overt hematopoietic disease. Rather, the transplantation of WBM and HSCs led to a more overt self-renewal phenotype indicating that the proliferative stress of inflammatory environment may contribute to the phenotype of *Kdm6b*-KO^{VAV} HSCs. One of the roles KDM6B plays in cells that has been widely studied is its role in inflammatory and environmental stresses[59,72,84]. Hematopoetic stem and progenitor cells were discovered to have toll-like receptors on their surface making them immunogenic[123]. This indicates that *Kdm6b* may be playing an important role in stress response in HSCs. Our RNA-SEQ indicated that loss of *Kdm6b* in HSCs leads to an increase in inflammatory signaling pathways including, NF-κB and IFNγ. Interestingly, numerous genes implicated in these pathways are overlapping and have been identified as driving HSC quiescence[139], as being immediate early response genes (IERs)[164], and as being top genetic markers defining aged HSCs[163] **(Table 3.1)**. These overlapping genes include but are not limited to: *Fos, Fosb, Jun, Dusp1, Egr1, Ier3,* and *Zfp36.*

Macrophage response to LPS stimulation indicated that, with the exception of *Bmp-2*[27], gene expression changes in the absence of *Kdm6b* is demethylase-independent[72]. Our ChIPmentation data for H3K27me3 indicates that the changes in gene expression driven by the loss of *Kdm6b* is also demethylase-independent. While

there were differences in peaks between control and Kdm6b-KO HSCs, they did not correlate with changes in gene expression. Previous experiments suggest that KDM6B may play a role in H3K4me3 in stress response in MDS[122], however, ChIPmentation for H3K4me3 showed no differences with 99.9% of the peaks overlapping. Taken together this suggests that loss of *Kdm6b* in HSCs leads to a proinflammatory state that is not dependent upon the previously identified chromatin modifications with which Kdm6b identifies.

The dysregulation in inflammatory signaling led us to explore the effect that varying stress agents would have on *Kdm6b*-KO^{VAV} HSCs. We saw that upon pIpC treatment, which mimics a viral infection and INFα response[136], HSCs lacking Kdm6b were no longer able to compete short-term in transplantation. In non-manipulated primary mice, two short pIpC treatments indicated that upon inflammatory stress, while control^{VAV} HSCs are capable of expanding the HSC population as well as the progenitor pool, *Kdm6b*-KO^{VAV} HSCs did not show an increase, but their progenitor population did. This suggests that Kdm6b is required for self-renewal of HSCs exposed to inflammatory stress. To compliment this, we saw that while *Kdm6b*-KO^{VAV} mice were able to regenerate the hematopoietic compartment after 5-FU, upon serial exposure they had a significant decrease in survival. Additionally, both 5-FU and pIpC treatment caused the inflammatory genes already upregulated in *Kdm6b*-KO^{VAV} HSCs to become even more so. Altogether, our experimental data suggests that Kdm6b plays an integral role in stress response and survival in HSCs and progenitors.

3.1.4 Kdm6b as a Therapeutic Target for AML

When we explored the role of Kdm6b in leukemic stem cells under oncogenic stress using the MLL-AF9 model, we saw that loss of a single allele or both alleles of *Kdm6b* leads to significant increases in survival and a reduction in leukemic stem cells. This suggests that KDM6B could be a potential therapeutic target of AML as well as the previously identified MDS, multiple myeloma and T-ALL[120–122].

A small chemical inhibitor, GSK-J4, was identified in 2012 as a H3K27me3 demethylase inhibitor that shows specificity to KDM6B and UTX[28]. This small molecule inhibitor works by mimicking α-ketoglutarate and preventing the binding of that necessary cofactor[28]. Since then many studies have looked at the power of inhibiting KDM6B *in vitro,* however, given that the inhibitor works on both demethylases it may have unintended consequences. In NICD driven T-ALL, UTX had been shown to play a tumor suppressor role while KDM6B acts as an oncogene[120]. One could argue that inhibiting KDM6B may be therapeutic, but concurrent inhibition of UTX may lead to a more aggressive disease. In example, while the previous paper by Ntzizchristos et al suggested that GSK-J4 is acting by inhibiting KDM6B in NICD driven T-ALL, Benyoucef et al showed that in TAL1 driven T-ALL GSK-J4 is acting by inhibiting UTX, which is an activator of TAL1[165]. This ambiguity of the mechanism of action of GSK-J4 is an example of why more specific inhibitors are needed. It was shown that altering the structural design of GSK-J4 with different chelating groups to disrupt Fe(II) interactions may create stronger inhibitors for KDM6B[166], however, these inhibitors have yet to be tested in a therapeutic setting.

3.2 Future Directions

3.2.1 Combinatorial Treatment of IFN and KDM6B inhibition

We have shown that Kdm6b is required for normal and leukemic stem cell self-renewal, and that loss of *Kdm6b* leads to increased survival in MLL-AF9 driven leukemia. Further loss of *Kdm6b* leads to the inability for progenitor cells to respond correctly to inflammatory and stress signals, and stimulating *Kdm6b*-KO^{VAV} HSCs to proliferate under stress leads to a differentiation cascade and eventual loss of the HSC compartment. Currently, we still need to investigate if pharmacological inhibition of Kdm6b using GSK-J4 also increases the survival of controls. Further, treating *Kdm6b*-KO^{VAV} mice transplanted with MLL-AF9+ transduced WBM with INFγ or pIpC may create a combinatorial effect and a more efficacious therapy.

3.2.2 *Fos/Jun* AP-1 Transcription Factor as a Possible Regulator of *Kdm6b* Demethylase-Independent Gene Expression

Despite the overall amount of work that has already gone into this project, the one piece of evidence we are missing is the exact mechanism by which Kdm6b is acting in HSCs. While we have shown that loss of *Kdm6b* in HSCs leads to demethylase-independent changes in gene expression with the majority of genes increasing in expression, we have not elucidated what is causing these gene expression changes. Of the genes that consistently show up as being involved in dysregulated pathways, two may hold the key: *Jun* and *Fos.* These two genes form the AP-1 transcription factor that like KDM6B has been shown to be necessary for neuronal development and repair[167,168], epidermal differentiation[169–172], stress-response[173–176], and TPA-induced HL-60

differentiation[177,178]. As IER genes they are immediately increased in expression upon stress stimulus and bind to the TPA-inducible enhancers (TRE) with the consensus binding site TGA(C/G)TCA[179]. Importantly, it has also been shown that AP-1 acts in a positive autoregulatory loop, where TPA causes AP-1 to bind to the *Jun* promoter and increase its own expression[180]. It has also been shown that AP-1 can increase glucocorticoids which in turn downregulate AP-1 activity[181], indicating that AP-1 target genes can serve as negative feedback loops for the transcription factor.

The macrophage stress-response promoter found in the first intron of *Kdm6b* contains two AP-1 TRE consensus sites, in addition to two NF-κB binding sites[27,104]. After LPS treatment in macrophages it was shown that NF-κB binds to this promoter resulting in increased *Kdm6b* expression[27]. *KDM6B* was shown to be necessary for TPA-induced HL-60 differentiation, and it has been identified as a TPA response gene[70] in addition to the IER genes *FOS* and *JUN*[177,178]. We hypothesize that in HSCs *Kdm6b* is a direct target of the AP-1 transcription factor containing *Jun* and *Fos* and that *Kdm6b* loss leads to the inability to regulate the feedback loop necessary to silence the AP-1 pathway in HSCs. In support of this, of the 49 previously identified IER genes, there is significant overlap, with 12 being overexpressed greater than 2-fold in *Kdm6b*-KO^{VAV} HSCs (p=1.6485x10^{-9}) **(Table 3.1)**. Additionally, *Erg1,* another highly dysregulated inflammatory gene, has been shown to interact with AP-1 at its consensus binding sites[182]. To test this, we will perform chromatin immunoprecipitation for FOS and JUN in HL-60 cells that are treated with PBS or stimulated to differentiation with TPA. Following this we will perform qPCR for the *KDM6B* promoter regions that contain the AP-1 binding motif. This will allow us to show

the direct interaction between the AP-1 transcription factor and *KDM6B* in response to stress and differentiation.

3.2.3 Does Genetic Inhibition of AP-1 Transcription Factor Genes Rescue *Kdm6b* Phenotype?

Because the AP-1 transcription factor was one of the first discovered, it has been widely studied in a variety of systems. The expression patterns of *FOS* and *JUN* been seen to be highly specific in human keratinocytes[170] and suppression of the AP-1 transcription factor in this system prevents differentiation[142]. The differential expression pattern of *FOS* showed that expression of the gene is not high in hematopoietic tissue unless it is undergoing differentiation, and it exhibits similar patterns in differentiating fetal membranes[183]. Induced prolonged expression of *Fos* in transgenic mouse HSCs caused decreased colony forming potential and forced the HSCs into G0/G1, but *Fos*-KO HSCs had no deficiencies[143]. Taken together, this indicates that the expression of *Fos* is highly regulated within the hematopoietic system, and aberrant expression can effect both HSC and differentiation. We hypothesize that the increased expression of *Fos* and *Jun* in *Kdm6b*-KO^{VAV} HSCs contributes to phenotype we observed and that reduction of their expression will lead to increased engraftment and restored inflammatory stress response.

We have generated shRNAs targeting *Fos* and *Jun* in GFP+ and mCherry+ constructs, respectively, as well as shLacZ controls. We will perform double transduction on c-Kit+ enriched WBM from control^{VAV} or *Kdm6b*-KO^{VAV} mice. These cells will be competitively transplanted and allowed to engraft. At four weeks post-transplant, we will treat the recipient micce with six-doses of pIpC for 12-days, and two-weeks post-treatment analyze HSCs. This system will allow us to see if reduction of *Fos, Jun,* or both

Fos and *Jun* concurrently are contributing to the phenotype. We will perform a similar experiment overexpressing *Fos* and *Jun* in control^{VAV} HSCs to determine if overexpression phenocopies loss of *Kdm6b.*

Taken together, these experiments should contribute to identifying the mechanism behind the phenotype we observed and should add significantly to the scientific contribution of this thesis.

3.3 Figures

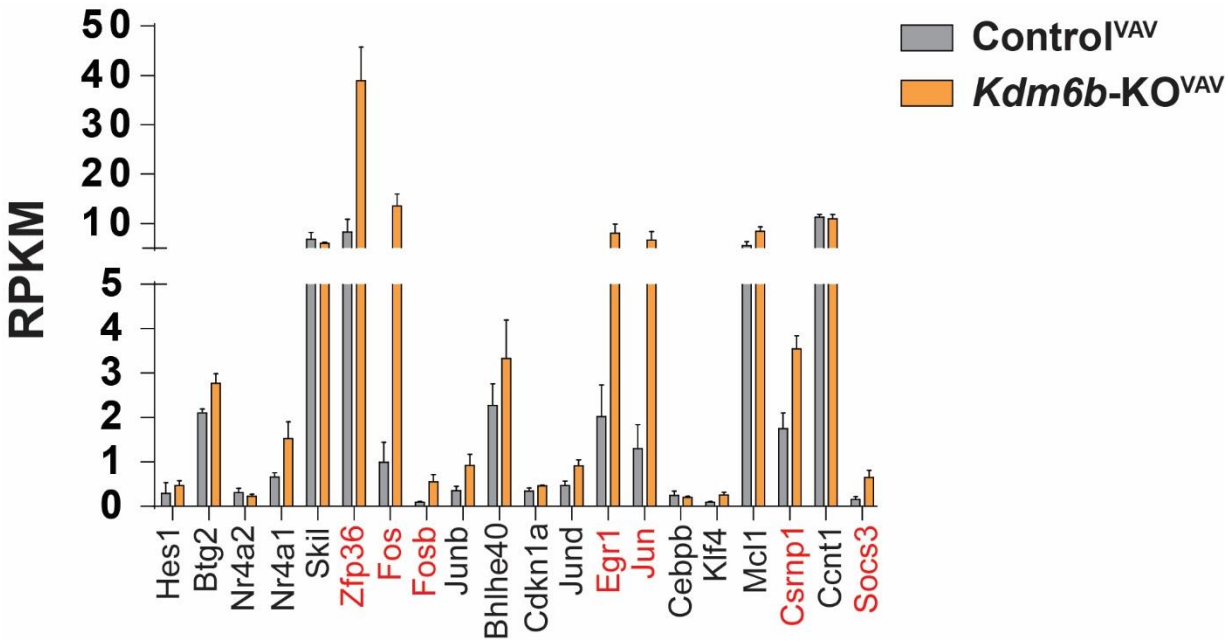

Figure 3.1 Aged HSC Gene Expression Signature

RPKM values from RNA-SEQ of the top 20 genes driving the aged HSC gene expression signature as identified by Kristina Kirschner et al[163] with significantly upregulated genes in Kdm6b-KO^{VAV} HSCs highlighted in red.

3.3 Tables

Table 3.1: Overlapping Gene Signatures in Kdm6b-KO^{VAV} HSCs

Gene	Quiescence	Immediate Early Response	Aged HSCs
Csf2rb2	X		
Csrnp1		X	X
Ctsf	X		
Dusp1	X	X	X
Dusp5		X	
Egr1		X	X
Eng	X		
Fam110a			X
Fos	X	X	X
Fosb	X	X	X
Gem		X	
Hbegf		X	
Id1			X
Ier2	X		X
Ier3		X	
Jun		X	X
Klc4	X		
Lrp10	X		
Nr4a3		X	
Ormdl3	X		
Per1			X
Rabac1	X		
Rrad	X		
Sertad1	X		
Slc3a2	X		
Stk38l	X		
Tgfbi	X		
Tmem189			X
Tspan7	X		
Ubxn6	X		
Zfp36	X	X	X

References

1. Grewal, S. I. S. & Klar, A. J. S. Chromosomal inheritance of epigenetic states in fission yeast during mitosis and meiosis. *Cell* **86,** 95–101 (1996).

2. Cavalli, G. & Paro, G. The Drosophila Fab-7 chromosomal element conveys epigenetic inheritance during mitosis and meiosis. *Cell* **93,** 505–518 (1998).

3. Morgan, H. D., Sutherland, H. G. E., Martin, D. I. K. & Whitelaw, E. Epigenetic inheritance at the agouti locus in the mouse. *Nature Genetics* **23,** 314–318 (1999).

4. Ringrose, L. & Paro, R. Polycomb/Trithorax response elements and epigenetic memory of cell identity. *Development* **134,** 223–232 (2007).

5. Kuzmichev, A. Histone methyltransferase activity associated with a human multiprotein complex containing the Enhancer of Zeste protein. *Genes & Development* **16,** 2893–2905 (2002).

6. Barski, A. *et al.* High-Resolution Profiling of Histone Methylations in the Human Genome. *Cell* **129,** 823–837 (2007).

7. Stock, J. K. *et al.* Ring1-mediated ubiquitination of H2A restrains poised RNA polymerase II at bivalent genes in mouse ES cells. *Nature Cell Biology* **9,** 1428–1435 (2007).

8. Heard, E. Delving into the diversity of facultative heterochromatin: the epigenetics of the inactive X chromosome. *Current Opinion in Genetics & Development* **15,** 482–489 (2005).

9. Plath, K. Role of Histone H3 Lysine 27 Methylation in X Inactivation. *Science* **300,** 131–135 (2003).

10. O'Carroll, D. *et al.* The Polycomb-Group Gene Ezh2 Is Required for Early Mouse Development. *Molecular and Cellular Biology* **21,** 4330–4336 (2001).

11. Pasini, D., Bracken, A. P., Jensen, M. R., Denchi, E. L. & Helin, K. Suz12 is essential for mouse development and for EZH2 histone methyltransferase activity. *The EMBO Journal* **23,** 4061–4071 (2004).

12. Boyer, L. A. *et al.* Polycomb complexes repress developmental regulators in murine embryonic stem cells. *Nature* **441,** 349–353 (2006).

13. Bracken, A. P. Genome-wide mapping of Polycomb target genes unravels their roles in cell fate transitions. *Genes & Development* **20,** 1123–1136 (2006).

14. Lee, T. I. *et al.* Control of Developmental Regulators by Polycomb in Human Embryonic Stem Cells. *Cell* **125,** 301–313 (2006).

15. Shi, Y. *et al.* Histone Demethylation Mediated by the Nuclear Amine Oxidase Homolog LSD1. *Cell* **119,** 941–953 (2004).

16. Klose, R. J., Kallin, E. M. & Zhang, Y. JmjC-domain-containing proteins and histone demethylation. *Nature Reviews Genetics* **7,** 715–727 (2006).

17. Tsukada, Y. *et al.* Histone demethylation by a family of JmjC domain-containing proteins. *Nature* **439,** 811–816 (2006).

18. Xiang, Y. *et al.* JMJD3 is a histone H3K27 demethylase. *Cell Research* **17,** 850–857 (2007).

19. Agger, K. *et al.* UTX and JMJD3 are histone H3K27 demethylases involved in HOX gene regulation and development. *Nature* **449,** 731 (2007).

20. Yamane, K. *et al.* JHDM2A, a JmjC-Containing H3K9 Demethylase, Facilitates Transcription Activation by Androgen Receptor. *Cell* **125,** 483–495 (2006).

21. Greenfield, A. The UTX gene escapes X inactivation in mice and humans. *Human Molecular Genetics* **7,** 737–742 (1998).

22. Hong, S. *et al.* Identification of JmjC domain-containing UTX and JMJD3 as histone H3 lysine 27 demethylases. *Proceedings of the National Academy of Sciences* **104,** 18439–18444 (2007).

23. Jones, S. E., Olsen, L. & Gajhede, M. Structural Basis of Histone Demethylase KDM6B Histone 3 Lysine 27 Specificity. *Biochemistry* **57,** 585–592 (2018).

24. Sengoku, T. & Yokoyama, S. Structural basis for histone H3 Lys 27 demethylation by UTX/KDM6A. *Genes & Development* **25,** 2266–2277 (2011).

25. Lee, M. G. *et al.* Demethylation of H3K27 Regulates Polycomb Recruitment and H2A Ubiquitination. *Science* **318,** 447–450 (2007).

26. Lan, F. *et al.* A histone H3 lysine 27 demethylase regulates animal posterior development. *Nature* **449,** 689–694 (2007).

27. De Santa, F. *et al.* The Histone H3 Lysine-27 Demethylase Jmjd3 Links Inflammation to Inhibition of Polycomb-Mediated Gene Silencing. *Cell* **130,** 1083–1094 (2007).

28. Kruidenier, L. *et al.* A selective jumonji H3K27 demethylase inhibitor modulates the proinflammatory macrophage response. *Nature* **488,** 404–408 (2012).

29. Kristensen, J. B. L. *et al.* Enzyme kinetic studies of histone demethylases KDM4C and KDM6A: Towards understanding selectivity of inhibitors targeting oncogenic histone demethylases. *FEBS Letters* **585,** 1951–1956 (2011).

30. Gehani, S. S. *et al.* Polycomb Group Protein Displacement and Gene Activation through MSK-Dependent H3K27me3S28 Phosphorylation. *Molecular Cell* **39,** 886–900 (2010).

31. Walport, L. J. *et al.* Arginine demethylation is catalysed by a subset of JmjC histone lysine demethylases. *Nature Communications* **7,** 11974 (2016).

32. Luo, J. *et al.* Acetylation of p53 augments its site-specific DNA binding both in vitro and in vivo. *Proceedings of the National Academy of Sciences* **101,** 2259–2264 (2004).

33. Sims, R. J. & Reinberg, D. Is there a code embedded in proteins that is based on post-translational modifications? *Nature Reviews Molecular Cell Biology* **9,** 815–820 (2008).

34. Chuikov, S. *et al.* Regulation of p53 activity through lysine methylation. *Nature* **432,** 353–360 (2004).

35. Kurash, J. K. *et al.* Methylation of p53 by Set7/9 Mediates p53 Acetylation and Activity In Vivo. *Molecular Cell* **29,** 392–400 (2008).

36. Huang, J. *et al.* Repression of p53 activity by Smyd2-mediated methylation. *Nature* **444,** 629–632 (2006).

37. Shi, X. *et al.* Modulation of p53 Function by SET8-Mediated Methylation at Lysine 382. *Molecular Cell* **27,** 636–646 (2007).

38. Solá, S. *et al.* p53 Interaction with JMJD3 Results in Its Nuclear Distribution during Mouse Neural Stem Cell Differentiation. *PLoS ONE* **6,** e18421 (2011).

39. Marikawa, Y. & Alarcón, V. B. Establishment of trophectoderm and inner cell mass lineages in the mouse embryo. *Molecular Reproduction and Development* **76,** 1019–1032 (2009).

40. Saha, B. *et al.* EED and KDM6B Coordinate the First Mammalian Cell Lineage Commitment To Ensure Embryo Implantation. *Molecular and Cellular Biology* **33,** 2691–2705 (2013).

41. Niwa, H. *et al.* Interaction between Oct3/4 and Cdx2 Determines Trophectoderm Differentiation. *Cell* **123,** 917–929 (2005).

42. Home, P. *et al.* GATA3 Is Selectively Expressed in the Trophectoderm of Peri-implantation Embryo and Directly Regulates *Cdx2* Gene Expression. *Journal of Biological Chemistry* **284,** 28729–28737 (2009).

43. Ralston, A. *et al.* Gata3 regulates trophoblast development downstream of Tead4 and in parallel to Cdx2. *Development* **137,** 395–403 (2010).

44. Chung, N. *et al.* Active H3K27me3 demethylation by KDM6B is required for normal development of bovine preimplantation embryos. *Epigenetics* **12,** 1048–1056 (2017).

45. Ying, Q.-L., Nichols, J., Chambers, I. & Smith, A. BMP Induction of Id Proteins Suppresses Differentiation and Sustains Embryonic Stem Cell Self-Renewal in Collaboration with STAT3. *Cell* **115,** 281–292 (2003).

46. Sato, N., Meijer, L., Skaltsounis, L., Greengard, P. & Brivanlou, A. H. Maintenance of pluripotency in human and mouse embryonic stem cells through activation of Wnt signaling by a pharmacological GSK-3-specific inhibitor. *Nature Medicine* **10,** 55–63 (2004).

47. Dahle, O., Kumar, A. & Kuehn, M. R. Nodal Signaling Recruits the Histone Demethylase Jmjd3 to Counteract Polycomb-Mediated Repression at Target Genes. *Science Signaling* **3,** ra48-ra48 (2010).

48. Fei, T. *et al.* Genome-wide mapping of SMAD target genes reveals the role of BMP signaling in embryonic stem cell fate determination. *Genome Research* **20,** 36–44 (2010).

49. Ye, L. *et al.* Histone Demethylases KDM4B and KDM6B Promotes Osteogenic Differentiation of Human MSCs. *Cell Stem Cell* **11,** 50–61 (2012).

50. Liu, D. *et al.* Demethylation of *IGFBP5* by Histone Demethylase KDM6B Promotes Mesenchymal Stem Cell-Mediated Periodontal Tissue Regeneration by Enhancing Osteogenic Differentiation and Anti-Inflammation Potentials: IGFBP5 Promotes MSC-Mediated Tissue Regeneration. *STEM CELLS* **33,** 2523–2536 (2015).

51. Xu, J., Yu, B., Hong, C. & Wang, C.-Y. KDM6B epigenetically regulates odontogenic differentiation of dental mesenchymal stem cells. *International Journal of Oral Science* **5,** 200–205 (2013).

52. Akizu, N., Estaras, C., Guerrero, L., Marti, E. & Martinez-Balbas, M. A. H3K27me3 regulates BMP activity in developing spinal cord. *Development* **137,** 2915–2925 (2010).

53. Jiang, W., Wang, J. & Zhang, Y. Histone H3K27me3 demethylases KDM6A and KDM6B modulate definitive endoderm differentiation from human ESCs by regulating WNT signaling pathway. *Cell Research* **23,** 122–130 (2013).

54. Ohtani, K. *et al.* Jmjd3 Controls Mesodermal and Cardiovascular Differentiation of Embryonic Stem Cells. *Circulation Research* **113,** 856–862 (2013).

55. Sen, G. L., Webster, D. E., Barragan, D. I., Chang, H. Y. & Khavari, P. A. Control of differentiation in a self-renewing mammalian tissue by the histone demethylase JMJD3. *Genes & Development* **22,** 1865–1870 (2008).

56. Iida, A. *et al.* Histone demethylase Jmjd3 is required for the development of subsets of retinal bipolar cells. *Proceedings of the National Academy of Sciences* **111,** 3751–3756 (2014).

57. Jepsen, K. *et al.* SMRT-mediated repression of an H3K27 demethylase in progression from neural stem cell to neuron. *Nature* **450,** 415–419 (2007).

58. Burgold, T. *et al.* The Histone H3 Lysine 27-Specific Demethylase Jmjd3 Is Required for Neural Commitment. *PLoS ONE* **3,** e3034 (2008).

59. Wijayatunge, R. *et al.* The histone lysine demethylase Kdm6b is required for activity-dependent preconditioning of hippocampal neuronal survival. *Molecular and Cellular Neuroscience* **61,** 187–200 (2014).

60. Wijayatunge, R. *et al.* The histone demethylase Kdm6b regulates a mature gene expression program in differentiating cerebellar granule neurons. *Molecular and Cellular Neuroscience* **87,** 4–17 (2018).

61. Park, D. H. *et al.* Activation of Neuronal Gene Expression by the JMJD3 Demethylase Is Required for Postnatal and Adult Brain Neurogenesis. *Cell Reports* **8,** 1290–1299 (2014).

62. Burgold, T. *et al.* The H3K27 Demethylase JMJD3 Is Required for Maintenance of the Embryonic Respiratory Neuronal Network, Neonatal Breathing, and Survival. *Cell Reports* **2,** 1244–1258 (2012).

63. Satoh, T. *et al.* The Jmjd3-Irf4 axis regulates M2 macrophage polarization and host responses against helminth infection. *Nature Immunology* **11,** 936–944 (2010).

64. Shpargel, K. B., Starmer, J., Yee, D., Pohlers, M. & Magnuson, T. KDM6 Demethylase Independent Loss of Histone H3 Lysine 27 Trimethylation during Early Embryonic Development. *PLoS Genetics* **10,** e1004507 (2014).

65. Hofstetter, C. *et al.* Inhibition of KDM6 activity during murine ESC differentiation induces DNA damage. *Journal of Cell Science* **129,** 788–803 (2016).

66. Williams, K. *et al.* The Histone Lysine Demethylase JMJD3/KDM6B Is Recruited to p53 Bound Promoters and Enhancer Elements in a p53 Dependent Manner. *PLoS ONE* **9,** e96545 (2014).

67. Akdemir, K. C. *et al.* Genome-wide profiling reveals stimulus-specific functions of p53 during differentiation and DNA damage of human embryonic stem cells. *Nucleic Acids Research* **42,** 205–223 (2014).

68. Zhao, W. *et al.* Jmjd3 Inhibits Reprogramming by Upregulating Expression of INK4a/Arf and Targeting PHF20 for Ubiquitination. *Cell* **152,** 1037–1050 (2013).

69. Miller, S. A., Mohn, S. E. & Weinmann, A. S. Jmjd3 and UTX Play a Demethylase-Independent Role in Chromatin Remodeling to Regulate T-Box Family Member-Dependent Gene Expression. *Molecular Cell* **40,** 594–605 (2010).

70. Chen, S. *et al.* The histone H3 Lys 27 demethylase JMJD3 regulates gene expression by impacting transcriptional elongation. *Genes & Development* **26,** 1364–1375 (2012).

71. Issaeva, I. *et al.* Knockdown of ALR (MLL2) Reveals ALR Target Genes and Leads to Alterations in Cell Adhesion and Growth. *Molecular and Cellular Biology* **27,** 1889–1903 (2007).

72. De Santa, F. *et al.* Jmjd3 contributes to the control of gene expression in LPS-activated macrophages. *The EMBO Journal* **28,** 3341–3352 (2009).

73. Das, N. D. *et al.* Gene networking and inflammatory pathway analysis in a JMJD3 knockdown human monocytic cell line: JMJD3 KNOCKDOWN-DEPENDENT MOLECULAR NETWORKING. *Cell Biochemistry and Function* **30,** 224–232 (2012).

74. Benoit, M., Desnues, B. & Mege, J.-L. Macrophage Polarization in Bacterial Infections. *The Journal of Immunology* **181,** 3733–3739 (2008).

75. Mantovani, A., Sozzani, S., Locati, M., Allavena, P. & Sica, A. Macrophage polarization: tumor-associated macrophages as a paradigm for polarized M2 mononuclear phagocytes. *Trends in Immunology* **23,** 549–555 (2002).

76. Gordon, S. Alternative activation of macrophages. *Nature Reviews Immunology* **3,** 23–35 (2003).

77. McLaren, J. E. & Ramji, D. P. Interferon gamma: A master regulator of atherosclerosis. *Cytokine & Growth Factor Reviews* **20,** 125–135 (2009).

78. Billiau, A. & Matthys, P. Interferon-γ: A historical perspective. *Cytokine & Growth Factor Reviews* **20,** 97–113 (2009).

79. Martinez, F. O., Helming, L. & Gordon, S. Alternative Activation of Macrophages: An Immunologic Functional Perspective. *Annual Review of Immunology* **27,** 451–483 (2009).

80. Yıldırım-Buharalıoğlu, G., Bond, M., Sala-Newby, G. B., Hindmarch, C. C. T. & Newby, A. C. Regulation of Epigenetic Modifiers, Including KDM6B, by Interferon-γ and Interleukin-4 in Human Macrophages. *Frontiers in Immunology* **8,** (2017).

81. Tang, Y. *et al.* Jmjd3 is essential for the epigenetic modulation of microglia phenotypes in the immune pathogenesis of Parkinson's disease. *Cell Death & Differentiation* **21,** 369–380 (2014).

82. Przanowski, P. *et al.* The signal transducers Stat1 and Stat3 and their novel target Jmjd3 drive the expression of inflammatory genes in microglia. *Journal of Molecular Medicine* **92,** 239–254 (2014).

83. Sherry-Lynes, M. M., Sengupta, S., Kulkarni, S. & Cochran, B. H. Regulation of the JMJD3 (KDM6B) histone demethylase in glioblastoma stem cells by STAT3. *PLOS ONE* **12,** e0174775 (2017).

84. Yan, Q. *et al.* Jmjd3-mediated epigenetic regulation of inflammatory cytokine gene expression in serum amyloid A-stimulated macrophages. *Cellular Signalling* **26,** 1783–1791 (2014).

85. Mozes, G., Friedman, N. & Shainkin-Kestenbaum, R. Serum amyloid A: an extremely sensitive marker for intensity of tissue damage in trauma patients and indicator of acute response in various diseases. *Journal of Trauma* **29,** 71–74 (1989).

86. Chambers, R., MacFarlane, D., Whicher, J. & Dieppe, P. Serum amyloid-A protein concentration in rheumatoid arthritis and its role in monitoring disease activity. *Annals of Rheumatic Diseases* **42,** 665–667 (1983).

87. da Silva, R. F., Lappalainen, J., Lee-Rueckert, M. & Kovanen, P. T. Conversion of human M-CSF macrophages into foam cells reduces their proinflammatory responses to classical M1-polarizing activation. *Atherosclerosis* **248,** 170–178 (2016).

88. Neele, A. E. *et al.* Macrophage Kdm6b controls the pro-fibrotic transcriptome signature of foam cells. *Epigenomics* **9,** 383–391 (2017).

89. Schoenborn, J. R. *et al.* Comprehensive epigenetic profiling identifies multiple distal regulatory elements directing transcription of the gene encoding interferon-γ. *Nature Immunology* **8,** 732–742 (2007).

90. Doñas, C. *et al.* The histone demethylase inhibitor GSK-J4 limits inflammation through the induction of a tolerogenic phenotype on DCs. *Journal of Autoimmunity* **75,** 105–117 (2016).

91. Manna, S. *et al.* Histone H3 Lysine 27 demethylases Jmjd3 and Utx are required for T-cell differentiation. *Nature Communications* **6,** (2015).

92. Anderton, J. A. *et al.* The H3K27me3 demethylase, KDM6B, is induced by Epstein–Barr virus and over-expressed in Hodgkin's Lymphoma. *Oncogene* **30,** 2037–2043 (2011).

93. Messer, H. G. P., Jacobs, D., Dhummakupt, A. & Bloom, D. C. Inhibition of H3K27me3-Specific Histone Demethylases JMJD3 and UTX Blocks Reactivation of Herpes Simplex Virus 1 in Trigeminal Ganglion Neurons. *Journal of Virology* **89,** 3417–3420 (2015).

94. Shan, J., Fu, L., Balasubramanian, M. N., Anthony, T. & Kilberg, M. S. ATF4-dependent Regulation of the JMJD3 Gene during Amino Acid Deprivation Can Be Rescued in Atf4-deficient Cells by Inhibition of Deacetylation. *Journal of Biological Chemistry* **287,** 36393–36403 (2012).

95. Guo, X. *et al.* Regulation of histone demethylase KDM6B by hypoxia-inducible factor-2. *Acta Biochimica et Biophysica Sinica* **47,** 106–113 (2015).

96. Ma, J. *et al.* KDM6B Elicits Cell Apoptosis by Promoting Nuclear Translocation of FOXO1 in Non-Small Cell Lung Cancer. *Cellular Physiology and Biochemistry* **37,** 201–213 (2015).

97. Laks, D. R. *et al.* Neurosphere Formation Is an Independent Predictor of Clinical Outcome in Malignant Glioma. *Stem Cells* **27,** 980–987 (2009).

98. Ene, C. I. *et al.* Histone Demethylase Jumonji D3 (JMJD3) as a Tumor Suppressor by Regulating p53 Protein Nuclear Stabilization. *PLoS ONE* **7,** e51407 (2012).

99. Lin, L.-J. *et al.* Integrated Analysis of Copy Number Alterations and Loss of Heterozygosity in Human Pancreatic Cancer Using a High-Resolution, Single Nucleotide Polymorphism Array. *Oncology* **75,** 102–112 (2008).

100. Yamamoto, K. *et al.* Loss of histone demethylase KDM6B enhances aggressiveness of pancreatic cancer through downregulation of C/EBPα. *Carcinogenesis* **35,** 2404–2414 (2014).

101. Deeb, K. K., Trump, D. L. & Johnson, C. S. Vitamin D signalling pathways in cancer: potential for anticancer therapeutics. *Nature Reviews Cancer* **7,** 684–700 (2007).

102. Giovannucci, E. The epidemiology of vitamin D and cancer incidence and mortality: A review (United States). *Cancer Causes & Control* **16,** 83–95 (2005).

103. Pereira, F. *et al.* KDM6B/JMJD3 histone demethylase is induced by vitamin D and modulates its effects in colon cancer cells. *Human Molecular Genetics* **20,** 4655–4665 (2011).

104. Agger, K. *et al.* The H3K27me3 demethylase JMJD3 contributes to the activation of the INK4A-ARF locus in response to oncogene- and stress-induced senescence. *Genes & Development* **23,** 1171–1176 (2009).

105. Barradas, M. *et al.* Histone demethylase JMJD3 contributes to epigenetic control of INK4a/ARF by oncogenic RAS. *Genes & Development* **23,** 1177–1182 (2009).

106. Tokunaga, R. *et al.* The Prognostic Significance of Histone Lysine Demethylase JMJD3/KDM6B in Colorectal Cancer. *Annals of Surgical Oncology* **23,** 678–685 (2016).

107. Zhao, L. *et al.* JMJD3 promotes SAHF formation in senescent WI38 cells by triggering an interplay between demethylation and phosphorylation of RB protein. *Cell Death & Differentiation* **22,** 1630–1640 (2015).

108. McLaughlin-Drubin, M. E., Crum, C. P. & Münger, K. Human papillomavirus E7 oncoprotein induces KDM6A and KDM6B histone demethylase expression and causes epigenetic reprogramming. *Proceedings of the National Academy of Sciences* **108,** 2130–2135 (2011).

109. Gonzalez, S. L., Stremlau, M., He, X., Basile, J. R. & Munger, K. Degradation of the Retinoblastoma Tumor Suppressor by the Human Papillomavirus Type 16 E7 Oncoprotein Is Important for Functional Inactivation and Is Separable from Proteasomal Degradation of E7. *Journal of Virology* **75,** 7583–7591 (2001).

110. McLaughlin-Drubin, M. E., Park, D. & Munger, K. Tumor suppressor p16INK4A is necessary for survival of cervical carcinoma cell lines. *Proceedings of the National Academy of Sciences* **110,** 16175–16180 (2013).

111. Mathur, R. *et al.* Inhibition of demethylase KDM6B sensitizes diffuse large B-cell lymphoma to chemotherapeutic drugs. *Haematologica* **102,** 373–380 (2017).

112. Svotelis, A. *et al.* H3K27 demethylation by JMJD3 at a poised enhancer of anti-apoptotic gene *BCL2* determines ERα ligand dependency: H3K27 demethylation by JMJD3 determines ERα ligand dependency. *The EMBO Journal* **30,** 3947–3961 (2011).

113. Ramadoss, S., Chen, X. & Wang, C.-Y. Histone Demethylase KDM6B Promotes Epithelial-Mesenchymal Transition. *Journal of Biological Chemistry* **287,** 44508–44517 (2012).

114. Cregan, S. *et al.* Kdm6a and Kdm6b: Altered expression in malignant pleural mesothelioma. *International Journal of Oncology* **50,** 1044–1052 (2017).

115. Abdel-Wahab, O. & Levine, R. L. Mutations in epigenetic modifiers in the pathogenesis and therapy of acute myeloid leukemia. *Blood* **121,** 3563–3572 (2013).

116. Greenblatt, S. M. & Nimer, S. D. Chromatin modifiers and the promise of epigenetic therapy in acute leukemia. *Leukemia* **28,** 1396–1406 (2014).

117. The Cancer Genome Atlas Research Network. Genomic and Epigenomic Landscapes of Adult De Novo Acute Myeloid Leukemia. *New England Journal of Medicine* **368,** 2059–2074 (2013).

118. Mar, B. G. *et al.* Sequencing histone-modifying enzymes identifies UTX mutations in acute lymphoblastic leukemia. *Leukemia* **26,** 1881–1883 (2012).

119. Kiel, M. J. *et al.* Genomic analyses reveal recurrent mutations in epigenetic modifiers and the JAK–STAT pathway in Sézary syndrome. *Nature Communications* **6,** (2015).

120. Ntziachristos, P. *et al.* Contrasting roles of histone 3 lysine 27 demethylases in acute lymphoblastic leukaemia. *Nature* **514,** 513–517 (2014).

121. Ohguchi, H. *et al.* KDM6B modulates MAPK pathway mediating multiple myeloma cell growth and survival. *Leukemia* **31,** 2661–2669 (2017).

122. Wei, Y. *et al.* Global H3K4me3 genome mapping reveals alterations of innate immunity signaling and overexpression of JMJD3 in human myelodysplastic syndrome CD34+ cells. *Leukemia* **27,** 2177–2186 (2013).

123. Nagai, Y. *et al.* Toll-like Receptors on Hematopoietic Progenitor Cells Stimulate Innate Immune System Replenishment. *Immunity* **24,** 801–812 (2006).

124. Mochizuki-Kashio, M. *et al.* Dependency on the polycomb gene Ezh2 distinguishes fetal from adult hematopoietic stem cells. *Blood* **118,** 6553–6561 (2011).

125. Pedersen, M. T. & Helin, K. Histone demethylases in development and disease. *Trends in Cell Biology* **20,** 662–671 (2010).

126. Bannister, A. J. & Kouzarides, T. Regulation of chromatin by histone modifications. *Cell Research* **21,** 381–395 (2011).

127. Van der Meulen, J. *et al.* The H3K27me3 demethylase UTX is a gender-specific tumor suppressor in T-cell acute lymphoblastic leukemia. *Blood* **125,** 13–21 (2015).

128. Georgiades, P. *et al.* vavCre Transgenic mice: A tool for mutagenesis in hematopoietic and endothelial lineages. *genesis* **34,** 251–256 (2002).

129. Iwamori, N., Iwamori, T. & Matzuk, M. M. H3K27 demethylase, JMJD3, regulates fragmentation of spermatogonial cysts. *PLoS ONE* **8,** e72689 (2013).

130. Hu, Y. & Smyth, G. K. ELDA: Extreme limiting dilution analysis for comparing depleted and enriched populations in stem cell and other assays. *Journal of Immunological Methods* **347,** 70–78 (2009).

131. Krivtsov, A. V. *et al.* Transformation from committed progenitor to leukaemia stem cell initiated by MLL-AF9. *Nature* **442,** 818–822 (2006).

132. Mootha, V. K. *et al.* PGC-1α-responsive genes involved in oxidative phosphorylation are coordinately downregulated in human diabetes. *Nature Genetics* **34,** 267–273 (2003).

133. Subramanian, A. *et al.* Gene set enrichment analysis: A knowledge-based approach for interpreting genome-wide expression profiles. *Proceedings of the National Academy of Sciences* **102,** 15545–15550 (2005).

134. Schmidl, C., Rendeiro, A. F., Sheffield, N. C. & Bock, C. ChIPmentation: fast, robust, low-input ChIP-seq for histones and transcription factors. *Nature Methods* **12,** 963–965 (2015).

135. Kuhn, R., Schwenk, F., Aguet, M. & Rajewsky, K. Inducible gene targeting in mice. *Science* **269,** 1427–1429 (1995).

136. Fortier, M.-E. *et al.* The viral mimic, polyinosinic:polycytidylic acid, induces fever in rats via an interleukin-1-dependent mechanism. *Am. J. Physiol. Regul. Integr. Comp. Physiol.* **287,** R759-766 (2004).

137. Wang, C. *et al.* UTX regulates mesoderm differentiation of embryonic stem cells independent of H3K27 demethylase activity. *Proc. Natl. Acad. Sci. U.S.A.* **109,** 15324–15329 (2012).

138. Velasco-Hernandez, T., Säwén, P., Bryder, D. & Cammenga, J. Potential Pitfalls of the Mx1-Cre System: Implications for Experimental Modeling of Normal and Malignant Hematopoiesis. *Stem Cell Reports* **7,** 11–18 (2016).

139. Venezia, T. A. *et al.* Molecular Signatures of Proliferation and Quiescence in Hematopoietic Stem Cells. *PLoS Biology* **2,** e301 (2004).

140. Yamazaki, S. *et al.* The AP-1 transcription factor JunB is required for Th17 cell differentiation. *Scientific Reports* **7,** 17402 (2017).

141. Leppä, S., Eriksson, M., Saffrich, R., Ansorge, W. & Bohmann, D. Complex functions of AP-1 transcription factors in differentiation and survival of PC12 cells. *Mol. Cell. Biol.* **21,** 4369–4378 (2001).

142. Han, B. *et al.* Suppression of AP1 transcription factor function in keratinocyte suppresses differentiation. *PLoS ONE* **7,** e36941 (2012).

143. Okada, S., Fukuda, T., Inada, K. & Tokuhisa, T. Prolonged expression of c-fos suppresses cell cycle entry of dormant hematopoietic stem cells. *Blood* **93,** 816–825 (1999).

144. Rossi, D. J. *et al.* Cell intrinsic alterations underlie hematopoietic stem cell aging. *Proceedings of the National Academy of Sciences* **102,** 9194–9199 (2005).

145. Beerman, I., Maloney, W. J., Weissmann, I. L. & Rossi, D. J. Stem cells and the aging hematopoietic system. *Current Opinion in Immunology* **22,** 500–506 (2010).

146. Dobin, A. *et al.* STAR: ultrafast universal RNA-seq aligner. *Bioinformatics* **29,** 15–21 (2013).

147. Liao, Y., Smyth, G. K. & Shi, W. featureCounts: an efficient general purpose program for assigning sequence reads to genomic features. *Bioinformatics* **30,** 923–930 (2014).

148. Liao, Y., Smyth, G. K. & Shi, W. The Subread aligner: fast, accurate and scalable read mapping by seed-and-vote. *Nucleic Acids Research* **41,** e108–e108 (2013).

149. Patro, R., Mount, S. M. & Kingsford, C. Sailfish enables alignment-free isoform quantification from RNA-seq reads using lightweight algorithms. *Nature Biotechnology* **32,** 462–464 (2014).

150. Wang, L., Wang, S. & Li, W. RSeQC: quality control of RNA-seq experiments. *Bioinformatics* **28,** 2184–2185 (2012).

151. Wang, L. *et al.* Measure transcript integrity using RNA-seq data. *BMC Bioinformatics* **17,** (2016).

152. Langmead, B. & Salzberg, S. L. Fast gapped-read alignment with Bowtie 2. *Nature Methods* **9,** 357–359 (2012).

153. Starmer, J. & Magnuson, T. Detecting broad domains and narrow peaks in ChIP-seq data with hiddenDomains. *BMC Bioinformatics* **17,** (2016).

154. Carroll, T. S., Liang, Z., Salama, R., Stark, R. & de Santiago, I. Impact of artifact removal on ChIP quality metrics in ChIP-seq and ChIP-exo data. *Frontiers in Genetics* **5,** (2014).

155. Ramírez, F. *et al.* deepTools2: a next generation web server for deep-sequencing data analysis. *Nucleic Acids Research* **44,** W160–W165 (2016).

156. Neph, S. *et al.* BEDOPS: high-performance genomic feature operations. *Bioinformatics* **28,** 1919–1920 (2012).

157. Challen, G. A. *et al.* Dnmt3a is essential for hematopoietic stem cell differentiation. *Nature Genetics* **44,** 23–31 (2012).

158. Li, Z. *et al.* Deletion of Tet2 in mice leads to dysregulated hematopoietic stem cells and subsequent development of myeloid malignancies. *Blood* **118,** 4509–4518 (2011).

159. Kunimoto, H. *et al.* Tet2 disruption leads to enhanced self-renewal and altered differentiation of fetal liver hematopoietic stem cells. *Scientific Reports* **2,** (2012).

160. Pan, F. *et al.* Tet2 loss leads to hypermutagenicity in haematopoietic stem/progenitor cells. *Nature Communications* **8,** 15102 (2017).

161. He, J., Nguyen, A. T. & Zhang, Y. KDM2b/JHDM1b, an H3K36me2-specific demethylase, is required for initiation and maintenance of acute myeloid leukemia. *Blood* **117,** 3869–3880 (2011).

162. Andricovich, J., Kai, Y., Peng, W., Foudi, A. & Tzatsos, A. Histone demethylase KDM2B regulates lineage commitment in normal and malignant hematopoiesis. *Journal of Clinical Investigation* **126,** 905–920 (2016).

163. Kirschner, K. *et al.* Proliferation Drives Aging-Related Functional Decline in a Subpopulation of the Hematopoietic Stem Cell Compartment. *Cell Reports* **19,** 1503–1511 (2017).

164. Tullai, J. W. *et al.* Immediate-Early and Delayed Primary Response Genes Are Distinct in Function and Genomic Architecture. *Journal of Biological Chemistry* **282,** 23981–23995 (2007).

165. Benyoucef, A. *et al.* UTX inhibition as selective epigenetic therapy against TAL1-driven T-cell acute lymphoblastic leukemia. *Genes & Development* **30,** 508–521 (2016).

166. Hu, J. *et al.* Design and discovery of new pyrimidine coupled nitrogen aromatic rings as chelating groups of JMJD3 inhibitors. *Bioorganic & Medicinal Chemistry Letters* **26,** 721–725 (2016).

167. Velazquez, F. N., Caputto, B. L. & Boussin, F. D. c-Fos importance for brain development. *Aging* **7,** 1028–1029 (2015).

168. Raivich, G. *et al.* The AP-1 Transcription Factor c-Jun Is Required for Efficient Axonal Regeneration. *Neuron* **43,** 57–67 (2004).

169. Eckert, R. L. *et al.* AP1 Transcription Factors in Epidermal Differentiation and Skin Cancer. *Journal of Skin Cancer* **2013,** 1–9 (2013).

170. Mehic, D., Bakiri, L., Ghannadan, M., Wagner, E. F. & Tschachler, E. Fos and Jun Proteins Are Specifically Expressed During Differentiation of Human Keratinocytes. *Journal of Investigative Dermatology* **124,** 212–220 (2005).

171. Young, C. A., Rorke, E. A., Adhikary, G., Xu, W. & Eckert, R. L. Loss of epidermal AP1 transcription factor function reduces filaggrin level, alters chemokine expression and produces an ichthyosis-related phenotype. *Cell Death and Disease* **8,** e2840 (2017).

172. Rossi, A., Jang, S.-I., Ceci, R., Steinert, P. M. & Markova, N. G. Effect of AP1 Transcription Factors on the Regulation of Transcription in Normal Human Epidermal Keratinocytes. *Journal of Investigative Dermatology* **110,** 34–40 (1998).

173. Guyton, K., Xu, Q. & Holbrook, N. Induction of the mammalian stress response gene GADD153 by oxidative stress: role of AP-1 element. *The Biochemical Journal* **314,** 547–554 (1996).

174. Chan, R., Brown, E., Ericsson, A., Kovacs, K. & Sawchenko, P. A comparison of two immediate-early genes, c-fos and NGFI-B, as markers for functional activation in stress-related neuroendocrine circuitry. *The Journal of Neuroscience* **13,** 5126–5138 (1993).

175. Weichselbaum, R. R., Hallahan, D., Fuks, Z. & Kufe, D. Radiation induction of immediate early genes: Effectors of the radiation-stress response. *International Journal of Radiation Oncology*Biology*Physics* **30,** 229–234 (1994).

176. Lan, Q. X., Mercurius, K. O. & Davies, P. F. Stimulation of Transcription Factors NFκB and AP1 in Endothelial Cells Subjected to Shear Stress. *Biochemical and Biophysical Research Communications* **201,** 950–956 (1994).

177. Kolla, S. S. & Studzinski, G. P. Resolution of Multiple AP-1 Complexes in HL-60 Cells Induced to Differentiate by 1,25-Dihydroxyvitamin D3. *Journal of Cellular Physiology* **156,** 63–71 (1991).

178. Ma, L., Krishnamachary, N., Perbal, B. & Center, M. HL-60 cells isolated for resistance to vincristine are defective in 12-O-tetradecanoylphorbol-13-acetate

induced differentiation and the formation of a functional AP-1 complex. *Oncology Research* **4,** 291–298 (1992).

179. Zhou, H. Frequency and Distribution of AP-1 Sites in the Human Genome. *DNA Research* **12,** 139–150 (2005).

180. Angel, P., Hattori, K., Smeal, T. & Karin, M. The jun proto-oncogene is positively autoregulated by its product, Jun/AP-1. *Cell* **55,** 875–885 (1988).

181. Karin, M. & Chang. AP-1--glucocorticoid receptor crosstalk taken to a higher level. *Journal of Endocrinology* **169,** 447–451 (2001).

182. Nakashima, A., Ota, A. & Sabban, E. Interactions between Egr1 and AP1 factors in regulation of tyrosine hydroxylase transcription. *Brain Research. Molecular Brain Research* **112,** 61–69 (2003).

183. Muller, R., Muller, D. & Guilbert, L. Differential expression of c-fos in hematopoietic cells: correlation with differentiation of monomyelocytic cells in vitro. *The EMBO Journal* **3,** 1887–1890 (1984).